

Rita Ruohola

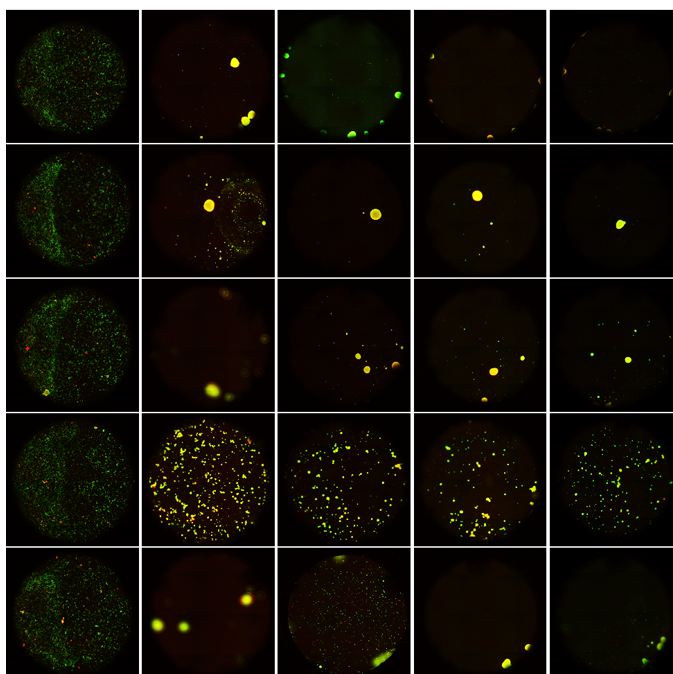
Viability and Survival of Cells in Alginate Gels

Master's thesis in Biotechnology

Supervisor: Berit Løkensgard Strand, IBT

May 2019

NTNU
Norwegian University of Science and Technology
Faculty of Natural Sciences
Department of Biotechnology and Food Science



Rita Ruohola

Viability and Survival of Cells in Alginate Gels

Master's thesis in Biotechnology
Supervisor: Berit Løkenstrand, IBT
May 2019

Norwegian University of Science and Technology
Faculty of Natural Sciences
Department of Biotechnology and Food Science



Preface

This thesis is a part of the master's degree program in the Faculty of Natural Sciences at the Norwegian University of Science and Technology. The work was carried out at the Department of Biotechnology in a collaboration with Sintef.

I would like to thank my supervisor Berit Løkensgard Strand, my co-supervisors Hanne Haslene-Hox and Daria Zaytseva-Zotova for their help and guidance throughout my master work. I would also like to thank Andrea Draget Hoel and Anette Vikenes for their help in the laboratory.

Finally, I would like to take the opportunity to thank Eric for his support for me throughout the project.

Trondheim, May 13th, 2019

Rita Ruohola

Abstract

Different biomaterials are studied for purposes of tissue engineering, drug development and many fields of research to serve as scaffolds for three-dimensional (3D) cell cultures to provide more authentic and tissue-like microenvironments for cells. A common approach for this is the use of hydrogels as the culture matrix. Use of hydrogels aims to mimic in vivo environment and provide more reliable results from in vitro studies.

Hydrogels are three-dimensional polymer networks with a flexible structure and resemblances to a natural extracellular environment with a high content of water. Those can be modified to obtain different mechanical and chemical features and have proven to be well suited for the purpose of biomaterial use. One of the most studied material for hydrogels for these purposes is alginate. Alginate is biopolymer originating commonly from algae and it has been shown to have many interesting and desirable features for biomaterial use. In this thesis a matrix material with the ability to support cell viability, survival and proliferation was searched through multiple screening experiments of different alginate-based hydrogels for encapsulation and cultivation of mammalian cells.

In the experiments conducted within this study, the cell viability inside and on top of the alginate-based hydrogels was followed over time periods from five to ten days. During these periods the cells were inspected at multiple time points and the overall survival was determined by Live/Dead assaying to qualitatively assess live and dead cells throughout the experiment. Furthermore, the morphology of the cells was also investigated in order to determine the capability of the material to promote cell attachment. The ability of cells to attach to their matrix is considered important for their viability and normal function. Two different cell lines were utilized in the experiments and the results obtained with each line were used to evaluate the viability promoting features of the gel matrix. The used cell lines were liver-derived HepG2 line and a myofibroblast line IMR90.

In the series of experiments, it was found that the use of alginate with incorporated RGD-peptide had a significant influence on promoting cell attachment when compared to gels with only unmodified alginate. Gels with different laminin peptides were also studied but these were not found to produce a similar effect as the RGD-peptide with both cell lines. Especially important the incorporation of RGD-peptide was found to be for the IMR90 cell line. The adhering of cells was further improved by increasing the amount of this cell attachment promoting peptide in the gels. The attachment implying morphology changes was only discovered in gels with 1% of alginate. Gels with a higher total amount of alginate were predicted to be harder to penetrate for cells due to higher stiffness of gels. Gels with RGD-modified alginate and less than 1% alginate were not studied because it was susceptible if this would make a stable gel.

Different treatment procedures were also studied in order to increase the survival of cells during the encapsulation process. It was concluded that by exposing cells to hypothermic conditions (+4 °C) before encapsulation the cells had a slightly higher rate of survival when compared to cells encapsulated in RT conditions. Washing of the alginate gels with cell culture media after encapsulation procedure was also found to improve cell survival. The effect of the total cell number on cell survival was studied briefly in the experiments. The results suggested that by increasing cells concentration from initial $7,7 \times 10^5$ cells/ml to a double or more the cells might have been more prone to adhere to the material. However, increasing of the cell number could reduce the survival rate of the encapsulated cells due to higher demand for oxygen and nutrients.

Abbreviations

2D	Two-dimensional
3D	Three-dimensional
CaCO ₃	Calcium carbonate
CLSM	Confocal laser scanning microscopy
DMEM	Dulbecco's Modified Eagle Medium for mammalian cell culture
DPBS	Dulbecco's Phosphate Buffered Saline
ECM	Extracellular matrix
EthD-1	Ethidium homodimer-1
FBS	Fetal Bovine Serum
GDL	Glucono- δ -lactone, Gluconolactone
GFP	Green fluorescent protein
G-block	Section of alginate chain consisting only of α -L-guluronic acid
HepG2	Hepatoma cell line from human liver
HEPES	Citrate-HEPES buffer
IF-water	Ion-free water
IMR90	Myofibroblast cell line from a human lung
L/D assay	Live/dead assay
M-block	Section of alginate chain consisting only of β -D-mannuronic acid
MEM NEAA	Minimum essential medium, Non-essential amino acids -solution for mammalian cell culture
OX	Oxidized alginate
PBS	Phosphate buffered saline
Pen-Strep	Penicillin Streptomycin
RFP	Red fluorescent protein
RPMI	Roswell Park Memorial Institute 1640 medium for cell culturing
RT	Room temperature
SP	Sodium pyruvate
T75	Cell culture flask with 75 cm ² surface area
T175	Cell culture flask with 175 cm ² surface area
UP-LVG	Ultra-pure low viscosity alginate with min.60 % guluronate

Table of Contents

Preface	i
Abstract	ii
Abbreviations	iii
Table of Contents	iv
1 Introduction	7
1.1 3D Cell culturing – Background	7
1.1.1 Hydrogels	8
1.1.2 Polysaccharide as a base of hydrogels	9
1.2 Alginate	10
1.2.1 Chemical structure	10
1.2.2 Features and applications of alginate	11
1.3 Grafted alginates	12
1.4 Cells for encapsulation	14
1.4.1 Fibroblasts	14
1.4.2 IMR90 and myofibroblasts	14
1.4.3 Hepatocytes	16
1.4.4 HepG2	16
2 Materials and Methods	17
2.1 Alginate solutions	17
2.1.1 Grafted alginates	17
2.2 the HEPES buffer	18
2.3 Cells in the experiments	19
2.3.1 Cell suspension for gelling experiments	19
2.3.2 Cold treatment of cells	19
2.3.3 Cell number	20
2.4 Gel preparation	21
2.4.1 Gel formation – Role of CaCO ₃ and GDL	21
2.4.2 Preparation of gels used for cell encapsulation	22
2.4.3 Preparation of gels for on-top cell cultivation	23
2.4.4 Washing of gels	23
	iv

2.5	Corning® Matrigel®	24
2.5.1	Cell cultivation on top of Matrigel matrix	24
2.5.2	Cell encapsulation into low concentration Matrigel	24
2.5.3	Cell encapsulation into high concentration Matrigel	24
2.6	Viability assessment	25
2.6.1	Imaging of gels with a light microscope	26
2.6.2	Imaging of gels with CLSM	27
3	Results	28
3.1	Survival of gel encapsulated IMR90 and HepG2 cells	28
3.2	Comparison of different gel conditions	31
3.3	Effect of cold treatment	34
3.4	Peptide grafted alginates in on-top cell cultivation	37
3.4.1	Results for IMR90	37
3.4.2	Results for HepG2	40
3.5	RGD-modified alginate for cell encapsulation	41
3.5.1	Results for IMR90	41
3.5.2	Results for HepG2	45
3.6	RGD-modified alginate for IMR90 encapsulation	48
3.7	Effect of stiffness and cell number on the survival of IMR90	54
3.7.1	Imaging of gels with CLSM	59
3.8	Matrigel as a material for matrix	65
3.8.1	Cell cultivation on top of Matrigel	65
3.8.2	Encapsulation of cells into high concentration Matrigel	66
3.8.3	Encapsulation of IMR90 into high concentration Matrigel	70
4	Discussion	73
4.1	Increasing the rate of survival	73
4.2	Enhancing viability by promoting cell attachment	74
4.3	Mechanical properties of ECM and the effect on cells	75
4.4	RGD-modified alginate and cell adhesion	78
4.5	Effect of the cell number	81
4.6	Imaging of gels and the L/D assay	82

4.7	Results obtained with Matrigel	84
4.7.1	Comparison of alginate gels and Matrigel	85
4.8	Future perspectives	86
5	Conclusion	88
6	References	89
	Appendix A. Citrate-HEPES buffer	94
	Appendix B. Cell culture mediums and sub cultivation	95
	Appendix C. List of Experiments	96

1 Introduction

1.1 3D Cell culturing – Background

Use of three-dimensional (3D) environment for cell culturing has been under excess research in recent years. A change into these 3D matrixes is thought to provide more tissue-like constructs and there is evidence that cells would behave more as they do in real tissues in 3D matrixes than they do in monolayer cultures. Cells cultured in a single-layer show difference in cell migration, growth and signal transduction to how they would behave in natural tissue. Use of 3D matrixes aims to sustain cell-cell communication and cell-matrix interactions and the interaction with the culture matrix is very different in 3D than in 2D. (1) The morphology of cells is found to be distinctively different in 2D compared to what is perceived in 3D cultures. In 2D cultures, cells grow in one layer and tend to spread along the surface. This causes changes in the apical-basal polarity of the cells. For epithelial cells this behavior is normal, but for many other cell types, the unnatural morphology induces changes in viability, proliferation, metabolism and differentiation. Many non-epithelial cells are more prone to grow in 3D-like environments found in different tissues and organs. (2)

3D matrixes can be used to provide the scaffold material for cells to mimic the extracellular matrix (ECM). Multiple different materials are currently in use or under research and there are already many commercially available products (e.g. Matrigel by BD Biosciences or ECM gel by Sigma-Aldrich) on the market. (3) Materials of both organic and inorganic origin are used as scaffold materials. These are for example different natural or synthetic polymers. Some of the most common materials used are collagen, agarose, laminin and fibronectin. Different cell lines have different requirements for their environment and the choice of scaffold material will affect the behavior and morphology of the cells. (4) In natural tissue, ECM has multiple unique functions and is involved in many vital operations. One of the most evident features of ECM is the physical structure that it provides. Within this structure the intercellular communication and exchange of gas and nutrients take place. (5) In addition to mechanical strength and stability, 3D matrixes must also provide similar conditions to natural ECM as for porosity and permeability to support and maintain chemical and physical interactions of encapsulated cells. (4)

Research on 3D cell matrices and tissue like ECM materials aims to develop methods for achieving novel therapies for regenerative medicine and tissue engineering and to replace the need for organ troublesome transplants in the future. For these purposes, the matrix material must be biocompatible and replicate the functions and properties of the natural tissue that it is designed to mimic. The material must also promote cell survival and in the case of stem cells, cell differentiation. In more simpler approaches, like in cell therapy methods, the material must support the normal exchange of metabolites, nutrients and gases of encapsulated cells while protecting them from immunological responses of the host. (6) Development of 3D cell matrixes seeks to provide new and better approaches for many different research methods that are currently in use. The 3D cell culture models are potential for drug and cancer research, where they could be used for replacing heavy animal tests that the screening experiments are currently relying on. A desire to replace animal tests with 3D in vitro models for toxicological studies is under research because many animal models have proven to be flawed and it is believed that tissue models could provide more accurate results in the future. (3)

Use of 3D models in the early stages of drug research could reduce the number of needed animal studies by detecting and recognizing ineffective and toxic candidates before they enter further trials. (4). Moreover, the use of 3D matrixes in cancer research as 3D tumor models has been under increasing interest. For long this has been done by using 2D cell cultures and in vivo tumor xenografts, but these methods have their constraints. Because of the absence of natural microenvironment cells in monolayer culture have different morphology and an altered pattern of protein synthesis that can significantly influence the outcome of studies.

A different approach for tumor studies are in vivo xenograft models, that usually mean transplantation of cancer cells of human origin into laboratory animals, thus providing the complex environment for the cells. But for this approach, the regular monitoring of tumor development has been a challenge. The relevance of these studies has also proven to be debatable in some cases, e.g. promising treatments have been found to be less effective in human patients than what had been observed in animal studies. In vitro 3D tumor models with a range of complexities from cell spheroids to models combining multiple cell lines can be used for studying e.g. cancer development and effects of therapeutic agents in more closely monitored and controlled environment. (7) Other useful approaches of 3D models are for studies of cell biology where the basic functions of the cell, like expression of genes and proteins, adhesion, proliferation and cell-cycle could be studied in more tissue-like environment. 3D cell culture approaches are also a matter of interest for stem cell research in order to study the differentiation of cells in a controlled environment with specific constructed features. (4)

1.1.1 Hydrogels

Hydrogels can be described as networks made of insoluble polymers with a capability to absorb and retain large volumes of water or other solvents. The great relative volume of solvent in hydrogels allows diffusion to happen much like in free liquids even though the material itself can share properties of solid materials. Hydrogels are often used in 3D cell culturing for their many preferable properties. (8) Generally, hydrogels are a vast group of materials, that can be divided into multiple categories based on the composition, ionic charge, physical structure, etc. They can be made from natural or synthetic polymers, or a combination of these, by using one or more polymers or certain chemicals like silica. (9)

Hydrogels are formed in a process called gelation. Gelation occurs when the polymeric chains in the system are crosslinked by physical or chemical bonds. Formation of hydrogels can be initiated in different ways and the gelation properties are characteristic for different polymers. Free counterions can initiate gelation in polymers with ionic properties, like polysaccharides with polycationic or polyanionic features. Changes in thermal conditions can trigger gelation in some polymers upon heating or cooling. Gelation point or gelling point is defined to have been reached when the system no longer flows. (8)

In medical and pharmaceutical context hydrogels possess many desirable features e.g. for purposes of biomedicine. The softness of hydrogels combined with high water retaining properties and the possibility of alteration of the chemical and biological backbone of the gel makes them versatile and biocompatible. The structure and properties of the gels can be tailored to mimic the features of different target tissues. Hydrogels have also been studied as for material for drug delivery. By encapsulating a drug inside of carrier material, the rate of release of the drug happens in a more controlled and predictable way and the delivery can be improved. Use hydrogels carriers can also be used to reduce the degradation of the drug. (9)

1.1.2 Polysaccharide as a base of hydrogels

Polysaccharides are long chained carbohydrates found almost everywhere in nature from multiple different origin and type. Cellulose being one of the most profuse ones is a structure providing polysaccharide found particularly in plants. Another abundant polysaccharide called chitin is found e.g. in shellfish and insects. Alginates are a family of different polysaccharides found in certain algae and bacteria. Polysaccharides are either linear or branched and can be composed of one type of monomer units (homoglycans) or a chain of different monomers (heteroglycans). (10)

Polysaccharides have properties that make them favorable for many industries. For the medical and pharmaceutical industry, the properties that spark great interest are e.g. nontoxicity and biocompatibility. Many hydrogels based on polysaccharides are found to have structural similarities to ECM because of the porosity and water-retaining abilities. Because of this, the use of hydrogels is being studied for many purposes e.g. encapsulating therapeutic proteins, peptides and vaccines can be encapsulated within the hydrogels. The ECM like structure is less likely to cause tissue irritation and stimulation of chronic inflammation compared to synthetic materials. This makes them potential candidates for regenerative medicine and drug delivery. (11)

Alginate-based hydrogels are recognized as a potential matrix material for cell encapsulation. Use of encapsulated cells can be beneficial for different industries, for example in processes of food production. For biomedical approaches, alginate is an interesting material due to its biocompatibility, permeability and stability in physiological conditions. (12)

1.2 Alginate

Alginates are polysaccharides that are produced by brown algae and bacteria. Alginates provide materials with many different mechanical properties that can be used in a variety of applications in many industries. The most important properties of alginates for industrial use are their ability to promote gelling, retain water and to function as a stabilizing agent. Alginate also has multiple different features that have made it suitable especially for pharmaceutical and medical industry. A lot of research is being done to study and utilize its structure and properties. (13)

1.2.1 Chemical structure

Alginate is non-branched polysaccharide consisting of two different subunits, β -D-mannuronic acid and α -L-guluronic acid (Figure 1). These two monomers are often abbreviated as G (guluronic acid) and M (mannuronic acid). The monomer sequence that emerges from the order of placement of these two has a great effect on the mechanical properties of the alginate. Unlike in many other polysaccharides, the sequence of an alginate polysaccharide chain is inhomogeneous. It is formed by sections or blocks of the same monomer units ('GG...' or 'MM...') with different lengths or with an altering sequence of one monomer by time (e.g. 'GMGMG...'). These two monomers have different chemical properties and therefore the monomer sequence has a great effect on the behavior of alginate. (13) (14)

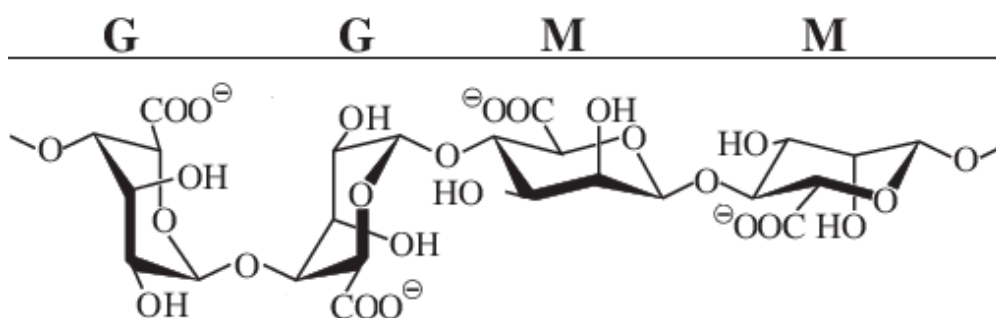


Figure 1. Chemical structure of alginate monomers and polymeric chain conformations.

Alginate is a polyanionic polymer and one of its key features is its ability to bind divalent cations (e.g. Ca^{2+} , Sr^{2+} , and Mg^{2+}). The binding of cationic ions initiates gel formation in regions with a high amount of guluronic acid. G-blocks, the long sections consisting only of this monomer G, are a vital precursor for the gelling properties of alginate. These monomers are diaxially linked and form cavity-like structures in the polymeric chain when two or more G monomers are next to each other in the polymer chain (Figure 1).

G-monomers are formed when β -D-mannuronic acid monomer (M) undergoes an epimerization and has its conformation changed from ${}^4\text{C}_1$ -form into ${}^1\text{C}_4$ -form in a two-step process resulting in an α -L-guluronic acid (G). This change in conformation in the glycosidic linkages between the alginate monomers, changes the geometry of the alginate backbone, creating these 'cavities' between G-monomers. These cavities are characteristic for G-blocks and are not found in di-equatorially linked M-blocks or between of equatorial-axial linked M and G monomers. These cavities have the ability to bind counter ions and upon binding initiate interchain interactions between other polymer chains with G-blocks

to form junction zones. These structures are often referred to as the egg-box model, that is the underlying feature of gel formation in alginate (Figure 2). (14)

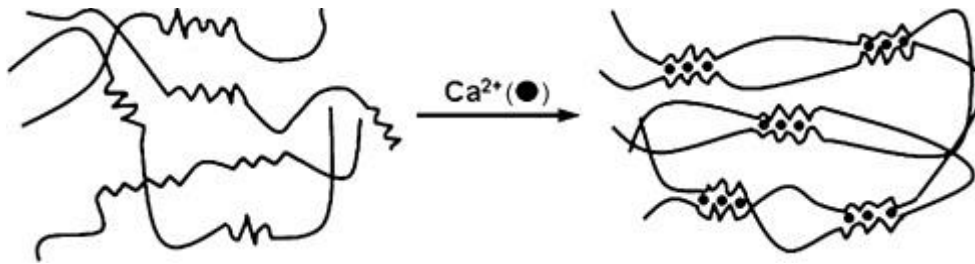


Figure 2. The egg-box model of alginate. Junction zones are formed when e.g. calcium ions are bound into G-blocks and form crosslinks. (Picture retrieved from an article by D.J. Mooney and K.Y. Lee (15))

1.2.2 Features and applications of alginate

Alginate has many qualities that make it a target of studies and research worldwide. From a biomedical point of view, its most interesting and beneficial features are biocompatibility and low toxicity combined with the ability to form structures with an ECM like textures. Many features of alginate-based hydrogels are favorable for purposes of tissue engineering, regenerative medicine and drug delivery. Alginate is also one of the most studied materials for cell encapsulation (12). In pharmaceutical applications alginate is used for administrating of both oral and injectable drugs and is used in products for controlled drug release. Due to its many beneficial features, alginate is a promising material for cell transplantation and culturing. Alginate-based hydrogels have been used both in 2D and 3D culturing but due to alginates inherent inability to promote cell adhesion, cell interaction promoting ligands should be incorporated into the alginate for these purposes. (15) One used approach is to couple cell adhesion promoting peptides into the alginate backbone (2).

The initial rate of diffusion of small molecules is fast in alginate-based hydrogels due to the nanoporous structure (pore size ~5 nm) that these gels often display. By alteration of the alginate used in these applications, it has been possible to increase the time of drug release. For example, the use of oxidized or partially oxidized alginate has led to more controlled release methods. The rate of release is also dependent on the chemical interactions between the drug and the alginate. Covalently bound molecules are released through chemical hydrolysis of cross-linker and ionically bound may be released only after the drug has dissociated from the carrier. Alginate-based hydrogels can also be used for different drugs simultaneously and are also proving to be a potential material for carrying protein-based drugs. (15)

Alginate beads have been used for encapsulation of insulin-producing pancreatic cells for the treatment of type 1 diabetes. This could provide an alternative method for treatment that would evade some of the problems and possible complications of current treatments such as fluctuations of glycemic index in blood. (12) For example, in some studies, xenografic cells have been encapsulated inside of alginate-based hydrogel beads. The use of the alginate beads was done to protect the implanted cells from immunoreactions of the host tissue without having to subject the patient to immunosuppressive drugs. (15)

1.3 Grafted alginates

Cells do not have receptors for binding to alginate and alginate-based hydrogels do not naturally promote cell adhesion due to a hydrophilic surface and low absorption of serum protein. This restricts the cells natural behavior and prevents cells from spreading and moving. This is particularly problematic for purposes of cell culturing and tissue engineering. Multiple different procedures have been developed to tackle this limitation. Many of these are based on the incorporation of different peptides into alginate backbone. (5) (16)

There are few different methods used for coupling of alginates and biologically active peptides. Customary this has been done by oxidizing alginate using carbodiimide chemistry in prior to peptide coupling, but this method has its limitations. If the oxidizing of alginate is done with periodate, the degree of coupled peptides will be higher than if done traditionally. Periodate oxidation induces a cleavage between the second and the third carbon in a ring of alginate monomer. This further increases the flexibility and degradability of the polymer. After oxidation with periodate, alginates are subjected to reductive amination before the actual coupling with peptides. (17)

In one approach alginate has been modified with a protein called laminin that is ECM protein found in the basement membrane. It is biologically active factor participating in e.g. cell adhesion, migration and neurite extension, but functions also as a structural component. Laminin protein has three chains A, B1 and B2. It binds to basement membrane proteins (e.g. collagen IV) and functions as a mediator to the basal lamina. IKVAV peptide is naturally part of the chain A of laminin and has five amino acids (isoleucine-lysine-valine-alanine-valine) in its sequence. It is an active region for cell adhesion and attachment (18). YIGSR (tyrosine-isoleucine-glycine-serine-arginine) peptide originating from a region of B1 chain of the laminin protein has been found to have an active role in cell attachment, migration and receptor binding. In many studies, YIGSR and IKVAV peptides among few other laminin related peptides have also been found to promote neurite outgrowth. (18) (19)

RGD (a peptide with arginine-glycine-aspartic acid included in the sequence) is a cell adhesion promoting peptide. It functions as a ligand for integrin receptors and since has been used extensively as model adhesion ligand. This peptide sequence is found in fibronectin in which it is the minimum essential component for promoting cell adhesion. RGD peptides are incorporated into alginate by chemical coupling. (20) (18) The tripeptide RGD functions as a cell attachment site for many adhesion promoting proteins (21).

Integrins are a vast group of cell adhesion receptors that are involved in multiple critical events like molecule anchoring, cell differentiation, and immune responses. Integrins are composed of two transmembrane subunits α and β , that are both found in various forms. Together these have found to compose over 20 different integrins with different specificities on the binding ligand. Depending on these subunits the receptor can bind different ECM proteins and many of these different integrins have found to bind to ECM proteins e.g. fibronectin, laminin or collagen that have these adhesive RGD sites. (21) (22)

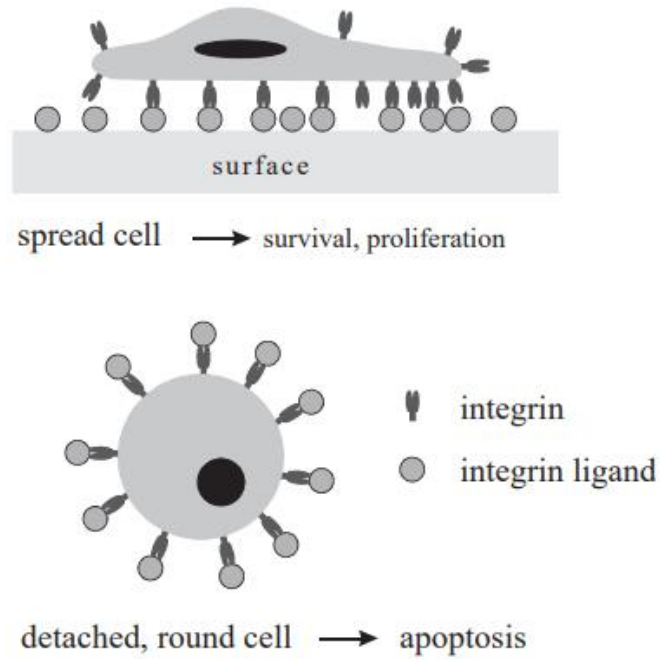


Figure 3. Cell fate dictated by attachment through integrin binding (21).

In order to promote cell adhesion, the RGD has to be coupled into the alginate backbone. If free RGD is introduced to cells it will bind to integrin receptors and prevent further cell attachment to any surface (Figure 3) (21). In a study by H.J. Kong et al. (2003) (23) RGD was found to support cell participation to gel formation and structure of alginate. The RGD in the modified alginate contributed to form a uniform dispersion of cells within the solution resulting in the crosslinked network by specific receptor-ligand binding, whereas cells in a solution of only unmodified alginate tended to form aggregates resulting in a less homogenous structure as a result of strong cell-cell interactions. (15)

1.4 Cells for encapsulation

Many different cell types are studied for purposes of tissue engineering. Approaches span from using stem cells to primary cell lines with different origins (autologous, heterologous, etc.). Use of cells as therapeutic agents, e.g. implantation of encapsulated hormone-producing cells, is also a great matter of interest and research towards utilizing different cell types is currently being studied. (6)

1.4.1 Fibroblasts

Fibroblasts are spindle-shaped cells that secrete collagenous proteins that make up the extracellular matrix (ECM) that provides mechanical strength for tissues. They belong to the family of connective tissue cells and many different types of fibroblasts are found from these tissues. Properties of the ECM in different tissues is determined by the composition of different the fibroblasts within the tissue. The base of connective tissue is the network formed by fibroblasts by connecting with each other and collagen fibrils. (24) The cells in connective tissue also participate in repair mechanisms and inflammatory responses (25).

As there is an important dependence of fibroblasts to the cell matrix, the fibroblasts are also dependent on each other and it is suggested that all fibroblasts are connected to each other and forming a network exceeding throughout the body. Indeed, the tendency of fibroblasts to connect can even be perceived in simple monolayered cell culture flask where fibroblasts connect through gap junctions visible under a microscope. In tissues, the fibroblasts have shown to form many kinds of cell-to-cell contacts. (26)

1.4.2 IMR90 and myofibroblasts

IMR90 was one of the cell lines used in experiments for this Thesis. IMR90 is a fibroblast line derived from human foetal lung of a 16-week-old fetus. It is a finite cell line with the reported capability of over 50 duplications before senescence (27). IMR90 cells are classified as myofibroblasts, fibroblasts that share similar features with differentiated smooth muscle cells. The IMR90 cells are similarly elongated (Figure 4) and regular as muscle cells and play a critical part in coordinated contraction. In comparison to other fibroblasts, IMR90 cells express much stronger efficiency of contraction. (28)

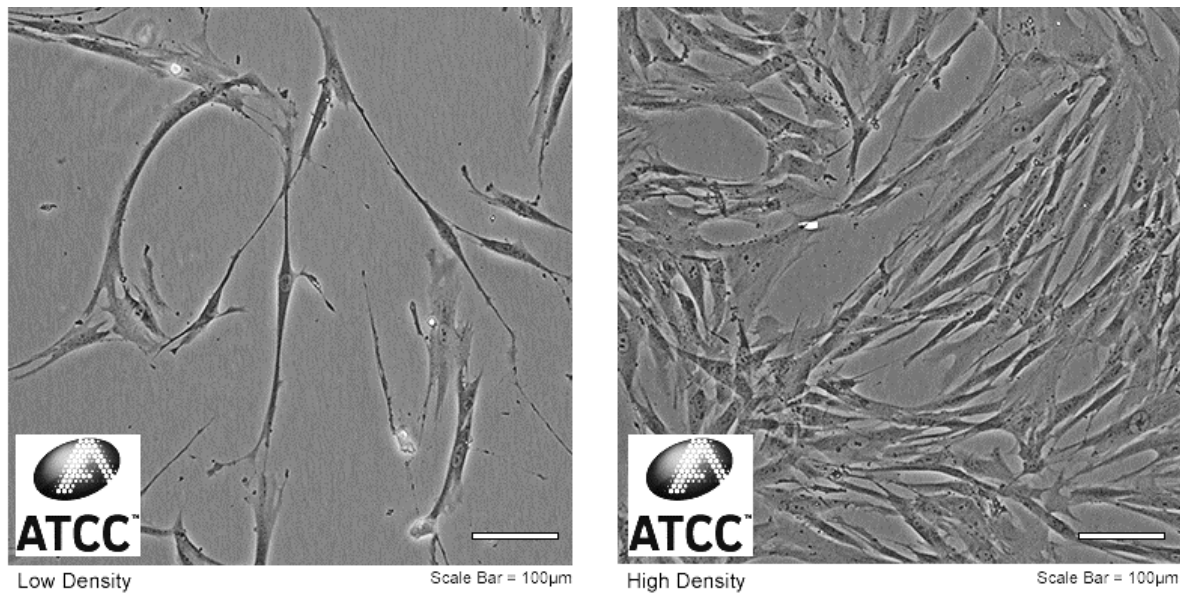


Figure 4. Morphology of IMR90 cells in monolayer cell culture with higher confluency on the right and lower confluency on the left. (Picture retrieved from ATCC website)

According to a study by Babiychuch et al. (1996) (28) metavinculin is a protein that is expressed by IMR90 but is not by other fibroblasts or smooth muscle cells. However, in later studies, metavinculin is stated to be found in great extent also in smooth muscle tissue. Metavinculin is a splice isoform of vinculin and they both are scaffold proteins mediating cell adhesion. Although the function of vinculin is rather well known, the full purpose of metavinculin is still somewhat unclear. It is currently believed to play part in mechanotransduction reactions, a process where mechanical stress experienced by sensor cell is converted into a signal in the multistep chain of events inducing a response in effector cells. (29) (30)

Myofibroblasts have a special role in the process of wound healing and scarring. Myofibroblasts are also the responsible factor of fibrosis that can affect decreasingly on the function of a healing organ. This is a problematic feature and in the western world scarring and fibrosis together has been estimated to be accountable for close to 50% of all chronic diseases. Because of this myofibroblasts are considered as important targets of therapeutic agents. (31)

Fibroblasts in connective tissue reside in collagenous ECM and experience relatively little external mechanical stress. Only after injury, these cells undergo a transformation that has an effect on the cells and their surrounding ECM. In the aftermath of an injury, the fibroblasts may transform first into a protomyofibroblast and then into differentiated myofibroblast. The assortment of proteins secreted by myofibroblasts include of e.g. increased amounts of type 1 and type 3 collagen, contractile proteins, growth factors, certain types of fibronectin and proteins regulating cell fate and cell cycle. The general composition of ECM changes from the collagen-rich environment into being principally fibronectin and fibrin-based. (31)

1.4.3 Hepatocytes

Hepatocytes are cells found in the liver where they are the primary factors performing the vital functions of the liver. There are multiple different hepatocytes which all have specialized to perform different roles in important mechanisms like detoxication and energy metabolism. (32)

The liver epithelia is distinct from other epithelial structures in the body. Different epithelial tissues confine networks for the circulation of bile and blood flow inside the liver. In these, the hepatocytes are polarized both structurally and functionally. Tight junctions are formed between hepatocytes in order to sustain a blood-bile barrier, whereas desmosomes, gap junctions and intermediate junctions are formed to maintain cell-cell connections and cohesive strength. (32)

Demand on engineered liver tissues to replace troublesome and potentially dangerous liver transplantations is undoubtedly a matter of great interest. Different approaches to develop platforms for hepatocyte culturing have tried to overcome the impediments of the others but the task has been found to be challenging and e.g. in some studies primary hepatocytes have proven to lose their viability and desired liver-specific features after isolation. (33)

1.4.4 HepG2

HepG2 cells are adherent epithelial cells derived from human liver. HepG2 is a cancerous cell line originating from hepatoblastoma or from hepatocarcinoma according to some references. HepG2 is widely used in research and studies of liver metabolism, liver toxicity, and oncogenesis (34). Despite being hepatoblastoma line, HepG2 shares many same characteristics as normal hepatocytes in the liver. HepG2 synthesizes serum proteins and exhibits changes in its growth rate and metabolism in vitro cultures as it would do in vivo. The doubling time of HepG2 increases as the number of cells in culture increases. (35) When cultured in monolayer HepG2 tends to form distinct clusters as cell number in the culture increases (Figure 5).

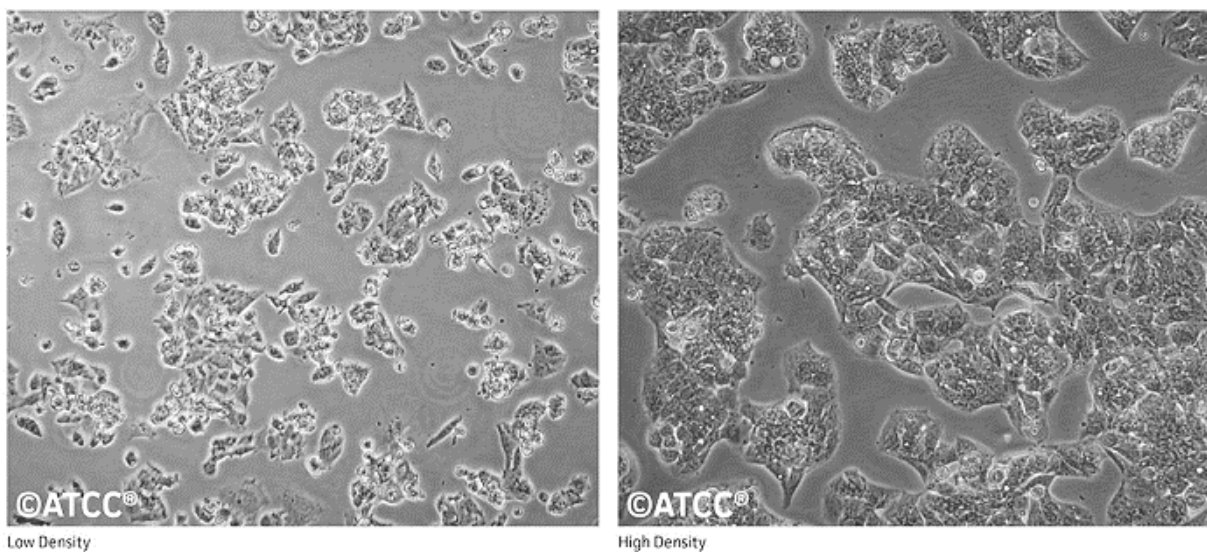


Figure 5. Morphology of HepG2 cells in monolayer cell culture with higher confluency on the right and lower confluency on the left (Picture retrieved from ATCC website)

2 Materials and Methods

2.1 Alginate solutions

Alginate gels were made from solutions containing dissolved alginate and buffer. The gel formation was initiated by the addition of a gelling agent. Alginate solutions used in these experiments contained 1,0 % and 2,0 % of alginate to make gels with 0,5% and 1% alginate as a final concentration. In the last experiment gels with 2% alginate content were used and for these solutions with 4% alginate were prepared.

To prepare the solutions the needed amount of alginate was weighed and added into HEPES buffer in a constant stirring in room temperature. Most common volume prepared was 10 ml with 0,1 g of UP-LVG for 1 % solution and 0,2 g UP-LVG for 2 % solution each dissolved in 10 g of HEPES-buffer. The concentration of HEPES used was the same as for cell-suspension in each experiment. Only in the second experiment where 25 mM HEPES was used for cell suspension, 10 mM HEPES was used for the alginate solution. The mixture was stirred for a minimum of three hours covered with parafilm to avoid evaporation. After mixing the solution was visually examined to assure that the alginate had properly dissolved. Solutions were then filtered with Thermo Scientific™ Nalgene Rapid-Flow filter with a pore size of 0,2 µm and stored in a fridge (+4 °C). Gels with 1 % alginate were used as bottom gels in the gel 'sandwich' method. Gels with different alginate contents were used for encapsulation of cells as 'top-gel' for the 'sandwich'.

The alginate used in the experiments was PRONOVA™ UP-LVG (Mw: 75-200), ultrapure sodium alginate with low viscosity (20-200 mPas) and a minimum of 60% guluronate content from NovaMatrix. Effects of peptide-modified alginates were studied in further experiments. In these, four grafted alginates were used together with PRONOVA™ UP-LVG alginate combined with these modified alginates and as a parallel.

2.1.1 Grafted alginates

In the fourth experiment alginates with different modifications were introduced into the experimental set up to study the effects of oxidization and cell adhesion promoting peptides coupled into the alginate has on cell survival. In experiments following the fourth, some of these modified alginates were further used. The alginates with peptide modifications used in the experiments described in this thesis had been oxidized prior to peptide coupling. The grafted alginates had been prepared in the study group at NTNU.

The peptide modified alginates had been grafted in the study group at NTNU. All alginates with inserted peptides had been oxidized with periodate and then exposed to reductive amination in prior to peptide coupling. The different alginates used in this experiment were oxidized UP-LVG with the degree of oxidation being 8%, UP-LVG coupled with IKVAV-peptide with 11% of the degree of substitution, UP-LVG coupled with YIGSR-peptide with 9% substitution and UP-LVG with coupled GRGDSP-peptide with 5% degree of substitution. The degree of substitution stands for moles of coupled peptide per one mole of alginate monomer. (17) The GRGDSP-peptide coupled alginate is referred to as RGD-modified alginate in further in the text because the RGD-sequence is the functional part of this peptide.

The grafted alginate solutions used in the on-top cultivation experiment had a ratio of 1:1 of the grafted alginate and the PRONOVA™ UP-LVG. For the preparation of the solutions, the grafted alginates were weighed in separate tubes to make 1 ml of each solution with 2% alginate. 25 mM HEPES-buffer was added, and the tubes were then left to stir in a table mixer in 20°C at 700 rpm for 2 hours. The solutions were stored at +4 °C overnight. The next day solutions were sterile filtered with 0,2 µm polyether-sulfone syringe filter by VWR. 2% PRONOVA™ UP-LVG alginate solution was prepared in prior to use as for previous experiments.

The working solutions were made by mixing each grafted alginate solution with 2% PRONOVA™ UP-LVG solution with a 1:1 ratio of the grafted alginate solution in a 5 ml tube. These were then mixed in table mixer minimum for 1 hour up to several hours depending on the visually observed viscosity of the solution mix. Solutions were stored in a fridge (+4 °C) and used within 24 hours. Alginate solutions with grafted alginates used in later experiments with different ratios of the modified and unmodified alginates were done in a similar way. The specific ratios are stated in the Results -section for each experiment separately.

2.2 the HEPES buffer

HEPES is a widely used buffer with pKa value in a 6-8 range. HEPES can be used to increase the buffering capacity of the media in cell suspension during the processing of cells outside a CO₂-controlled incubator. Citrate-HEPES buffer was used as a component in alginate- and CaCO₃-solutions and in cell suspensions in all the experiments. In the first experiment, the concentration of HEPES in the buffer was 10 mM for all gel conditions. In the second experiment, the 25 mM concentration of the HEPES buffer was introduced and the effect of increased concentration of the buffer on cells was compared to the initial 10 mM HEPES.

The formula of Citrate-HEPES buffer see Appendix A.

2.3 Cells in the experiments

In the experiments two cell lines IMR90 and HepG2 were utilized. Both cell lines were cultivated in surface treated cell culture flasks that promote cell attachment and growth in prior to encapsulations. For this cell culturing two flask sizes were used, T75 (75 cm²) for normal maintenance of the lines and T175 (175 cm²) for up-scaling before experiments. Growth media used for IMR90 line was DMEM (D5546) with 10% FBS, 1% l-glutamine, 1% Pen-Strep (100 U/ml), 1% NEAA and 0,1 mM SP. The growth media used in culturing HepG2 was RPMI with 10% FBS, 1% l-glutamine and 1% Pen-Strep (100 U/ml). Cells were cultured in an incubator at 37 °C with 5% CO₂ and 95% air in complete humidity. More information on cell culture mediums listed in Appendix B.

2.3.1 Cell suspension for gelling experiments

In a preparation for encapsulation experiment cell suspension was prepared. Cells cultured in T175 flasks were detached with trypsin (TrypLE™ Express (12605-010) by Gibco) and suspended into a corresponding medium. At this point HepG2 cells were filtered with 40 µm nylon cell strainer (by Corning) to remove any big cell clusters. The suspension was then centrifuged and the media was then discarded. To wash out the remaining media cells were resuspended into PBS and then again centrifuged. After centrifugation, PBS was removed and cells were resuspended into HEPES buffer and set aside to wait for the encapsulation step. In prior to this, CaCO₃ solution was mixed in cell-buffer suspension. For the experiments, the wanted number of cells was 50 000 per well (approx. $7,7 \times 10^5$ cells/ml) and the cell-buffer suspension used in each experiment were prepared in a manner to achieve this. For experiments where cells were cultivated on top of the gels, the cells were suspended in growth medium after washing with PBS.

The number of cells was determined before the washing with PBS. A 1 ml sample was collected from the cell suspension for cell count procedure after trypsinization and re-suspension into fresh media. If more than one cell culturing flask were needed all cells were suspended into the same suspension before the number of cells was determined.

2.3.2 Cold treatment of cells

In part of the experiments, the cells were prepared and encapsulated in very low temperatures (+4 °C). This was done to bring the cells into a hibernating state where cells would be less vulnerable to stress caused by changes in pH and mechanical forces due to pipetting and shaking of the plate during the encapsulation process.

If cell suspension was prepared for 'cold treatment' experiment the preparation of the suspension was done as normally to the point of washing with PBS after centrifugation. After this, the cells were resuspended into cold HEPES buffer (+4 °C) and then stored on ice until used in the encapsulation experiment. The total length of time the cells were kept in hypothermic conditions was approximately 1h in each experiment where the cold-treatment was used. After this, the encapsulated cells were either left to gradually warm to room temperature (2h gelling of alginate-based gels) before moving into an incubator to +37 °C or were directly transported into there (Matrigel-based gels).

2.3.3 Cell number

The number of cells for the suspension was determined by using a Trypan Blue assay and an automated cell counter (Countess™ II by Life technologies). The cell counter was programmed for counting cell lines with different morphologies and specific programs for HepG2 and IMR90 were used. Samples were prepared by mixing 10 µl of well-mixed cell suspension and 10 µl of Trypan Blue (by Life Technologies) in an Eppendorf tube. 10 µl of the sample was then transferred into a cell count chamber and inserted into the counter. Cell counter reported the number of cells in one milliliter and the percentage of dead cells. Three to four replicas were prepared from each suspension. Average of the samples was then calculated. The volume of HEPES buffer was determined from the total number of cells considering the wanted final number of cells (50 000/well) and the number of wells to be prepared.

2.4 Gel preparation

Gels used for the cell encapsulation were prepared aseptically in order to avoid possible contaminations from the environment or from equipment. The preparations were done in laminar flow hood whenever possible and but e.g. during shaking, incubation and imaging, the gels had to be protected by covering them with a lid. The needed equipment, tools and materials were autoclaved or disinfected with 80% ethanol beforehand. Alginate solutions were sterile filtered before use with a suitable filter.

2.4.1 Gel formation – Role of CaCO₃ and GDL

In experiments, Glucono- δ -lactone (C₆H₁₀O₆, GDL) from SigmaAldrich (G4750, MW:178,14 g/mol) was used. The CaCO₃ used was ViCALity ALBAFIL Precipitated Calcium Carbonate with a particle size of 0,7 μ m from Specialty Minerals Inc.

Gelling of alginate with Ca²⁺ will happen instantaneously and the gels can obtain inhomogeneous structure due to the rapid gelling event. This is not always an optimal feature and gradual gelling of the alginate was a more practical approach for these experiments. The calcium ions must be distributed evenly into the alginate solution before the gelling reaction is allowed to happen to achieve homogenous gelling. When insoluble CaCO₃ is mixed with alginate solution the Ca²⁺ ions are not released, and gelling will not be initiated. When GDL is then added to alginate solution with the CaCO₃, it induces hydrolysis reaction causing the release of Ca²⁺ ions into the solution leading to gradual gel formation. The rate of the gelling can be controlled with the particle size of the CaCO₃ where smaller particles release Ca²⁺ ions faster than bigger particles due to their relatively larger surface resulting in faster gelation.

CaCO₃ suspensions were prepared separately for each experiment. Amount of CaCO₃ was weighed according to the desired final concentration into 5 ml Eppendorf tube. Before use, 2 ml of IF-water was pipetted on the CaCO₃. The mixture was then suspended thoroughly and 500 μ l of it was transferred into 10 ml beaker. 2250 μ l of HEPES buffer was then added on the CaCO₃ suspension in the beaker. The suspension was kept on constant stirring during use to prevent CaCO₃ from sedimentation. GDL solutions too were prepared separately for each experiment. The needed amounts were weighed into 5 ml Eppendorf tubes and left to wait until the procedures prior to GDL addition had been completed. After these 2 ml of IF-water was added in the Eppendorf tube and the tube was vortexed until GDL had dissolved. The solution was then pipetted in the wells with the alginate-CaCO₃ solution.

Gels with 1,0 % alginate had a final concentration of 18 mM of CaCO₃ and 36 mM of GDL. Gels with 0,5 % alginate had a final concentration of 15 mM of CaCO₃ and 30 mM of GDL. In experiment 7 where gels with 2,0 % alginate content were studied the concentration of CaCO₃ and GDL were the same as for 1,0 % gels. In this experiment gels with different cell concentrations were prepared and studied. Same cell suspensions with the certain cell concentrations were used for gels despite the total amount of alginate.

2.4.2 Preparation of gels used for cell encapsulation

Gels used in cell encapsulation and cultivation had a two-layered structure as shown in Figure 6. To prepare this structure the gels were prepared in a two-step process. The cells were encapsulated inside the top gel and the bottom gel served as an insulating layer to prevent the cell attachment to the bottom of the well plate since the survival of the cells inside the gel matrix was the interest in these experiments. The gel 'sandwich' was prepared in such a way that gel layers formed evenly, and they did not mix with each other. Media was added on the gels with encapsulated cells 2 hours after from initiating the gelling event to ensure that the gels had formed properly.

The 1% bottom gels were made by pipetting 32,6 μl of 2% UP-LVG alginate solution on 96-well plates followed by 27,6 μl of 195 mM CaCO_3 suspension prepared in HEPES-buffer. The plates were then shaken at 2000 RPM for 30 s to mix these two solutions thoroughly. GDL solution was prepared only after the plates with pipetted alginate and CaCO_3 solution had been shaken. 2 ml of sterilized water was added on 139 mg of GDL and the mixture was mixed with vortex until the GDL had completely dissolved. 5 μl of the solution was then pipetted on each well of the 96-plate with the alginate- CaCO_3 -solution and the plate was again shaken at 2000 RPM for 30 s. If there were more than one plate the GDL was not added before the previous one had been finished with the shaking step. GDL solution was always prepared just before use. The plates were then left to gel overnight minimum. If the casting of the top gels were to be done the next day the bottom gels were left to gel in room temperature to assure the gel formation was complete before continuing. If the time between the two casting steps was longer (e.g. over a weekend) the bottom gels were stored in a fridge (+4 $^{\circ}\text{C}$) to prevent extent water evaporation and to minimize the risk of microbial growth.

For the top gels, 32,6 μl of alginate solution was pipetted on the bottom gels followed by 27,6 μl CaCO_3 solution containing the cells. The plate was then shaken in a plate shaker at 2000 RPM for 30 s. GDL was added in a similar step as for the bottom gels. After GDL addition and the second mixing step, the plates were left to gel in room temperature for two hours before 37 $^{\circ}\text{C}$ medium was added in the wells. After the media addition, the plates were transferred into an incubator at 37 $^{\circ}\text{C}$ with 5 % of CO_2 . Different alginate concentrations for top-gels were used in the course of this study, the final alginate concentrations in gels are stated in the Results section for each experiment separately. The sandwich method was applied to all experiments where the cells were encapsulated inside of gels to avoid cell attachment to the well surface because cells had been detected to do so in experiments conducted earlier for this project.

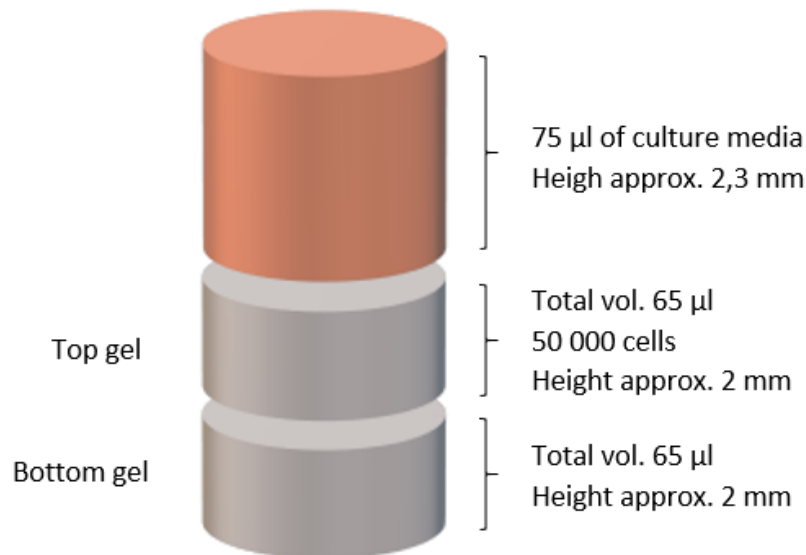


Figure 6. Illustration of the two-layered structure of a gel in one well of 96-well plate.

The approximated height of one gel layer is 2 mm. The height of the sandwich structure is approx.4 mm. The diameter of a gel is approx. 6,4 mm and the surface area of one well in 96-well plate is 0,32 cm². In all experiments, black BRAND 96 Well pureGrade™ microplates with a transparent flat bottom and untreated surface were used. The plates were pre-sterilized and individually packed with a transparent lid.

2.4.3 Preparation of gels for on-top cell cultivation

The process of gel preparation was different for Experiment 4, where the gels were used for cell cultivation on top of the gels instead of encapsulating them inside the gel. For this experiment grafted alginates were also used. The gel preparation process for on top cell cultivation was similar to the preparation of bottom gels. First 32,6 µl of 2% alginate solution was pipetted on 96-well plates followed by 27,6 µl of 195 mM CaCO₃ suspension. After this, plates were shaken for 30 s at 2000 RPM for thorough mixing. GDL solution (5 µl) was added after the first mixing and plate was again mixed for 30 s at 2000 RPM. Plates were then left to gel for two hours at room temperature. After gelling 75 µl of cell suspension prepared into growth media with 6.67E+05 cells/ml was added on top of the gels. Plates were then transformed into an incubator at 37 °C with 5 % of CO₂.

2.4.4 Washing of gels

Washing of gels was performed on gels with encapsulated cells 2 h after initiation of the gelling event. 150 µl of cell culture media was added on the gels and incubated for 30 min in an incubator (+37 °C and 5% CO₂). After the 30 min, the media was discarded and replaced. If more than one washing step was performed another 150 µl of cell culture media was added. At the end of the washing procedure, a volume of 75 µl of fresh cell culture media was added on the gels. Cell culture media specific for each cell line was used for wash procedures at all times.

2.5 Corning® Matrigel®

Corning™ Matrigel™ Matrix Phenol Red Free (REF 356237, lot. 8050007) with a concentration of 10,7 mg/ml was used in experiments for this Thesis. The original vial of Matrigel had been pre-divided into smaller volumes to avoid multiple freezing-thawing steps of the material. This matrix solution is recommended for fluorescence-based assays. Gels made from Matrigel are initially transparent and colorless.

2.5.1 Cell cultivation on top of Matrigel matrix

For cultivation of cells on top of the Matrigel matrix, 1 ml of Matrigel was thawed overnight on ice inside a cold room (+4 °C). 800 µl of Matrigel-solution was diluted with 56 µl PBS and mixed by pipetting in order to dilute the Matrigel into 10,0 mg/ml concentration. Gels with a volume of 65 µl were prepared for the cultivation of IMR90 and HepG2 cells. The gels were left to form for at least 1 h in RT before the cell-media suspension was added on the gels.

2.5.2 Cell encapsulation into low concentration Matrigel

For encapsulation of cells, the Matrigel matrix was diluted to a concentration of 7 mg/ml with PBS and 48,5 µl of this diluted Matrigel was then pipetted into 96-well plate. 16,5 µl of cell suspension with 3.01E+6 cells/ml suspended in culture medium was added in the wells with Matrigel and then mixed 2000 rpm for 30 s. The final number of cells in one well was approx. 50 000. Plates were then transferred to an incubator (37 °C, 5% CO₂) for 1 hour before 75 µl of cell culture media was added on the gels. After media addition, the incubation was continued under the same conditions. The final concentration of Matrigel was approx. 5 mg/ml.

Matrigel is in liquid phase between 0-10 °C and the gelling is initiated by an increase in temperature. When used for encapsulation of cells the cell suspension had to be tempered to +4 °C to prevent premature gelling of the matrix. For this, cells were suspended into cell culture media which was then chilled and kept on ice prior to use.

2.5.3 Cell encapsulation into high concentration Matrigel

For this experiment Matrigel in a concentration of 10 mg/ml was needed. Again, the Matrigel stock solution of 10,7 mg/ml was used. The cells were prepared into a cell-media suspension as for previous experiments with Matrigel. The number of cells in the suspension was determined and the total number of cells needed for all gels to be prepared was separated into a tube. The separated amount of the cell suspension was then centrifuged, and the supernatant was carefully discarded. Hence the concentration of Matrigel stock solution was 0,7 mg/ml higher as intended, the cell pellet was suspended in a small amount of PBS. The needed volume of Matrigel to obtain the 10 mg/ml concentration was then added into the cell-PBS suspension and the solution was then mixed by pipetting up and down. After mixing the cell-Matrigel suspension was pipetted in wells of 96 well plate with 65 µl for each gel. The plate was then transferred into the incubator at 37 °C and 5% CO₂. 75 µl of cell culture media was added on the gels after a minimum of 1 h of gelling.

2.6 Viability assessment

Viability and survival of the encapsulated cells were assessed for over time periods between 5 to 10 days. Depending on the experiment, the viability was examined daily, every other day or less frequently. Regardless of the general frequency of the viability assessment, the viability was determined in the day of the encapsulation, again after approximately 24 hours and on the second day from the encapsulation procedure in all experiments. On the day of the encapsulation (Day 0), the LIVE/DEAD (L/D) assay was performed approximately one hour from the addition of the growth medium on the gels. Two to four replicas were prepared for each condition for each time point. All of them were examined and imaged.

For assessment of the viability, the alginate gels with encapsulated cells were analyzed with LIVE/DEAD® Viability/Cytotoxicity Kit for mammalian cells by Molecular Probes™. The assay is a two-color fluorescence viability assay based on two dyes, calcein AM and ethidium homodimer (EthD-1) that enable detection of live and dead cells simultaneously. Calcein AM is converted into fluorescent calcein by intracellular esterase activity that then produces uniform green-colored fluorescence when it enters into a living cell. The other stain EthD-1 causes dead and dying cells to fluorescence in red by crossing through the damaged cell membrane and binding to the nucleus. The binding to the nucleic acids causes the EthD-1 to increase fluorescence intensity. EthD-1 cannot bind through an intact plasma membrane. (LIVE/DEAD® Viability/Cytotoxicity Kit protocol (36)) This method is a qualitative way to assess the viability of the cells and the overall survival. No quantitative analysis of the cell numbers were performed.

The staining solution was prepared in 5 ml of 1×DPBS (D1283 by SigmaAldrich) with 10 µl of EthD-1 and 2,5 µl calcein AM. The assay was carried out by adding 75 µl of the staining solution on each gel sample in the 96-well plates. The cell growth media on top of the gels (75 µl) was not removed before addition of the staining solution. The plates were incubated minimum of 45 min in room temperature and then imaged under a microscope. Because the staining chemicals are toxic to cells in long term exposure new gel samples were stained and examined for each separate assessment point.

Two cells lines with different origin and morphology were used in the experiments. Because in some cases the strength of the detected fluorescent signal from L/D staining of cells was found to differ in a significant amount between the two cells lines in gels of the same age, the intensity and effect of L/D staining was tested on cells without the gel matrix. Cells were suspended into cell culture media (+37 °C) and pipetted on 96-well plate with approx. 50 000 cells/well and the L/D staining solution was added soon after. The plate was then incubated in RT for 45 min and then imaged. From Figure 7 can be seen that there are no significant differences between fluorescent signals between cell the lines. For HepG2 the GFP signal might be considered to be slightly higher, but the difference could be also due to clustering of the HepG2 cells and not due to the effectivity of staining. It was also found that in many cases as the age of the gels prolonged the less visible fluorescence the calcein stain produced. The change appeared somewhat gradually after the first days and caused the live cells to seem vague and hard to detect on the microscope imaging. This was compensated on the later experiments by increasing the volume of the calcein AM to 2,5-fold from the initial volume.

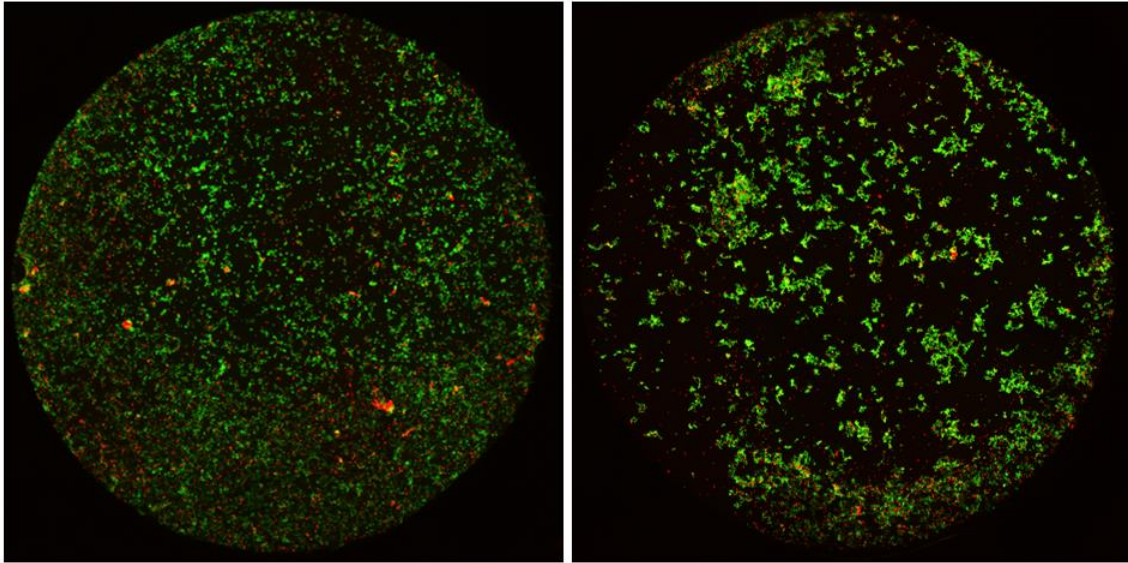


Figure 7. L/D imaging of IMR90 (left) and HepG2 (right) cells without matrix. The diameter of the gels is approx. 6,4 mm.

2.6.1 Imaging of gels with a light microscope

EVOS™ FL Auto Imaging System (AMAFD1000) microscope was used for imaging of gels with 4× and 10× objectives and the announced working distance of the condenser was 60 mm. The wavelengths for the 'light cubes' used were Ex 530 nm/Em 593 nm for RFP and Ex 470 nm/Em 525 nm for GFP. The microscope had settings for imaging 96-well plates with motorized X/Y scanning system. (37) Imaging covering the whole area of the well was used first in Experiment 3 (e.g. Figure 13 and Figure 14). The focus plane and light were adjusted manually in a similar manner as in normal imaging procedure. A 12-picture grid (4x3) was used in every full well surface covering image presented in here. The final picture was composed automatically by the imaging software.

In some of the pictures dark and circular spaces are visible as seen on the right in Figure 8. In a phase image of the same area (Figure 8 on the left) it can be seen that these are pockets of air entrapped inside the gel. These caused distortions in the focus in imaging on the sides of the air bubbles and in L/D images appeared as an inexplicable empty space.

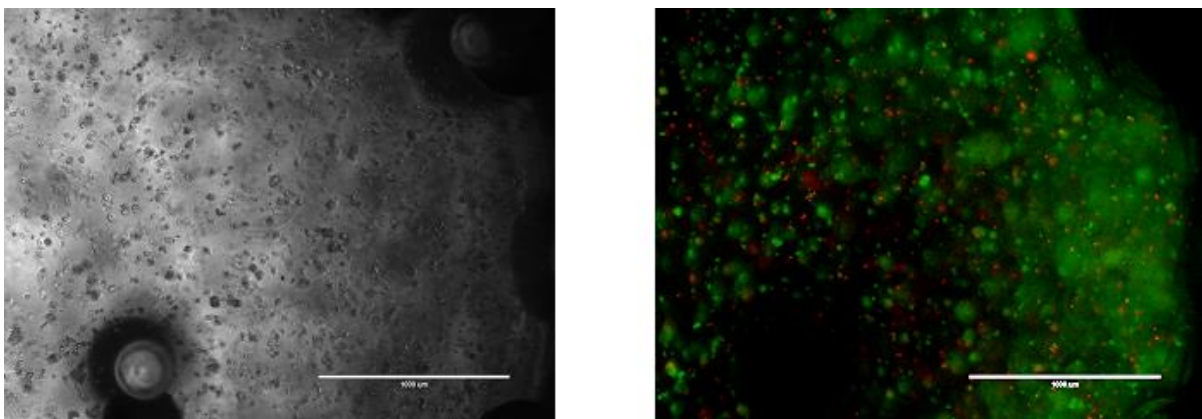


Figure 8. Air bubbles inside alginate gels visible in phase picture (original color and brightness) but not in L/D picture in a gel with encapsulated HepG2 cells. The scale is 1000 µm.

2.6.2 Imaging of gels with CLSM

In the last experiment, gels were imaged by using a confocal laser scanning microscopy (CLSM) in order to obtain three-dimensional schemes of the gel-matrixes to evaluate the distribution, morphology and number of cells in multiple layers simultaneously. The gels were stained by using the same L/D assay as in all other experiments. After addition of the L/D staining solution, the gels were incubated for 1 h in RT. For imaging with CLSM, the gels had to be removed from the 96-well plate and transferred into glass bottom petri dishes suitable for imaging with CLSM. The transfer was done by using a narrow spatula, the gels were dug out of the well. This was done inside a laminar flow hood with extra caution to avoid breaking the fragile gel-pellets. After removing the gels from the wells, they were no longer kept under cell culture media or staining solution and were kept in normal atmospheric conditions and not in an incubator.

Imaging was done by using an inverted confocal laser scanning microscope Zeiss LSM800 (Carl Zeiss) with motorized XY-stage. For imaging of cells in gels the C-apochromat 10x water-immersion objective (numerical aperture of 0.45, the working distance of 1.8 mm) was used. Excitation and emission maximum (Ex/Em) for L/D assay dyes used in the imaging were 494/517 nm for calcein and 528/617 nm for Ethd-1. The calcein was excited with 488 nm laser and emission was detected with 450-550 nm AiryScan detector at 514 nm. The EthD-1 was excited with 561 nm laser and emission was detected with 400-700 nm GaAsP detector at 617 nm. Imaging of the fluorophores was done in a two-step process where the z-stack was first obtained for Ethd-1 and then for calcein. All z-stacks images were edited for color balance (brightness and contrast) using ZEN 2.3 (blue edition) software.

3 Results

For this thesis, a series of experiments were done in order to find critical variables, estimate the effect of different parameters and compare differences in cell survival and behavior of different cell lines within different hydrogel matrixes. The use of alginate-based gel matrixes for cell encapsulation is also compared to a commercially available cell matrix material. In the experiments two different cell lines, IMR90 and HepG2 were used. IMR90 is a line of fibroblasts from human lung and HepG2 is a cancerous line of human liver cells.

In the Results section the experiments conducted within this thesis are presented in the order they were carried out, except the experiments with Matrigel that are presented in a separate section. All experiments with alginate-based hydrogels conducted within this thesis are also listed in Appendix C. with their corresponding experiment number, aim and all sample conditions.

3.1 Survival of gel encapsulated IMR90 and HepG2 cells

In the first experiment, the behavior and differences between the two cell lines were the main interest of the experiment conducted within a relatively short follow-up period and only one gel condition. Also, the effect of washing of the gel with cell culture media was compared to a no-wash treatment. The viability of the encapsulated cells was assessed daily over a five-day period including the encapsulation day. The cell culture media was not changed in the first experiment during the follow-up period. The washing was done with 150 μ l of cell culture media including 10% FBS over a duration of 30 min.

The pictures of L/D assay obtained with a light microscope for IMR90 are represented in Figure 9. On the pictures taken on the day of the encapsulation (Day 0), the amount of light had to be increased to detect any live cells. As a result, the amount of background signal of the green fluorescent has also increased and caused a green-colored blur in the background of the pictures.

From the same Figure 9, it can be seen that the number of dead cells was highest on Day 2 and especially high in the 'no wash' -sample. However, there are fewer dead cells visible in further samples. This could be explained by individual differences between the samples on different days or that the dead cells have fully degraded after the Day 2 and thus did not cause a detectable signal in the later viability assessments. Although this might have resulted in an increase in the background signal. A decrease in the total number of cells witnessed after Day 2 could support this. The number of live cells was higher in the wash-treatment group on the last assessment point on Day 4. This could suggest that washing of the gels after cell encapsulation could increase the survival rate of the cells for IMR90.

Viability and survival of encapsulated HepG2 cells were followed in a similar manner. The results of the L/D assaying from the five-day follow-up are represented in Figure 10. The viability of HepG2 did not seem to decrease as significantly as it did for IMR90 during a similar period. The relatively small differences between the two treatment groups could be explained by possible differences in the samples, e.g. differences in cell distribution or in imaging where one image represents just one part of the whole well. It appears that the washing of the gels after encapsulation did not have a markable effect on the survival of HepG2 cells.

IMR90

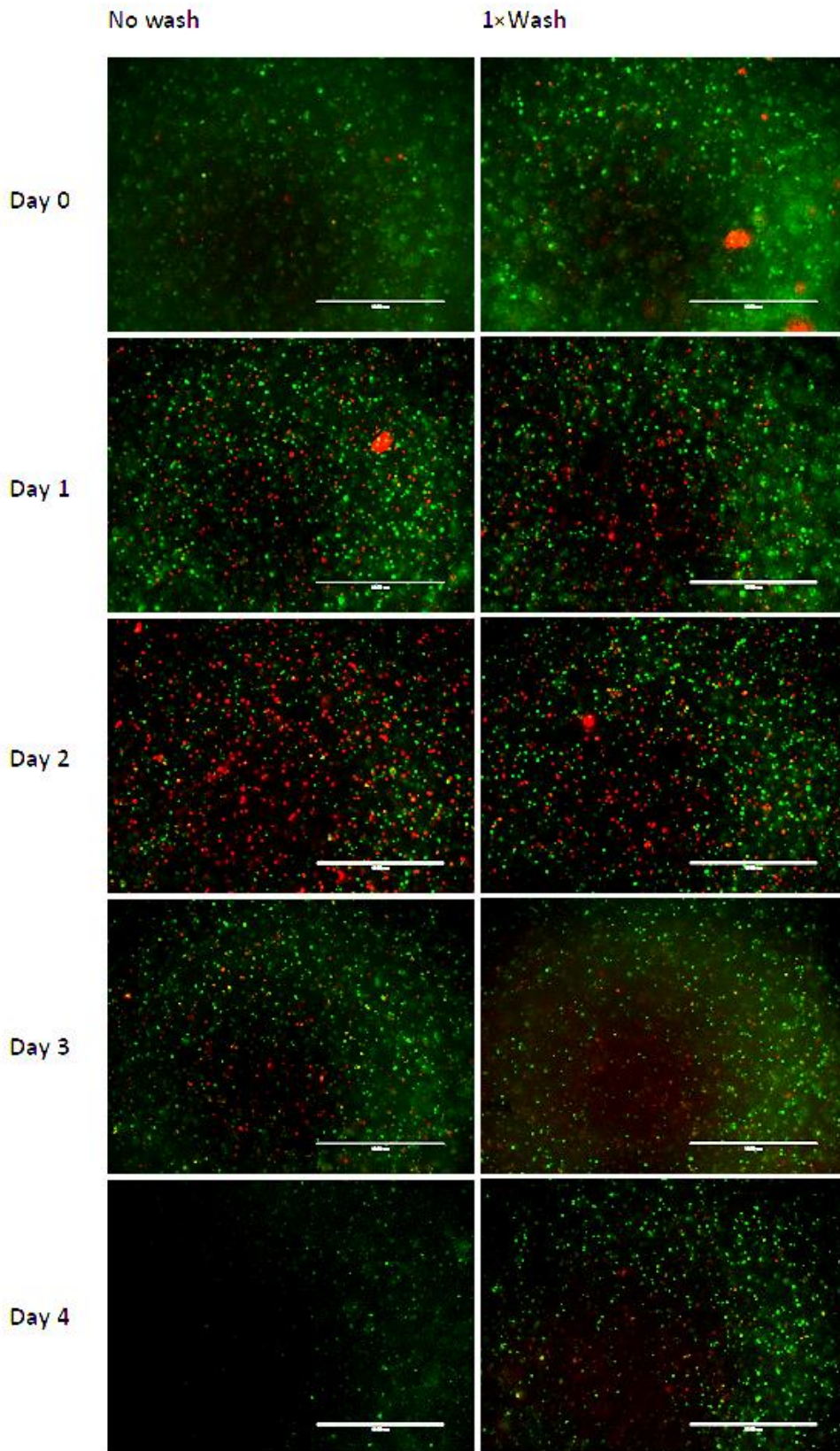


Figure 9. Live/dead imaging of encapsulated IMR90 cells. The scale in the images is 1000 μm . The color saturation increased in the image.

HepG2

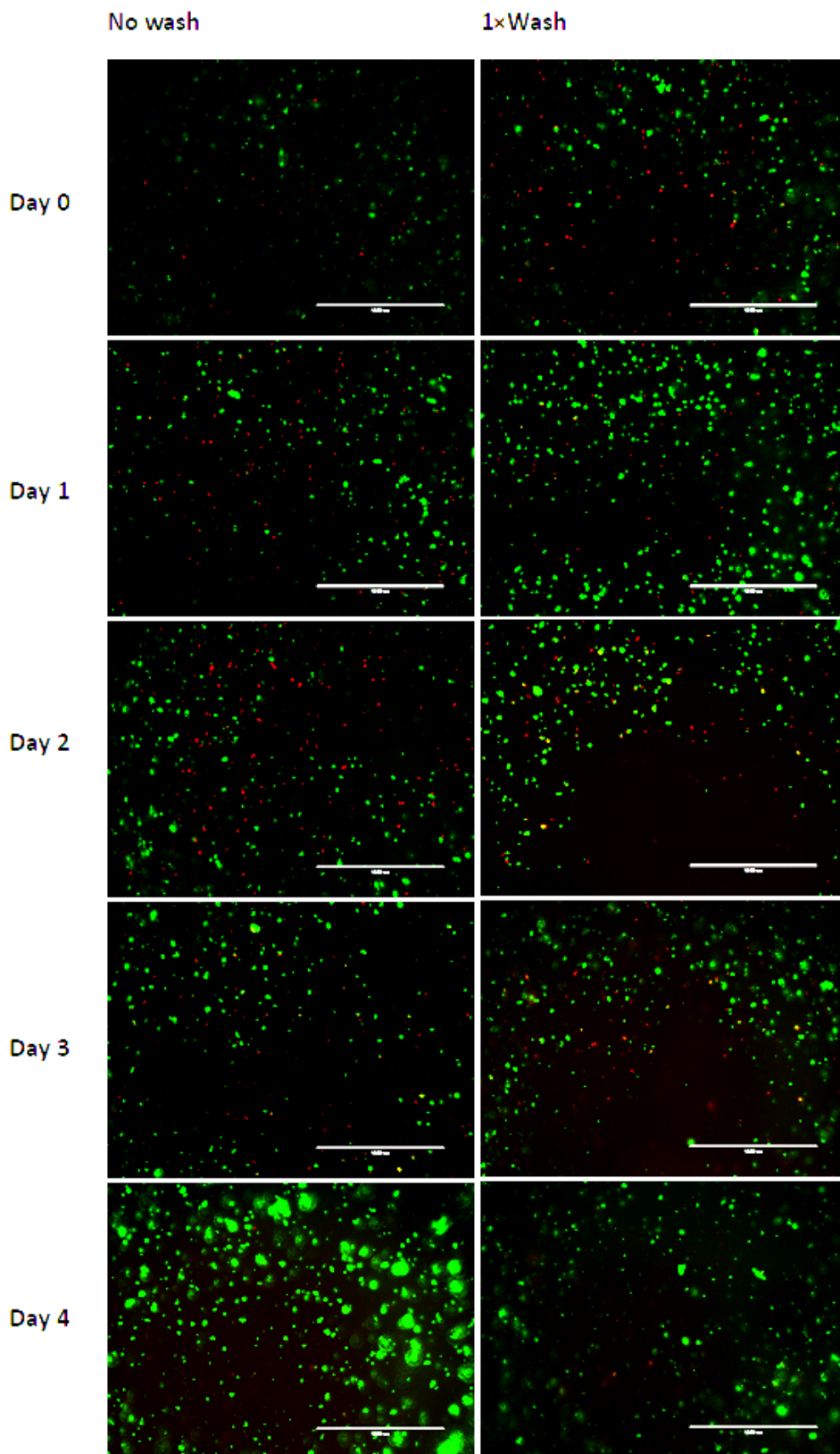


Figure 10. Live/dead imaging of encapsulated HepG2 cells. The scale in the images is 1000 μm . The color saturation increased in the image.

3.2 Comparison of different gel conditions

In the second experiment, the effect of different gel conditions on cell survival was studied. The different treatments in this experiment were increasing of the number of washes after the encapsulation procedure and changing of the 10 mM HEPES-buffer to 25 mM HEPES-buffer. The washes were increased from 1×150 µl of cell culture media to 2×150 µl in 30 min interval. Conditions similar as in the first experiment were used as a control. The period of viability follow-up was prolonged from the 5 days in the first experiment, to 8 days for gels with IMR90 and to 7 days for gels with HepG2. The viability of the cells was assessed at five-time points for all conditions during this period. The medium was changed once during the experiment for all gels. For HepG2 this was on the Day 2 and for IMR90 on Day 3. The media was changed only after the L/D assay had been carried out. The changes of culture media were performed after L/D assaying also in all further experiments.

Images obtained from L/D assaying performed on gels with IMR90 cells are shown in Figure 11. As in the first experiment, a great number of cells seemed to die during the first days after encapsulation in the wash-treatment and in the control group. In gels where 25 mM HEPES was used, similar behavior was not detected. On Day 6 and later only very few cells in total are detected, suggesting a poor survival in the later stages of the experiment. During this experiment, the detected signal for live cells was generally weaker than during the first experiment for IMR90. Due to this the color saturation of the IMR90 images had to be artificially increased to have presentable pictures to compare with the images obtained with HepG2 line. For further experiments, the volume of calcein-AM stain for L/D assay was increased to in order to obtain a more observable signal.

Imaging of the live and dead HepG2 cells during the second experiment is shown in Figure 12. Unlike in the first experiment, a great number of dead cells occurred in the wash-treatment group on the first days of the follow-up period. A high ratio of cells was dead on Day 1 and Day 2. In controversy to this, the total rate of survival of HepG2 cells seemed still highest for the wash-treatment group at multiple time-points and especially on the last day of the follow-up.

It was concluded that the wash-treatment was the most favorable for IMR90 and also for HepG2. The use of 25 mM HEPES-buffer did not seem to increase cell survival for either cell lines. The concentration of HEPES was increased because in experiments outside of this thesis, (carried out by Daria Zaytseva-Zotova, a postdoc at the faculty of biotechnology at NTNU) it had been found that higher concentration of HEPES buffered the changes in pH more better and helped to maintain it closer to pH 7. This was considered beneficial for cell survival and because of this the 25 mM HEPES-buffer was chosen to be used in all experiments that followed the second experiment. According to ThermoFisher Scientific 25 mM HEPES is the most common concentration to be used. (38)

IMR90

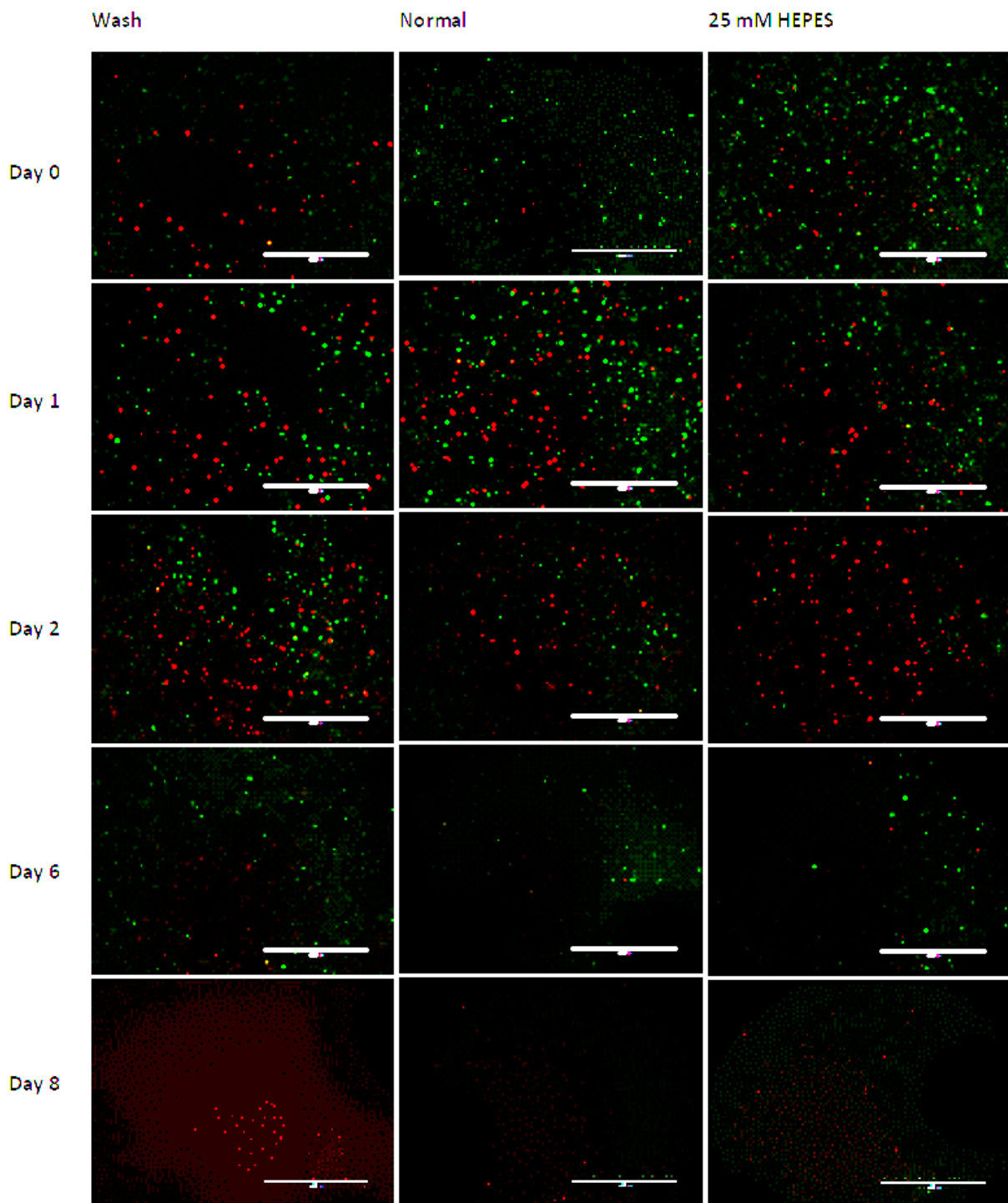


Figure 11. Live/dead imaging of encapsulated IMR90 cells with different treatments and gel conditions. The scale in the images is 1000 μm . Color saturation increased in the image.

HepG2

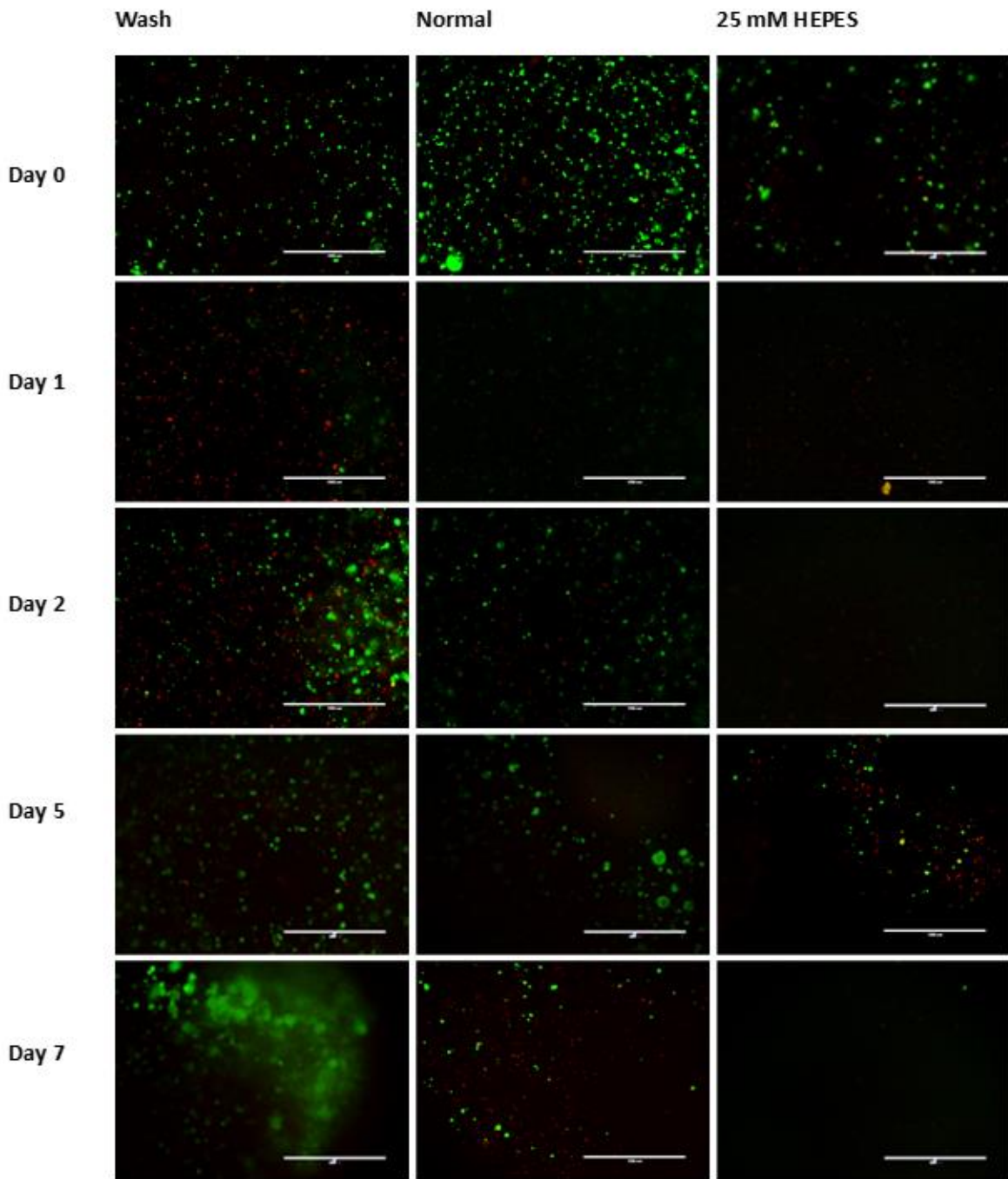


Figure 12. Live/dead imaging of encapsulated HepG2 cells with different treatments and gel conditions. The scale in the images is 1000 μm .

3.3 Effect of cold treatment

The effect of temperature on the cells during the encapsulation process was the main focus in the third experiment. Encapsulation temperature of +4 °C was compared to room temperature conditions that had been used in all previous experiments. In practice, all solutions used in the encapsulation procedure were either cold (+4 °C) or room temperature including cell suspensions, etc. Again, two cell lines HepG2 and IMR90 were used, resulting in a total of four different parallel conditions. Each were washed twice with 150 µl of cell culture medium in 30 min intervals after two hours of gelling in RT on the day of the cell encapsulation. The media was changed daily excluding days 6 and 7 from the encapsulation for HepG2 and days 4 and 5 from encapsulation for IMR90. The viability of the cells inside the gels was followed over a 10-day period, daily during the first three days including encapsulation day and then less frequently.

In this and further experiments, imaging was done so that one height in the gels covering the full surface of the gel in a 96-well plate was imaged in order to gain information about the distribution of the cells, overall survival and possible migration of cells during the follow-up period. The area was imaged in 12 overlapping sections and these separate pictures were then combined to one by the imaging program. However, as the imaging covers only one plane from the height of the gel structure the image does not represent the whole 3D matrix. The imaged planes represented the highest numbers of cells visible within the gel structure in each picture. If the cells were distributed on multiple different planes a height for obtaining the best representative image was chosen. Any exceptions or abnormalities in here or in further experiments are stated. In some of these images 'stitching lines' from joining the 12 separate images can be seen as straight vertical or perpendicular lines. These are not structures in the gel. Because the images represent an area covering the whole well, the cells appear smaller in size than in images for previous experiments. This should not be interpreted as a weaker signal of L/D assay.

For IMR90 the effect of encapsulation temperature on the cells was found negligible for overall survival rate in this experiment (Figure 13). The pictures taken after performing the L/D assay on both treatments seem to promote similar cell viability and survival throughout the 10-day follow-up period with one difference where the number of dead cells was found to be higher in the normal treatment on Day 0. This could indicate that the cold-treatment might have protected the cells during encapsulation but this did not seem to have an effect on the total survival rate in the end. The total number of live cells was high during the first days after encapsulation and then gradually decreased with the age of the gels. On Day 10, there were no live cells visible in the pictures. Since IMR90 had shown poor survival over longer periods inside the gel this was an expected outcome.

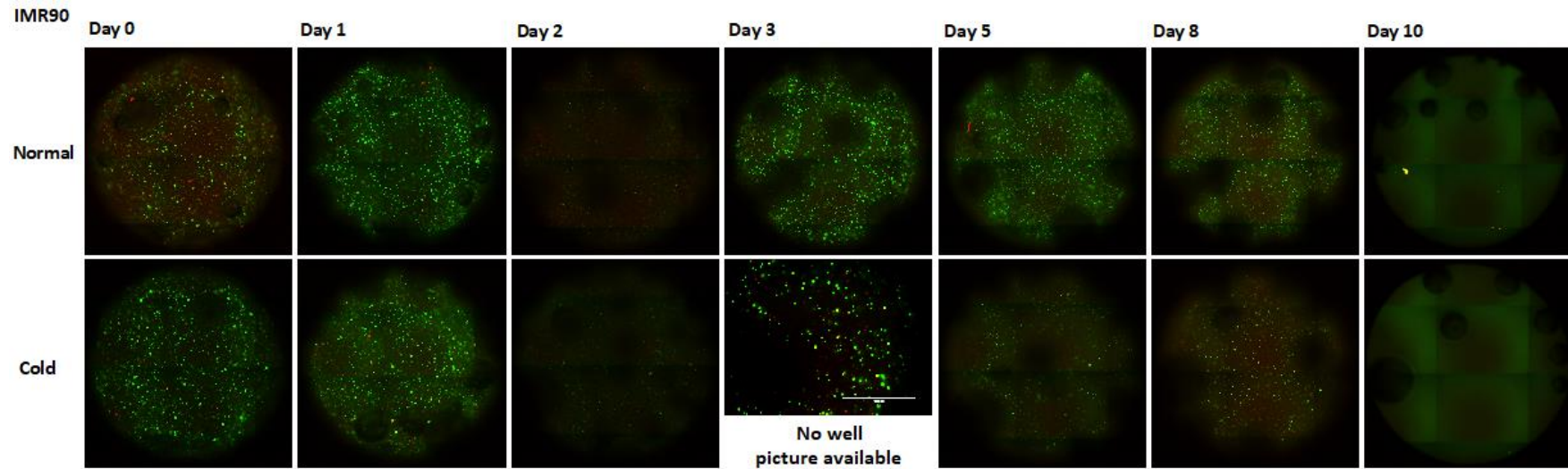


Figure 13. IMR90 cells in Experiment 3. For the image from Day 3 for cold treatment, the scale is 1000 μ m. Color saturation increased in the image.

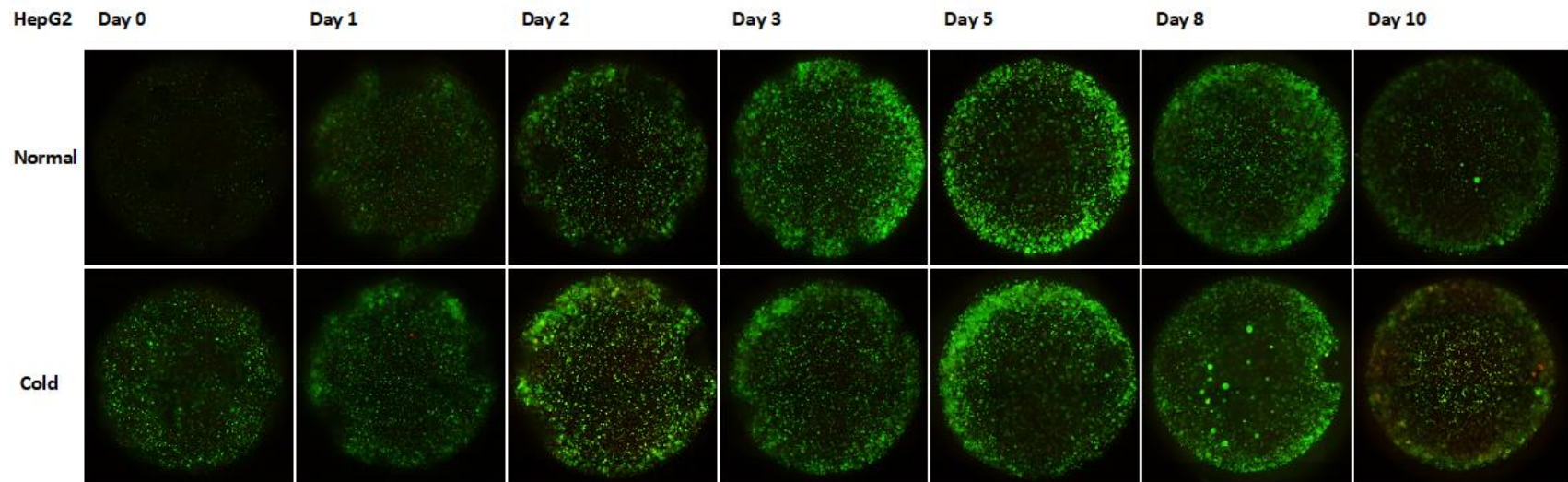


Figure 14. HepG2 cells in Experiment 3. In the images, the diameter of the gel is approx. 6,4 mm.

The imaging done on Day 0 for HepG2 was very vague for Normal treatment compared to images of cold treatment gels (Figure 14). The reason for this is not unambiguous because the staining solution used for L/D assay was the same and the assay was performed at the same time for all samples under the same incubation conditions (RT). Pictures taken from the parallels also displayed similar differences between the two treatments (Figures not provided here). The amount of calcein in staining solution was increased by $\times 2,5$ times for all assays performed after Day 1. Despite the vagueness, a great number of live cells can still be detected from the pictures. On Day 0, the number of live cells seemed higher for cells in the Cold treatment but on Day 1 and forward the differences were less markable. On Day 8 cells in the cold treated gels seemed to have formed visible clusters possibly indicating proliferation of cells.

The staining in L/D assay seemed to function differently in samples with cells from different cell lines. In Experiment 3 the same staining solution was used for all samples under the same conditions at multiple time points. Assaying of gels with IMR90 cells on Day 0, 3, 6, 8 and 10 was carried out at the same time as For HepG2 samples on Day 2, 5, 8, 10 and 12. During these particular days, the same staining solution was used for both lines. Because both signals in samples with IMR90 cells were found to be very vague throughout the follow-up the color saturation of Figure 13 has been increased in order to have the cells visible. This has not been done for the image of HepG2 (Figure 14). Despite this, the cells are still more visible in the samples with HepG2 cells.

In this experiment, the cell culture media in the wells was changed daily which was more frequently than in other experiments. Unlike expected, this did not seem to have an obvious influence on survival of IMR90. For HepG2 this might have been the critical change that resulted in the higher viability through-out the follow-up period.

3.4 Peptide grafted alginates in on-top cell cultivation

The fourth experiment had a different setup compared to the first three experiments. In this experiment, the cells were seeded on top of the alginate gels instead of encapsulating them inside of them. The gels used had a total of 1% alginate with a 1:1 ratio of grafted alginate and PRONOVA™ UP LVG alginate as used in previous experiments. Because the cells were added on top of gels, the two-layered sandwich-method was not used and gels with only one layer were prepared. Three different peptide-modified and one oxidized alginate were used in the experiment. The sample compositions were as follows:

- 1,0 % UP-LVG (control)
- 1,0 % UP-LVG + IKVAV-modified alginate (1:1)
- 1,0 % UP-LVG + YIGSR-modified alginate (1:1)
- 1,0 % UP-LVG + RGD-modified alginate (1:1)
- 1,0 % UP-LVG + oxidized alginate (1:1)

The unmodified PRONOVA™ UP LVG -alginate was used as a control material. Viability of the cells was followed daily for five days. The cell culture media was not changed once during the five-day experiment. Cells were prepared in RT and washing of gels was not performed at any point. In the figures representing results from imaging, the UP-LVG alginate has been abbreviated UM as unmodified alginate. Samples with peptide modified alginate have been abbreviated accordingly to the coupled peptide in the samples as IKVAV, YIGSR and RGD. The 'OX' stands for samples with UP-LVG and oxidized alginate.

3.4.1 Results for IMR90

For IMR90 the viability on the day of the cell seeding (Day 0) looked similar to all conditions and the number of live cells was high (Figure 15). Dead cells are visible in all pictures, but total amounts were relatively low compared to live cells. Imaging done on Day 0 is done from the same height for all samples resulting in decently focused and clear pictures for all conditions. On Day 1 same height of imaging was again used for all samples this time resulting in well-focused images only with some of the gels. From Figure 15 can be seen that cells were on a different plane on gels with YIGSR-modified alginate and oxidized alginate. This might have been due to swelling of the gel after media addition. On Day 2 and forward imaging was done on the plane of best focus.

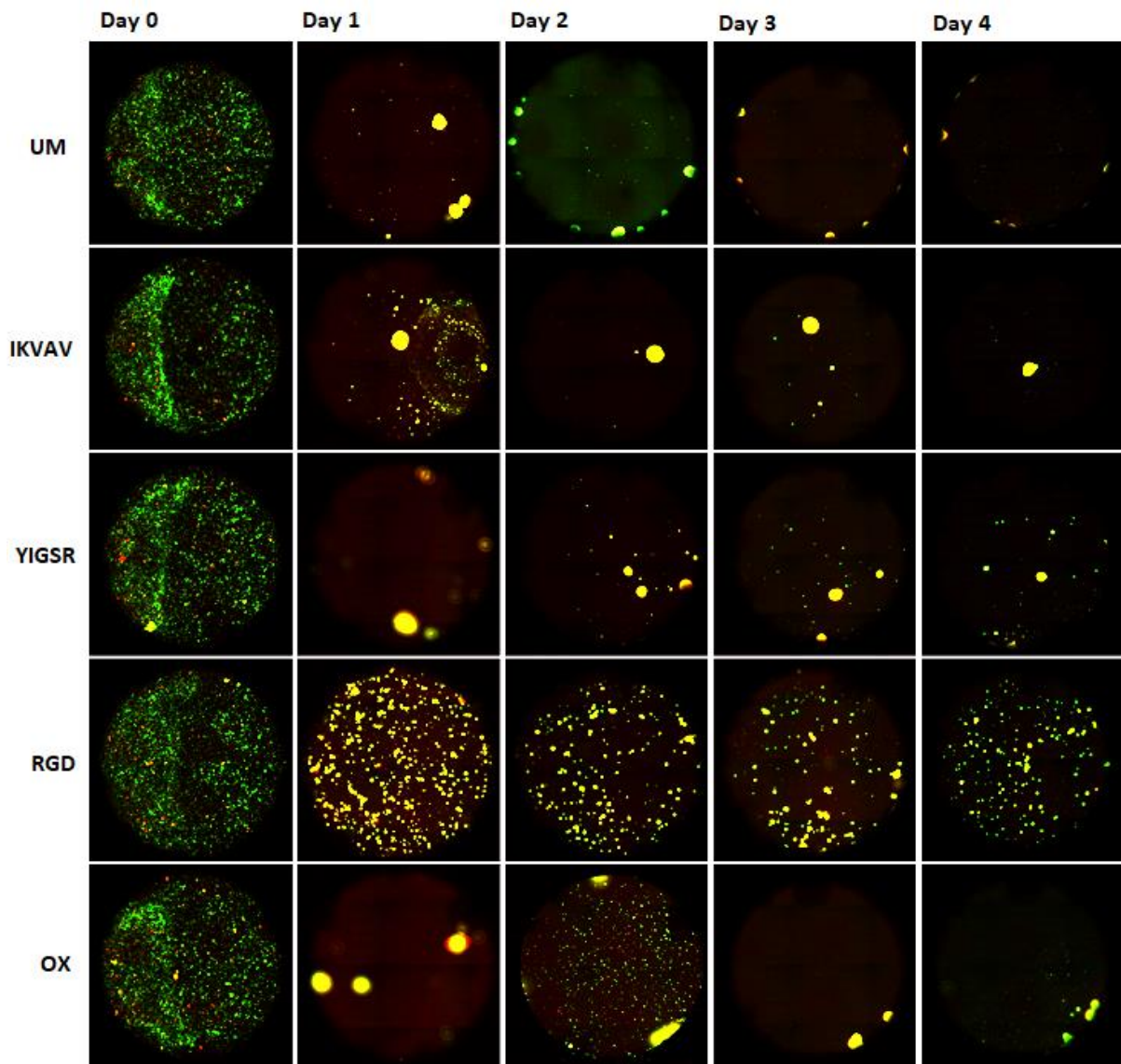


Figure 15. IMR90 cells cultivated on top of hydrogels with different grafted alginates in Experiment 4. In the images, the diameter of the gel is approx. 6,4 mm. Color saturation increased in the image.

In L/D assay the live cells are stained green and dead cells red. However, in many images in this experiment, the cells seemed strikingly yellow. This is due to clustering of cells with both live and dead cells that then under L/D staining transmit overlapping signals appearing yellow especially in the images covering the whole well area. With a closer look of the images (Figure 16) it can be seen that the dead and live cells are separate but found in close proximity with each other thus causing the yellowish signal.

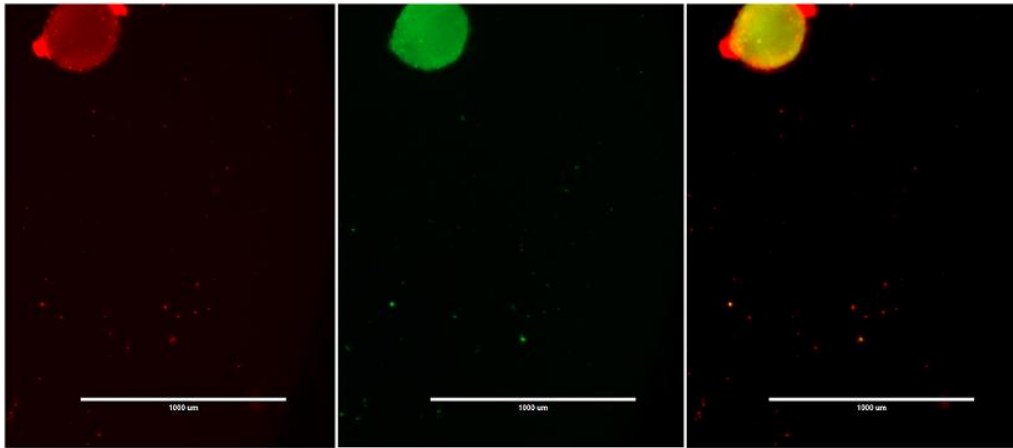


Figure 16. IMR90 cells on a gel with oxidized alginate during Day 1. Imaging of RFP, GFP and both (L/D) under a light microscope at the same location. The scale is 1000 μm . (Original color and brightness)

When seeded on top of gels the cells formed clusters in most sample groups. This might imply that the cells did not adhere to the gel surface. For IMR90 the RGD-modified alginate showcased better results for cell survival than the other alginates tested. Similar clustering was not detected at the same extent, and the cells were distributed over the surface more evenly than in other gels. Some cells were found to spread over (Figure 17) and to showcase morphology typical for fibroblasts (Figure 4) indicating an attachment on the surface. For IMR90 cells the viability was found to be highest on gels with RGD-modified alginate throughout the control period.

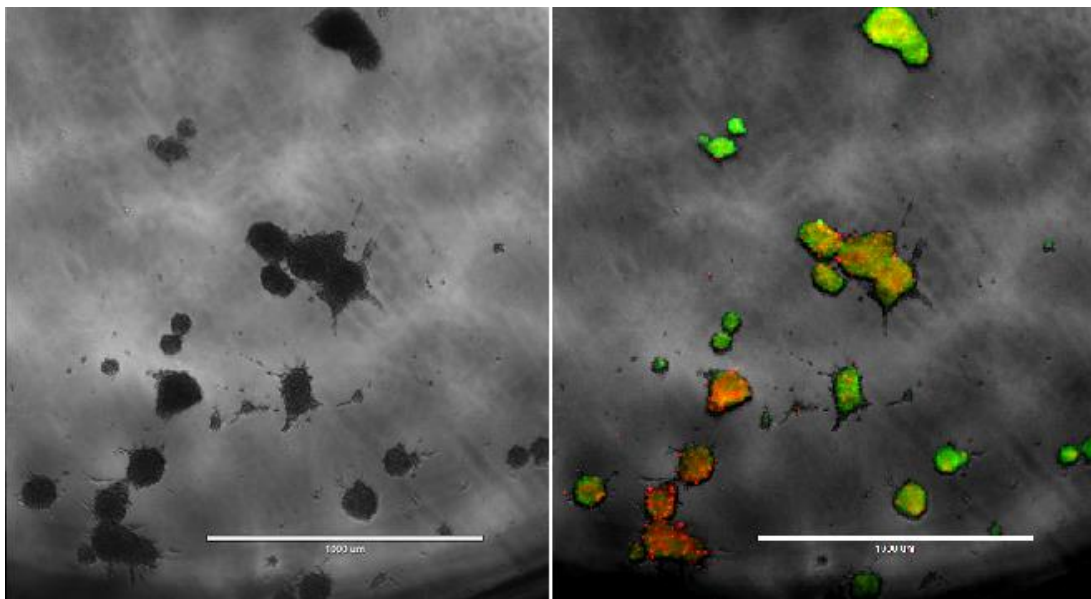


Figure 17. Phase image and image of L/D assay of IMR90 cells cultivated on top of gel with RGD-modified alginate. The scale is 1000 μm . (Original color and brightness)

3.4.2 Results for HepG2

Cultivation of HepG2 cells on top of a similar panel of gels was tested in Experiment 4. In the images from Day 0, the total number of cells is high and only a few dead cells are visible (Figure 18). Cells have also distributed evenly across the surface of the gel. The situation had changed dramatically after approximately 24 hours. L/D assaying on Day 1 revealed that only a fraction of the cells was longer visible and the number of dead cells had increased. The cells had formed clusters with both live and dead cells within the first 24 h. However, for gels with RGD-modified and oxidized alginate, the clustering seemed less extensive. The plane of best focus changed also for these gels after one day of incubation with growth medium as it did for the gels with IMR90.

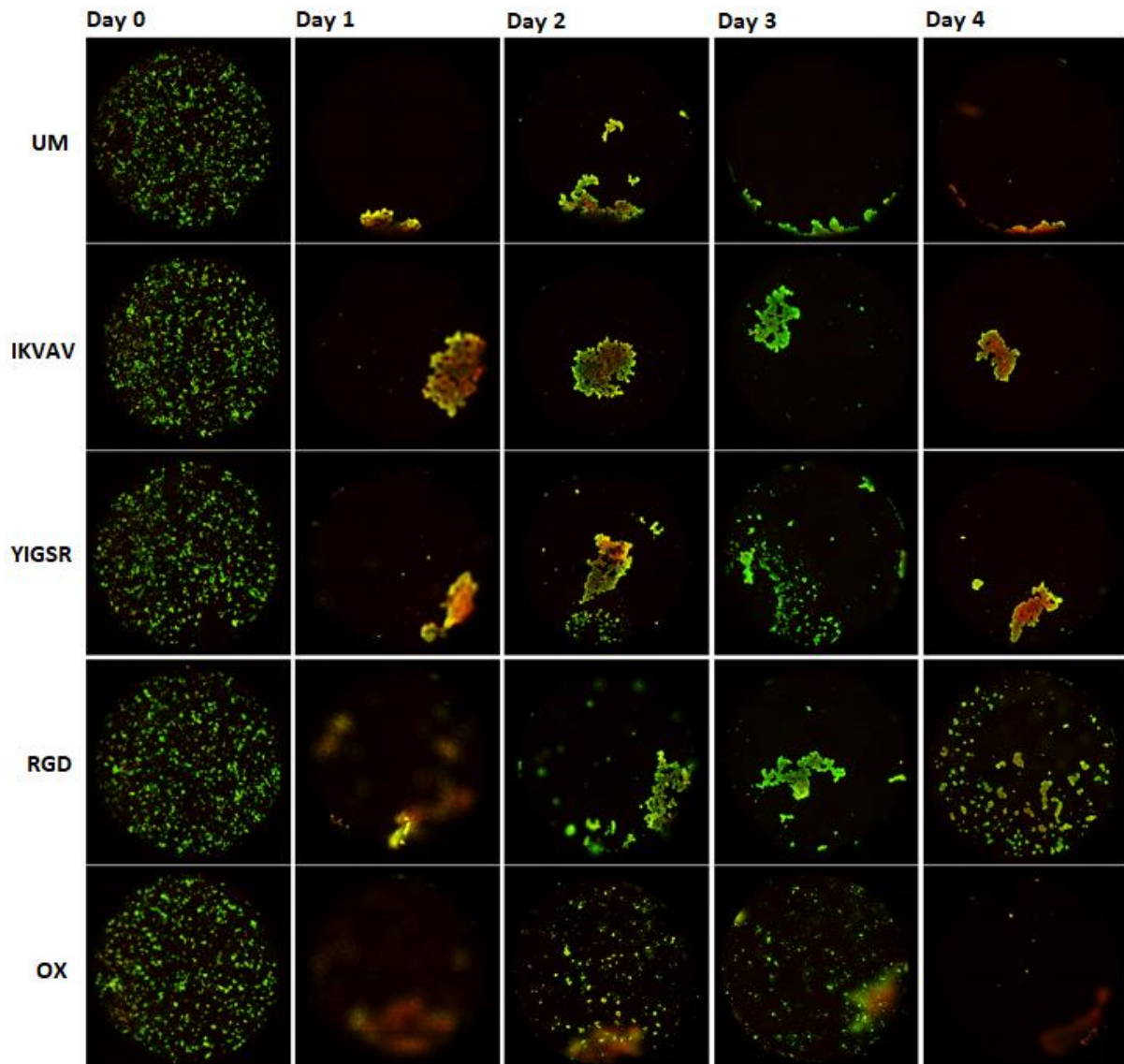


Figure 18. HepG2 cells cultivated on top of hydrogels with different grafted alginates in Experiment 4. In the images, the diameter of the gel is approx. 6,4 mm.

The survival rate of HepG2 cells was generally higher in all conditions compared to survival of IMR90. HepG2 did not seem to favor only one material as clearly as IMR90, although the best result from the last day of the control for HepG2 was the RGD-modified alginate too.

3.5 RGD-modified alginate for cell encapsulation

Since an indication that gels with RGD-modified alginate could promote cell adhesion was discovered in the fourth experiment, the RGD-modified alginate was chosen to be further tested for cell encapsulation. In this experiment alginate coupled with the RGD peptide was mixed in a 1:1 ratio with UP-LVG alginate and with oxidized alginate. Due to the weaker mechanical properties of gels made with grafted alginates the amount of alginate in gels was increased to 1% from the initial 0,5% for these gels. For control gels with only UP-LVG alginate, the 0,5% was still used. 1% bottom gel with UP-LVG was used for all conditions. The conditions for gels used for encapsulation were;

0,5 % UP-LVG (control)

1,0 % UP-LVG + RGD-modified alginate (1:1)

1,0 % OX + RGD-modified alginate (1:1)

For this experiment, cells were prepared and processed in cold temperature (+4 °C) as done in Experiment 3. The viability of cells was followed over a 10-day period. During this period the culture media was changed twice, on Day 2 and Day 5 for both cell lines. All gels were washed 2×150 µl in a 30 min interval at +37 °C, on the day of encapsulation after 2 h gelling. The RGD-modified alginate was the same as used in the previous experiment. This exact same alginate was also used in further experiments whenever RGD-modified alginate was used.

3.5.1 Results for IMR90

On the day of encapsulation, the viability of cells seemed eligible for gels with only UP-LVG and with UP-LVG+RGD-modified alginates. In gels with OX+RGD-modified alginates, the viability seemed weaker than for other conditions (Figure 19). After approx. 24 h the number of live cells seemed more constant for all conditions without a markable number of dead cells, but still a little less for gels with OX+RGD-alginate. On Day 2 the situation had changed to the opposite when the number of live cells seemed much higher in gels with OX+RGD-modified alginates and appeared to be having decreased in other gel conditions. Similar behavior continued throughout the control period.

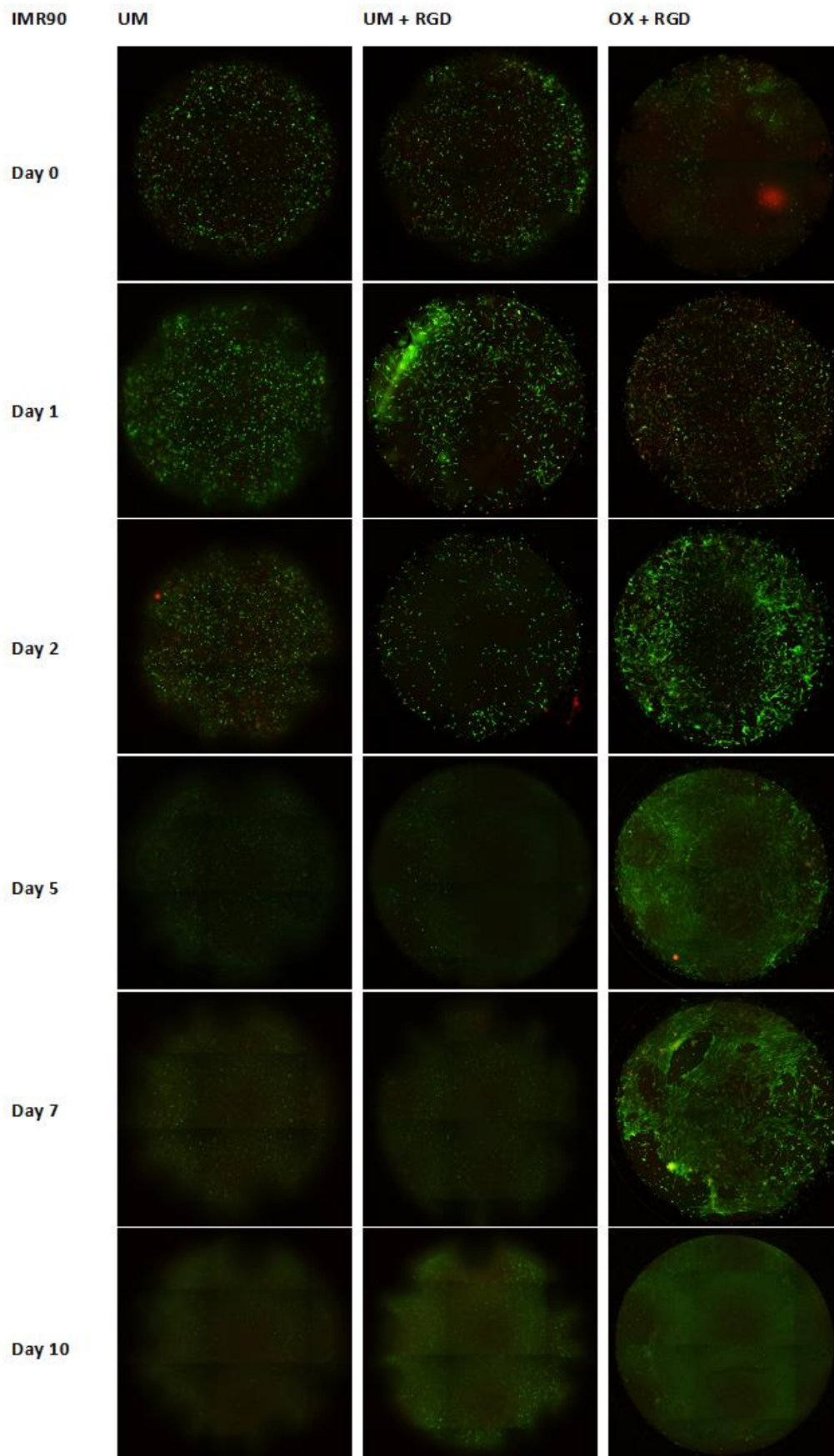


Figure 19. L/D imaging of IMR90 cells encapsulated in alginate gels with modified alginates. In the images the diameter of the gel is approx. 6,4 mm.

In a closer look of the images from Day 1 approx. 24 h after the encapsulation, cells seemed to have attached in gel all samples with RGD-modified alginate (Figure 20). Although the number of dead cells seemed to be higher in gel with OX+RGD alginates, also the number of live cells appeared to be higher than in gel with UP-LVG+RGD-modified alginate. In these images, the cells seem to be growing on one plane of height in the sample because hardly any cells are poorly focused and even cells with the elongated shape appear clearly and with a definite outline. If distributed in a 3D matrix a great number of cells should have been out of the focus range with this type of imaging.

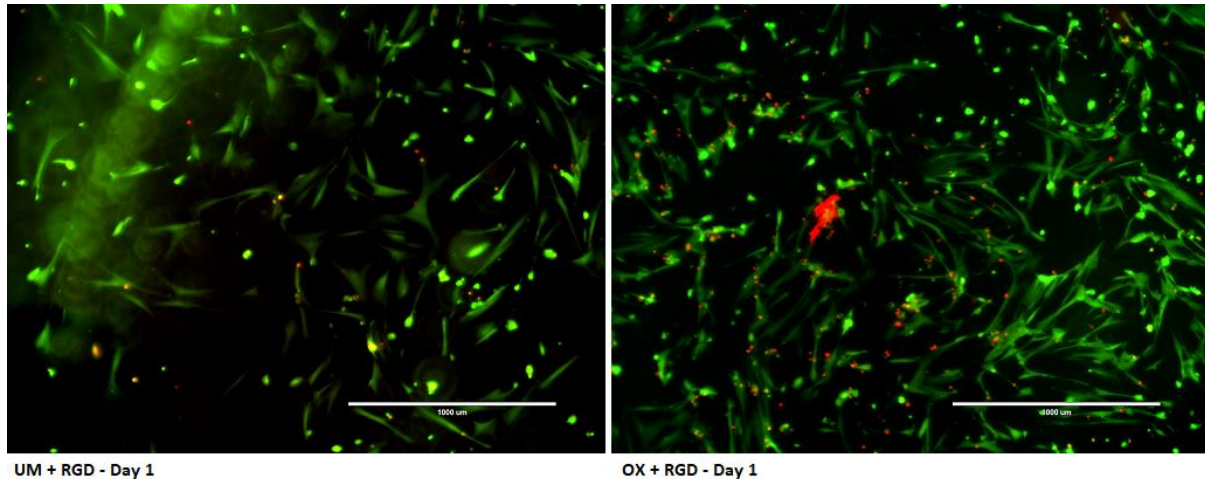


Figure 20. L/D imaging of IMR90 cells in gels with UP-LVG+RDG -alginates (left) and oxidized + RGD-modified alginates (right) on Day 1. The scale is 1000 μm .

On Day 1 the number of detected live cells seemed higher in gels with OX+RGD alginate and both parallels prepared for L/D assay displayed very similar results. Simultaneously the samples of UP-LVG+RGD alginate showed inconsistency for cell attachment. In Figure 21 are images of the two parallels of UP-LVG+RGD alginate gels from Day 1. The other parallel is on the left. On the middle and the right is the second parallel sample imaged at two different heights. In the image in the middle, the spreading of cells is indicating attachment but on the left image, this is not observed.

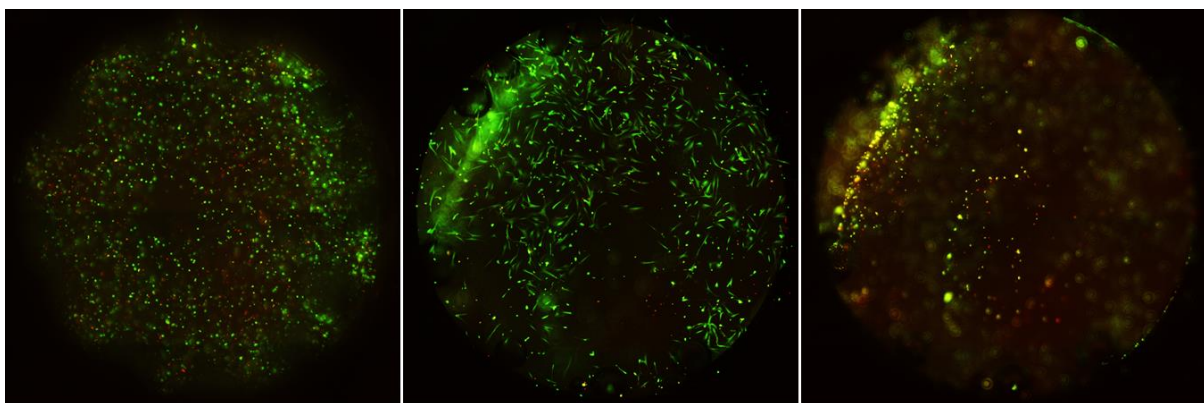


Figure 21. L/D imaging of IMR90 cells in UP-LVG+RGD alginate gels on Day 1. On the left parallel sample with no found indication of cell attachment. On the other two, the same sample imaged from different heights, the image of the lower part of gel in the middle and upper part in the right. In the images the diameter of the gel is approx. 6,4 mm.

During the experiment, more similar contradictions were observed between parallels with the UP-LVG+RGD-modified alginates. It was also observed that in some cases cells were found to have distributed in two locations. In some occasion, a small number of cells were found in the upper parts of the gel where they had distributed in multiple layers expressing a circular shape, that did not indicate attachment to the material. Besides this, a considerable number of cells could be found well beneath from this. The cells found in the lower part of the gel were growing in one distinct layer and displayed signs of attachment to a surface. Between these was a layer of the gel matrix with a negligible number of cells.

If the possible potential to support cell attachment in UP-LVG+RGD alginate gels was somewhat inconsistent, the results obtained from OX+RGD alginate gels seemed more coherent. The morphology of cells indicated attachment to a surface on Day 1 (Figure 20) and the number of live cells seemed to remain relatively high throughout the follow-up period despite the day of encapsulation. As with UP-LVG+RGD-modified alginate gels, cells that seemed to have attached were found in the lower part of the gel, growing in a distinct single layer. However, in samples with OX+RGD alginate cells were not found above the distinct cell layer.

Like in previous experiments the GFP signal from live cells seemed to fade as the age of the encapsulated cells prolonged, interestingly less in the OX+RGD alginate gels. The fading of the live signal could be due to a decrease in metabolic activity in IMR90. This could also explain why the signal was generally stronger for cells in OX+RGD alginate gels even though the staining solution and time of incubation had been the same for all samples at each point of L/D assaying. But in the images obtained on Day 10 also the gels with OX+RGD modified alginates displayed faded GFP signal. The images of gels with OX+RGD alginates also displayed rather high confluency of cells which might be the cause of a decrease in the metabolic activity.

After the encapsulation experiment, it was discovered that the combination OX+RGD alginates did not form a gel under the used parameters. Considering that multiple washing steps and media changes had been performed for these samples it was possible that the eventual amount of the OX+RGD alginate had decreased during the experiment. From this perspective, the results obtained from L/D analysis of samples with OX+RGD alginates could be considered to be somewhat intriguing. The samples did portray higher viability compared to the other gel conditions. Also, cells showcased better attachment in these samples than in other conditions in this experiment or in the previous experiment, where cells were casted on top of the gels (Figure 15 and Figure 17). This might be due that the RGD-peptide in the non-gelled alginate solution had bound either to the surface of the bottom gel or to the well plate.

In the encapsulation process, the cells are added into alginate solution with CaCO_3 and GDL. Loss of the material during the washing procedure would reasonably explain the decrease in the cell number in OX+RGD alginate samples on Day 0. The increase in number after the first day and later could be due to cell proliferation. However, there has not been an indication of IMR90 proliferation in previous experiments.

In every gel where the distinct plane of cells was found it had formed on a certain height of the gels. Nevertheless, the cells might not have attached to the surface of the 96-well plate because it was possible to image separate individual cells below the single layer structure. Another apparent layer in the gel structure besides the bottom of the well was the intersection of the two gel layers. This could have explained why the cells were found from the same height in each sample.

In all samples where the indication of cell attachment was found, the cells were growing in this distinct layer in lower parts of the gel structure. Because of this, the possibility of the cells growing in the bottom of the well plate underneath the matrix had to be considered. In order to determine this better, the IMR90 cells were cultivated on a well plate surface for 24 h to judge if they were prone to attach to it, regardless of the non-favoring surface for cell attachment of the well plate. Also, another sample was cultivated for 72 h to understand their ability to survive and proliferate on this non-favoring surface. Results for this are presented in Figure 22. The morphology the IMR90 cells had obtained after 24 h indicated an attachment to the plate surface (left). The shape of the cells is similar as in samples with OX+RGD alginates in Figure 20.

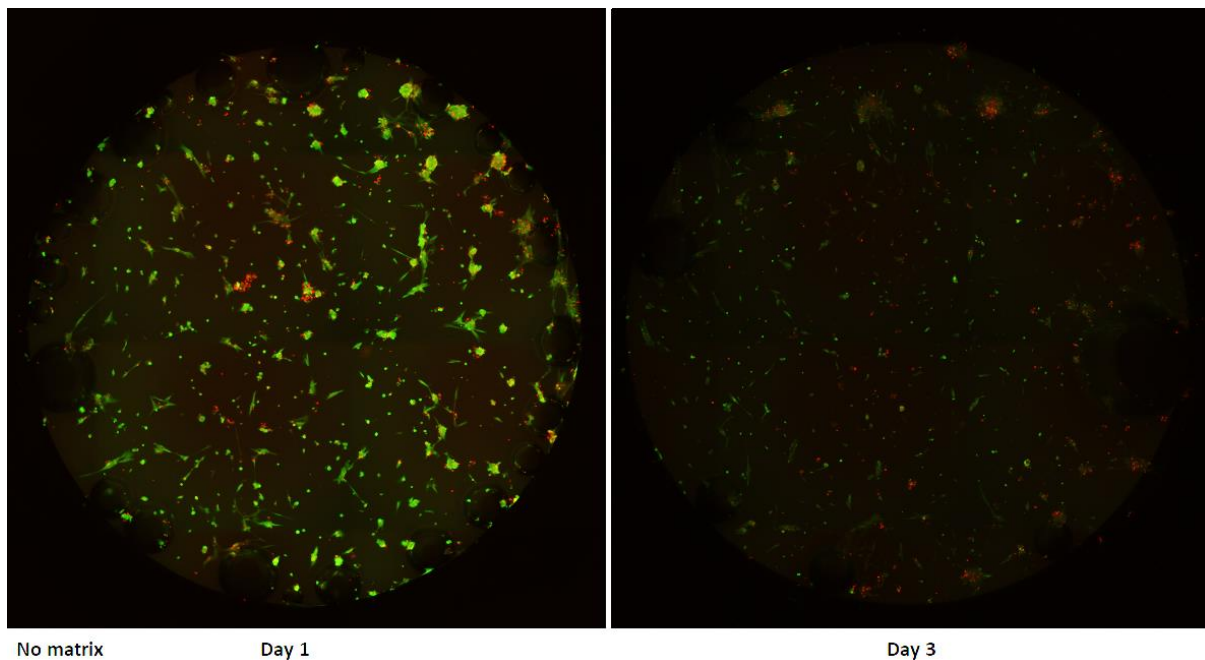


Figure 22. IMR90 cells cultured without gel matrix on 96-well plate. Imaged after approx. 24 h and 72 h of incubation in +37 °C and 5% CO₂. The diameter of the gel is approx. 6,4 mm.

Interestingly the cells did not seem to have proliferated during 72 h period in the samples without matrix as they seemed to have done in the samples with OX+RGD alginate from Day 2 and forward (Figure 19). Also, the RFP and GFP signals in L/D imaging are relatively vague in Figure 22 in the image obtained on Day 3. This could suggest a diminished metabolic activity, especially because the cells were in straight contact with the staining solution without a gel structure as a mechanical barrier.

3.5.2 Results for HepG2

The results obtained from a similar experiment with HepG2 cell line correlated with the results gained from the experiment with IMR90. The viability seemed weakest for cells in OX+RGD alginate samples on the day of encapsulation but increased over the control period and it seemed to be highest in the samples with OX+RGD alginates on the last day of the follow-up from the three comparison groups, although the viability seemed high in all conditions. An increase in GFP signal over the follow-up period can be seen from Figure 23. Similar development had been detected also during Experiment 3 (Figure 14).

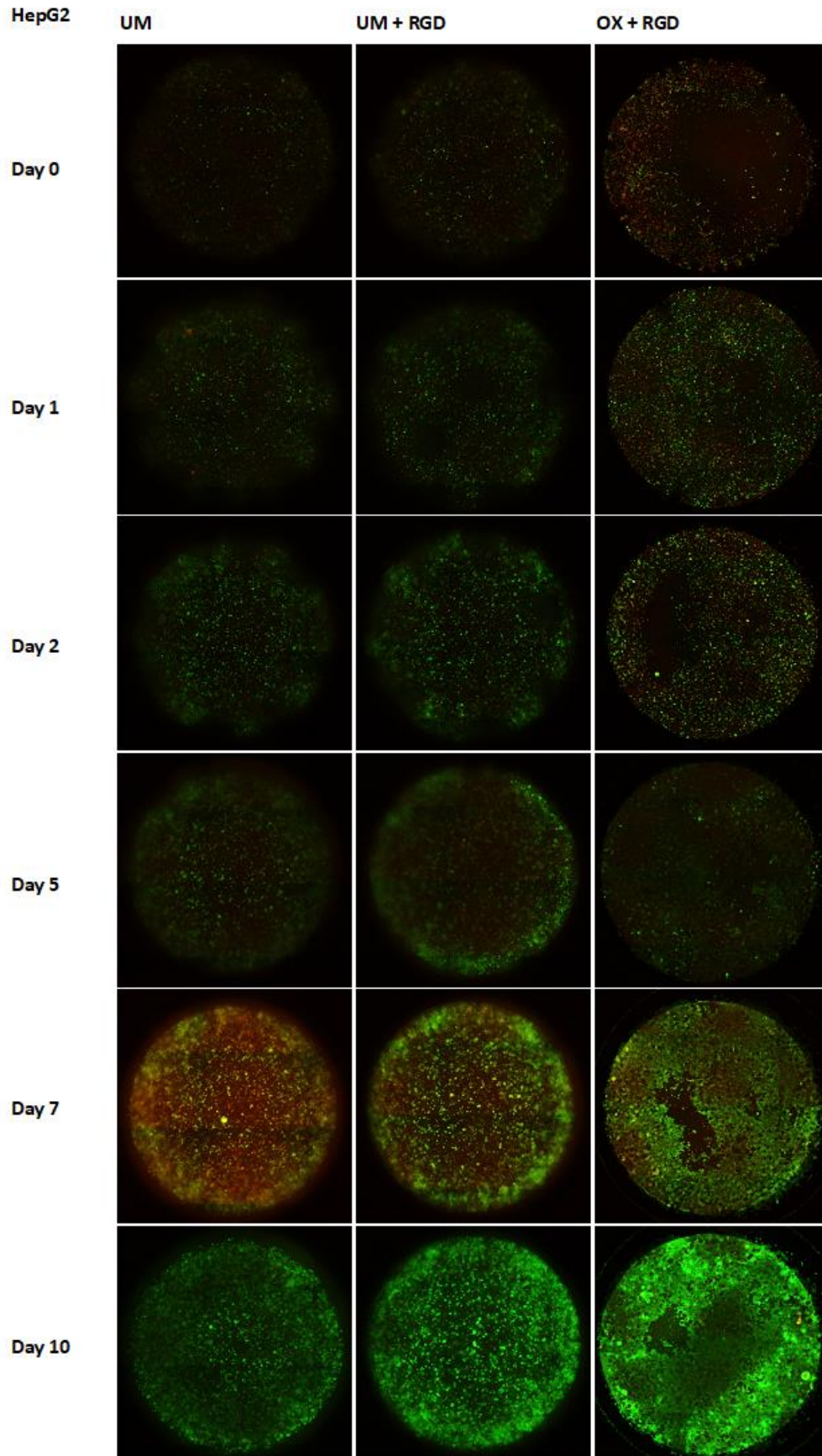


Figure 23. L/D imaging of HepG2 cells encapsulated in alginate gels. In the images the diameter of the gels is approx. 6,4 mm.

All materials seemed to support the viability of HepG2 cells, and the total number of live cells was relatively high throughout the term of the follow-up and even seemed to increase during it. However, cells in the samples with oxidized and RGD modified alginate expressed different behavior than cells in the other gels did (Figure 24). In these samples, the cells formed a more uniform structure when compared to cells in other gels and seemed to have grown more separately from each other and much like in previous experiments. Cells in the OX+RGD alginate gels seemed also to be less vertically distributed than in gels with UP-LVG+RGD alginate and UP-LVG alginate only. This might have been due to the attachment on the bottom gel or the well plate as with IMR90 cells because the OX+RGD alginates did not form a gel.

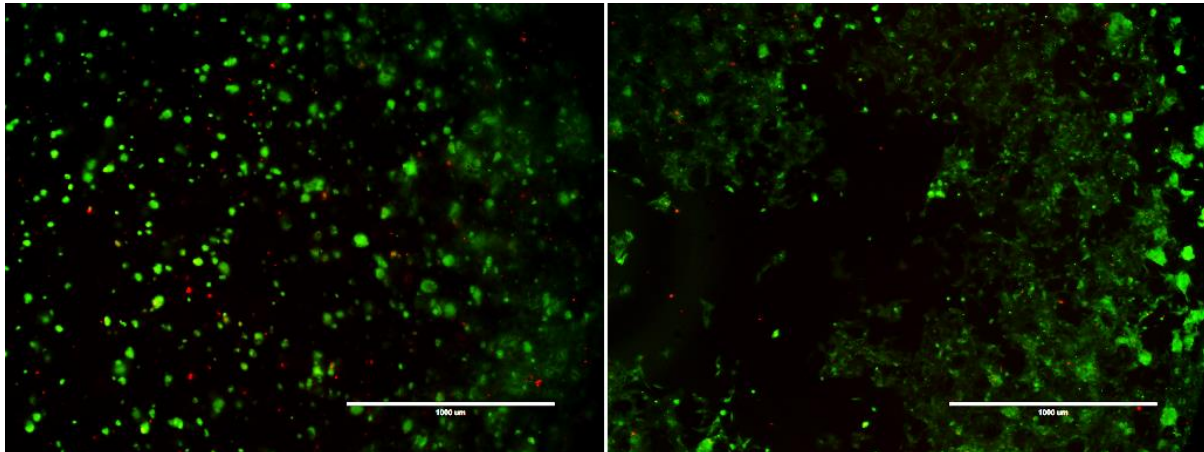


Figure 24. L/D imaging of HepG2 cells inside gels with just UP-LVG (on the left) and oxidized + RGD alginate (on the right) on Day 5. The scale is 1000 μm .

In an image taken with $\times 10$ objective (Figure 25) the sheet-like growth is more visible. The cells seem to have attached to a surface causing them to spread along with it and to form clusters much like the HepG2 does when cultured in 2D cell culture flasks (Figure 5). This indicates that the cells had indeed been able to attach a surface of some kind.

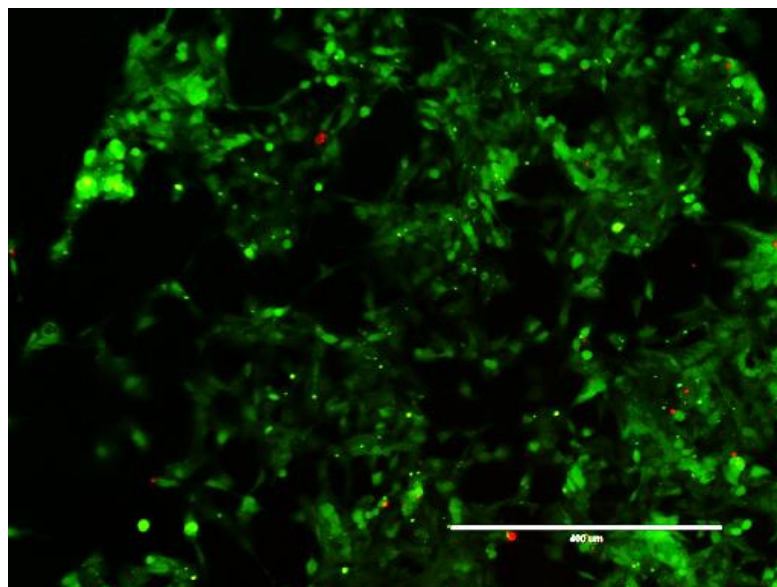


Figure 25. L/D imaging of HepG2 cells in the sample with oxidized and RGD modified alginate on Day 5 imaged with $\times 10$ objective. The scale is 400 μm .

3.6 RGD-modified alginate for IMR90 encapsulation

It was decided that only IMR90 cells were to be used in Experiment 6 because in this experiment many of the used conditions had been already studied in Experiment 5 with both cell lines. Because supporting the viability of IMR90 had proven to be generally more difficult and the results obtained from L/D assaying in the previous experiment had been inconsistent in some of the conditions, there was greater interest for repeating the experiment with IMR90 and less need for repetition with HepG2 line.

The experiment with UM+RGD alginate was decided to be repeated because an indication of cell attachment of IMR90 cells to the material was detected in gels during the first days of the control period (as seen in Figure 20) and also on some of the samples later on. But because a part of the samples did not indicate any attachment, the results had been generally more or less inconclusive. In addition of repeating the 1:1 ratio of UP-LVG+RGD alginate gels, also a 1:3 ratio UP-LVG+RGD alginate gels were chosen to be tested in this experiment to study if an increase in the amount of RGD-peptide in the gels would result in an increase the cell attachment. In addition, a repetition of OX+RGD alginate gels was decided to be carried out due to the peculiar results obtained, even though it did not form a gel after the addition of the gelling agent.

For this experiment, 0,5% UM alginate gels were used as a control as before. A gel condition with UP-LVG with oxidized alginate was introduced as another control. The UP-LVG+OX alginate gel shares similar structural features with the gels with UP-LVG+RGD alginates and was thought to be more relevant control for them. With this control, the possible effects of the RGD-peptide or the structural difference alone could be evaluated better. Generally, gels with oxidized alginate have weaker structure than gels with only UP-LVG alginate. This applies to gels with RGD-modified alginate a well. The different gel conditions used for encapsulation in this experiment were;

- 0,5 % UP-LVG (control)
- 1,0 % UP-LVG+RGD-modified alginate (1:1)
- 1,0 % UP-LVG+RGD-modified alginate (1:3)
- 1,0 % OX+RGD-modified alginate (1:1)
- 1,0 % OX+UP-LVG (control, 1:1)

The sandwich method was applied on all the gels in Experiment 6 and again bottom gel with 1% UP-LVG alginate was used. Similar washing as in the previous experiment was performed on all gels (2×150 µl with 30 min interval) and 75 µl cell culture media was added on gels after washing and changed twice during the control period on Day 2 and Day 5. As in Experiment 5 viability of the cells were followed over a 10-day period. Two parallels were prepared and imaged at each time point. Results of this are represented in Figure 26. Images covering the whole well surface are taken from the height where the highest number of cells were found in each time point.

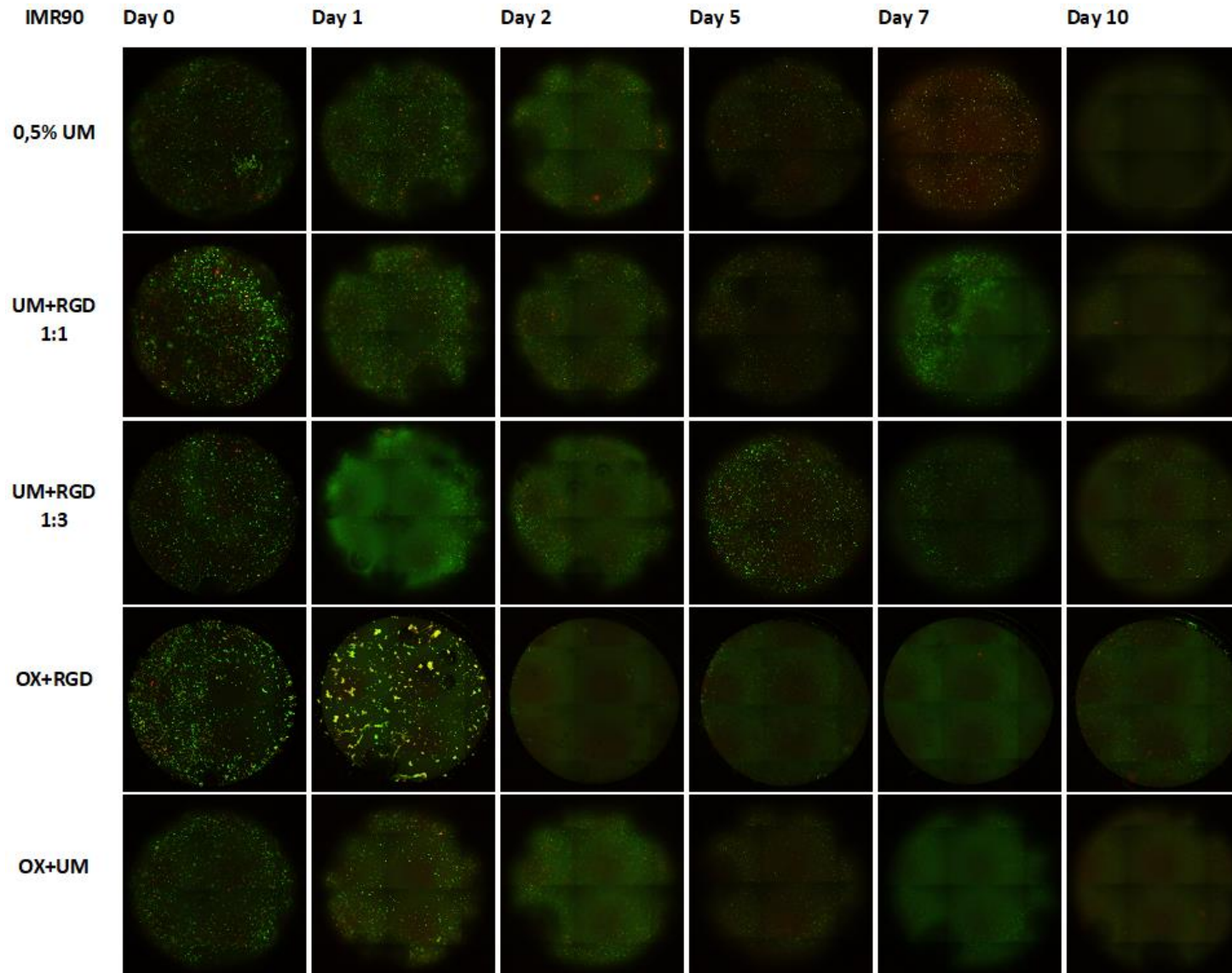


Figure 26. L/D imaging of IMR90 cells encapsulated in gels in Experiment 6. In the images the diameter of one gel is approx. 6,4 mm.

In the process of imaging the gels, some of the samples appeared to be outside of the focus range from the upper parts of the gel. In these cases, the cells inside a gel structure could be detected, but it was not possible to obtain a well-focused picture. For some of the samples, this resulted in images that showcase the viability of the cells, but the morphology is harder to interpret. Also, in the images covering the entire area of one plane in a gel (as in Figure 26), the non-focused cells can add up to the background signal of the L/D assay and appear more vague than they would under a properly focused image. Since the range of the microscope should have covered the full height of the two-layered gel structure it is possible that the gel or the top layer of the gel had detached and was floating in the cell culture media. In most cases, this was experienced only in the other parallel making it possible to study the distribution and estimate the viability of the cells in the range of the focus. However, it should be considered that in Figure 26 the image of the sample with UP-LVG+RGD alginates and with 1:1 ratio on Day 7 was partly out of focus range as described above.

Cells indicating attachment were discovered in gels with UP-LVG+RGD alginate and especially in gels with a higher percentage of RGD-modified alginate. In images taken during Day 5 and Day 7 (Figure 27), live (green) cells with an elongated structure can be seen for some of the cells. This time the cells with this natural fibroblast shape were most likely growing inside of the 3D gel structure. In images in Figure 27 only a few cells are on the focus plane of the microscope and the rest of them are either above it or below it, meaning that the cells did not grow in one layer. Furthermore, the cells did not reside in the lower parts of the gel, but rather high in the whole sandwich structure which also suggests that cells were inside the gel and had adhered on it.

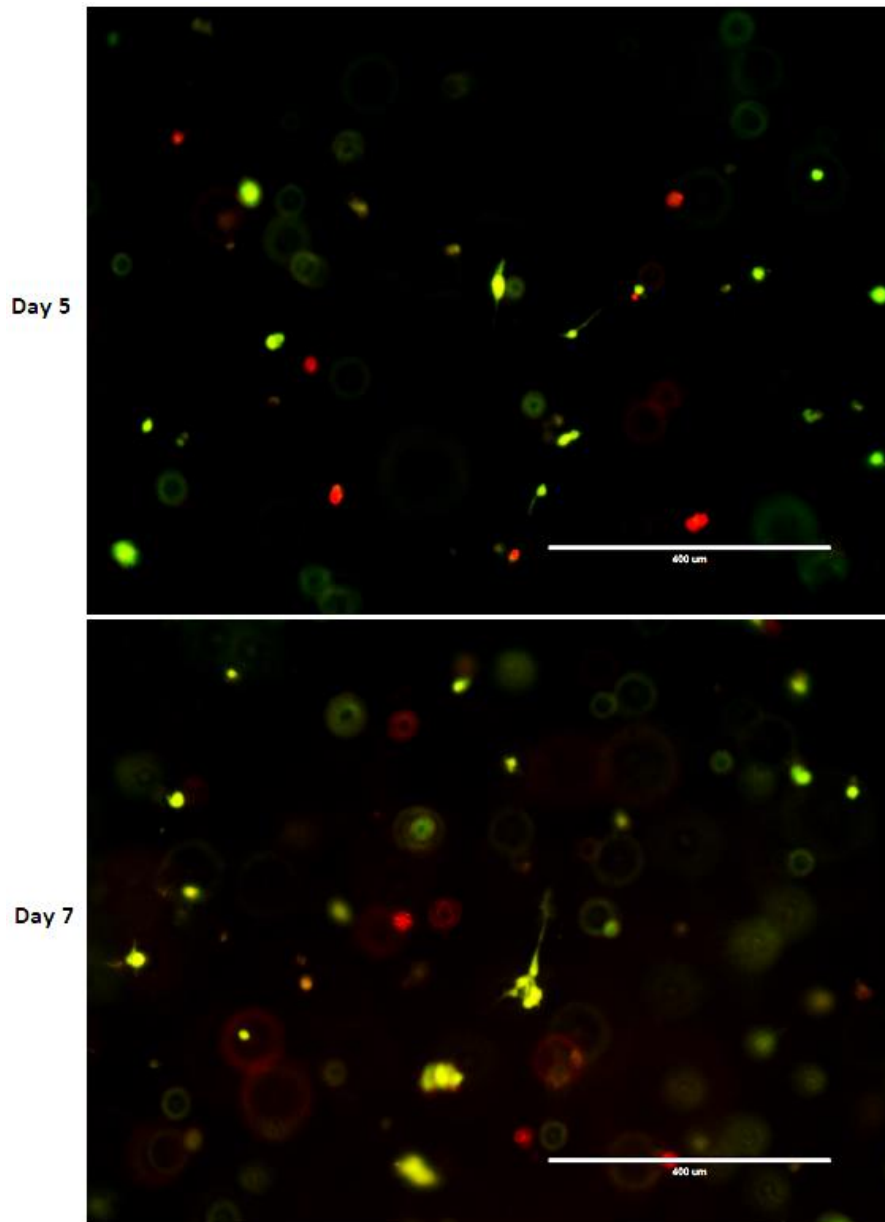


Figure 27. L/D imaging of IMR90 cells inside UP-LVG+RGD-modified alginate (1:3) alginate gels on Day 5 and Day 7. Imaged with the 10× objective. Brightness and contrast increased by 20%. The scale is 400 μm.

Morphology changes indicating cell attachment were also discovered in UP-LVG+RGD alginate gels with a smaller amount of RGD-alginate (1:1 ratio) (Figure 28) but in these gels, the number of attached cells was smaller and the cells appeared less elongated as in gels with the 1:3 ratio.

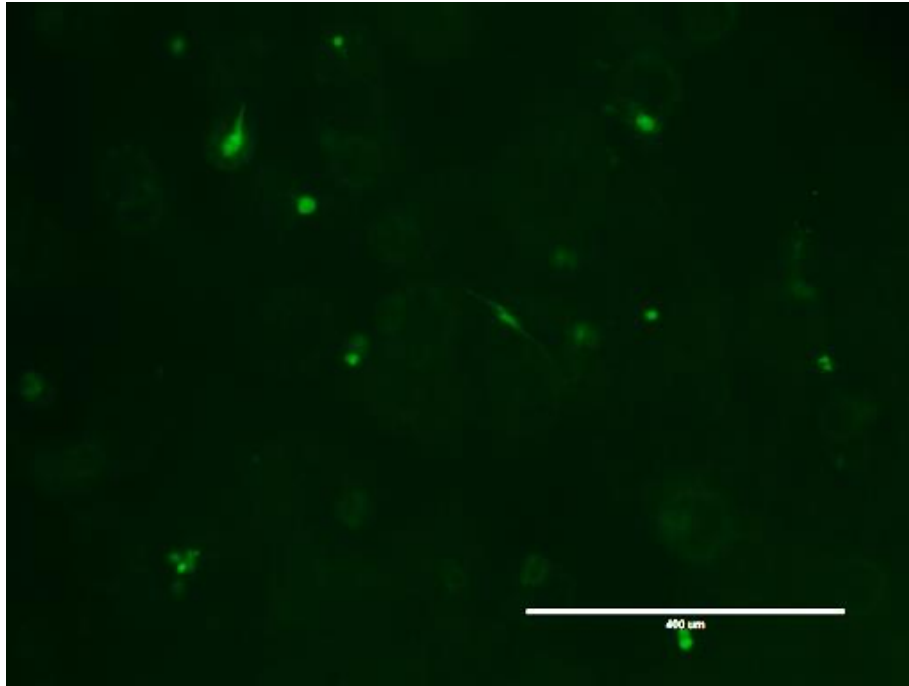


Figure 28. Imaging of live IMR90 cells inside gel with UP-LVG+RGD alginate in a 1:1 ratio a week after encapsulation (Day 7). Imaged with x10 objective, 400 μm scale.

The difference in survival rate between the two control conditions was found to be relatively little, but in L/D imaging the live cells were more apparent in gels with only UP-LVG alginate (Figure 26). This might have been due to the higher metabolic activity of the cells in these gels or to higher background signal in UP-LVG+OX gels as a result of binding of calcein-stain into the oxidized alginate. During the control period, no indication of cell attachment was detected in the UP-LVG+OX gels. This supports the likely relevance of the RGD-peptide for cell attachment over the structural difference between the different gels. Despite that the UP-LVG+OX control had a 1:1 ratio of the modified and unmodified alginate and in gels with 1:1 ratio of UP-LVG and RGD-modified alginate the cell attachment was found to be less significant than in gels with higher ratio of RGD-modified alginate, it was unlikely to be caused by the difference in alginate ratio.

In the fifth experiment the results obtained from gels with OX+RGD alginates it was debated whether the cells had migrated in the bottom of the well or were growing on top of the bottom gels. When L/D assay was performed on Day 2 to the sample with OX+RGD alginate, the cells were found to have formed a similar monolayer structure as previously. To study if the cells were growing on the bottom of the well plate, the gel samples were dug out and both the well plate and the separate gel were then examined. It was found that a majority of the cells were indeed attached to the untreated surface of the well and only a few cells were found on the gel (Figure 29). The same procedure was done again on Day 10 and again, the majority cells were found to grow in the bottom of the well and only a few were found on the gel.

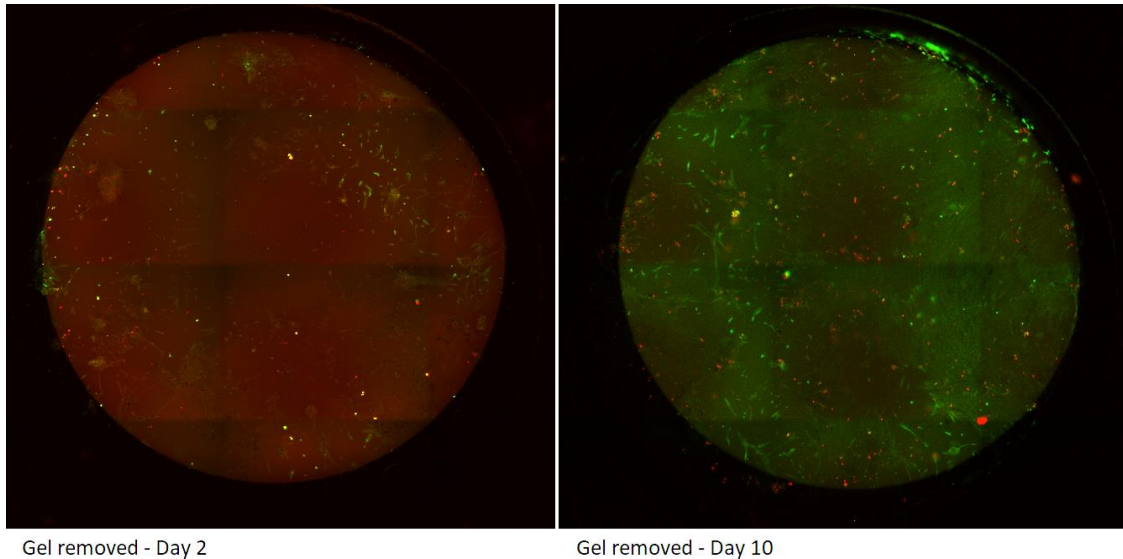


Figure 29. L/D imaging of IMR90 cells on 96-well plate surface after removing the bottom gel on Day 2 (left) and Day 10 (right) of OX+RGD alginate sample. The diameter of is approx. 6,4 mm.

On Day 10 a small number of cells were found on a higher level of the gel structure above the cell layer that was found to grow on the surface of the well plate. Like the cells growing on the bottom of the well, these cells were also found on one distinct height and but were most likely growing on top of the initial bottom gel. Interestingly the shape of some of the cells indicated an attachment to the material (Figure 30). Because no cell attachment promoting compounds were originally in the bottom gel it is possible that RGD-peptides from the non-gelled alginate solution had bound to its surface.

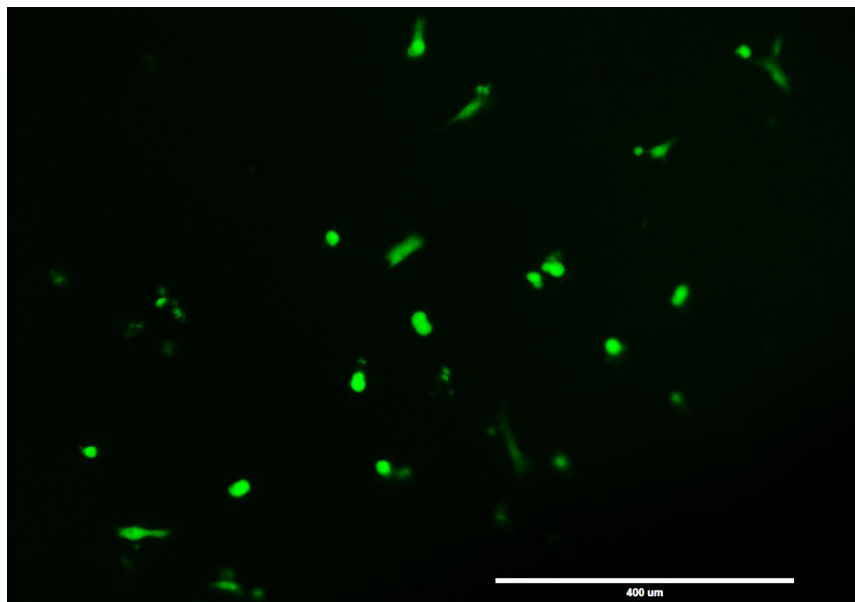


Figure 30. GFP imaging of IMR90 cells on top of 1% UP-LVG bottom gel on Day 10, imaged with x10 objective. The scale is 400 μm .

When compared to results obtained from Experiment 4 (Figure 15) where IMR90 cells were cultivated on top of different alginate gels, the morphology of the cells in Figure 30 resembles the one of those that were cultivated on top of gels with RGD-modified alginate (Figure 17).

3.7 Effect of stiffness and cell number on the survival of IMR90

In the seventh experiment, the effects of gel stiffness and cell number were studied. It was hypothesized that by increasing the number of cells inside of gels the cells would have a better chance of connecting and interacting with each other resulting in higher viability. Stiffness was increased because in studies with Matrigel the gels with higher Matrigel concentration and thus higher stiffness had expressed increased cell attachment and because in some cases the cells had preferred the rigid untreated surface of the well plate over gel matrix. Since the use of RGD-modified alginate had proven to promote cell adhering, it was used for every condition excluding the control sample in this experiment. The conditions in this experiment were following;

1% UP-LVG+OX 1:2 with 1×cells (50 000 cells/gel)
1% UP-LVG+RGD modified alginate 1:2, 1×cells
1% UP-LVG+RGD modified alginate 1:2, 2×cells
1% UP-LVG+RGD modified alginate 1:2, 4×cells
2% UP-LVG+RGD modified alginate 1:2, 1×cells
2% UP-LVG+RGD modified alginate 1:2, 2×cells

The two-layered structure with 1% UP-LVG bottom gel was again used for all conditions and the gels were washed twice with 150 µl cell culturing media after 2 h of gelling on the day of encapsulation. The cells were suspended into cold (+4 °C) 25 mM HEPES-buffer and kept on ice in prior to use. After the washings, 75 µl of cell culture media was added on the gels. The media was changed twice during the 10-day follow-up period on Day 3 and Day 6. Figure 31 and Figure 32 present the images obtained from the screening of a representative plane inside of each gel, covering the whole surface of the well for every gel condition in each control point.

The L/D staining was found to be vague for all gel conditions in images taken on Day 1 and Day 5 but also to some extent on Day 10. In the images taken on these days, the total number of cells seems smaller compared to other points of L/D assaying in Figure 31 and Figure 32 but when examined more closely the cells numbers were higher than it appears in images covering the well surface. On the day of the encapsulation, the number of cells seems lower than expected for the control sample and sample with 1% gel and 1×cells. For other samples, the amount of visible live cells was more coherent with the initial cell concentrations used for each sample group at this point.

On the day after the encapsulation, a high number of dead cells were visible in many samples. Similar behavior had been detected also in earlier experiments and the reason behind this could have been caused by the stress of the encapsulation process. On the image of the sample with 4×cells on Day 7 the overall viability seems rather poor, but this is due to a vague signal from live/dead cells that resided in lower parts of the gel. Although found at close proximity of the bottom, the cells were growing in multiple layers suggesting that they had not migrated out of the gel on to plate bottom.

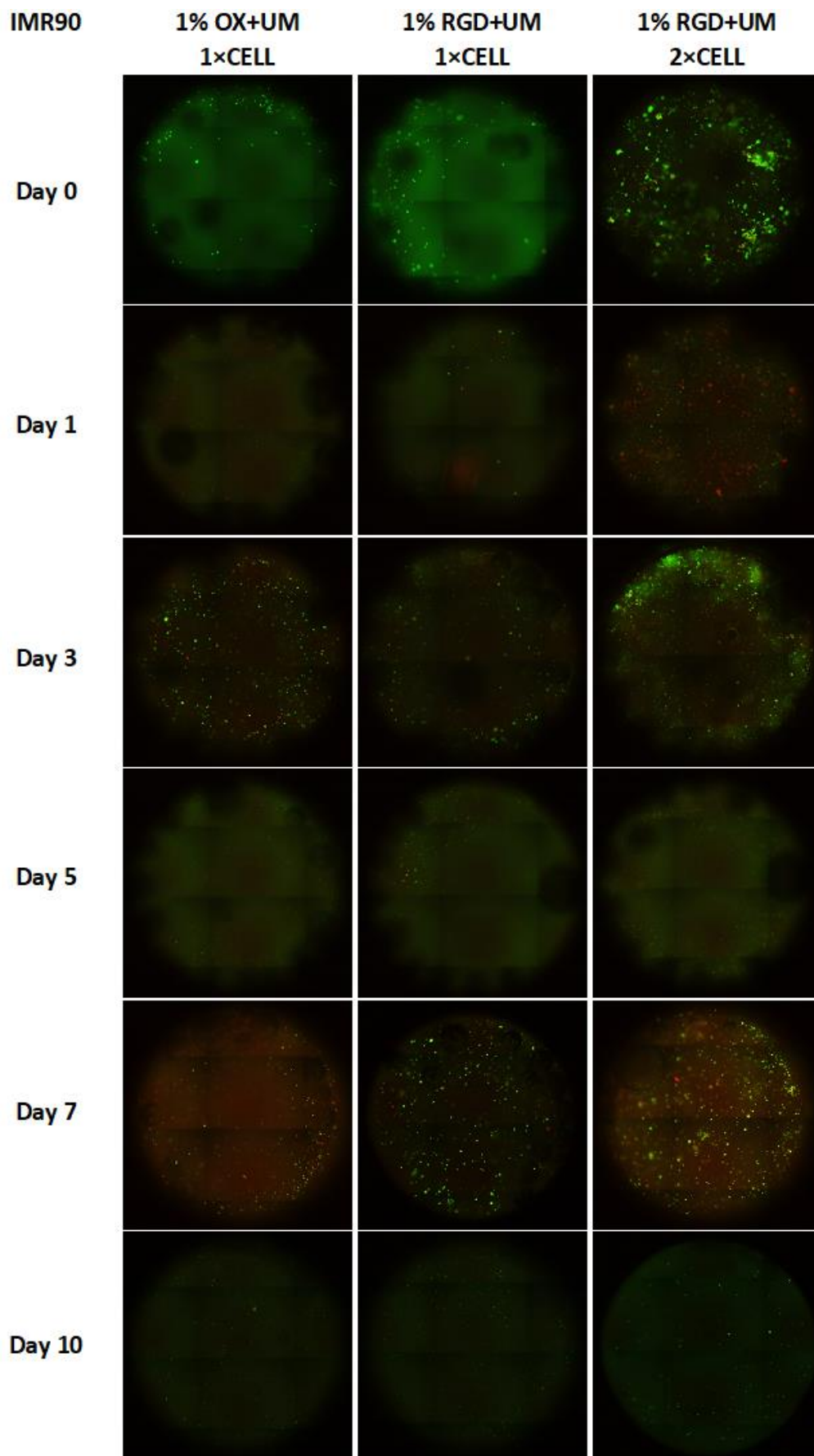


Figure 31. L/D Imaging of IMR90 in Experiment 7. The diameter of one gel is approx. 6,4 mm.

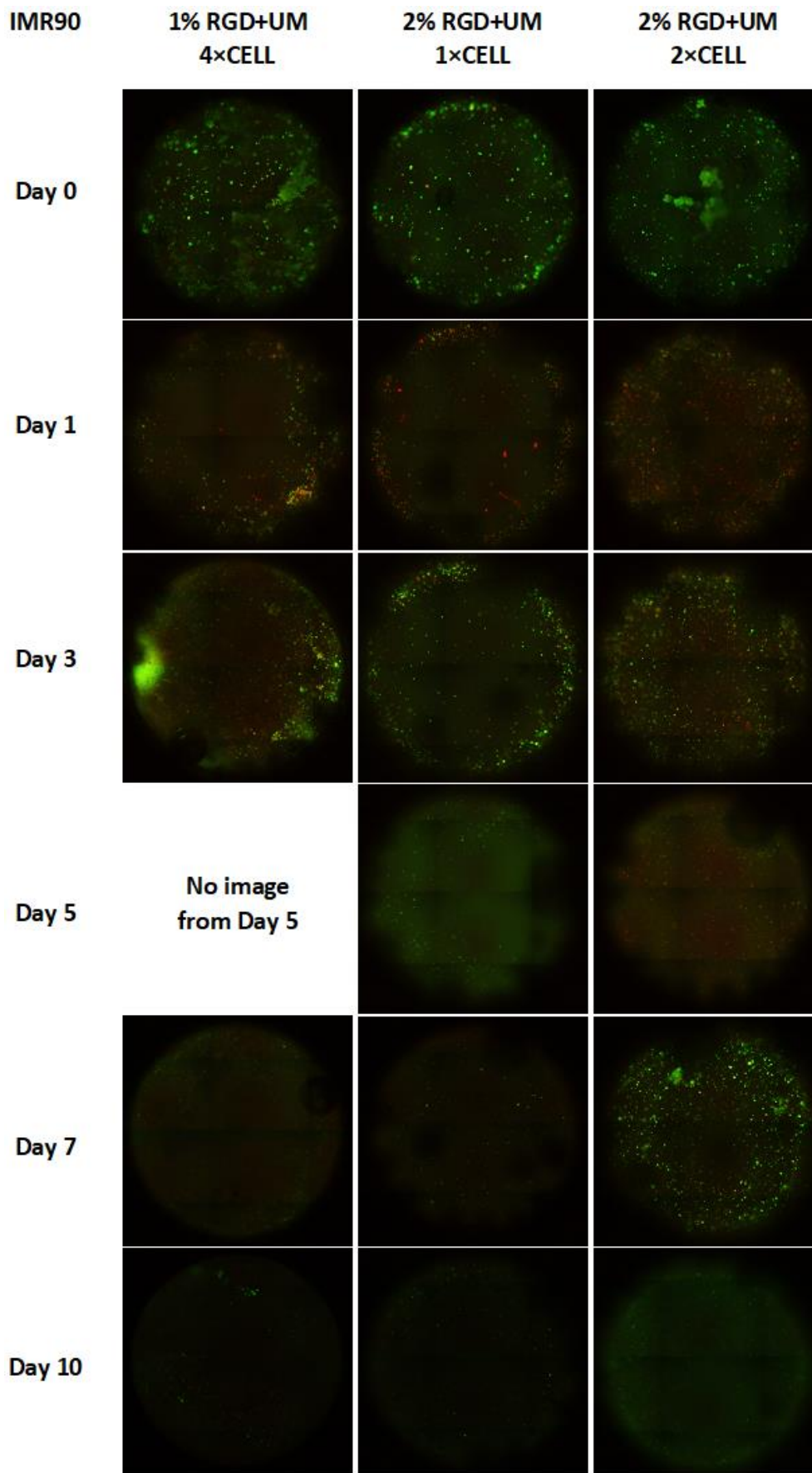


Figure 32. L/D Imaging of IMR90 in Experiment 7. The diameter of one gel is approx. 6,4 mm.

In samples with 1% gels, the results seemed most promising for cell attachment. The first elongated cells depicting of attachment were found just after 24 h from encapsulation in the sample with 4×cells (Figure 33). This was remarkable because in previous experiments it had taken several days before cells exhibiting similar morphology had been detected.

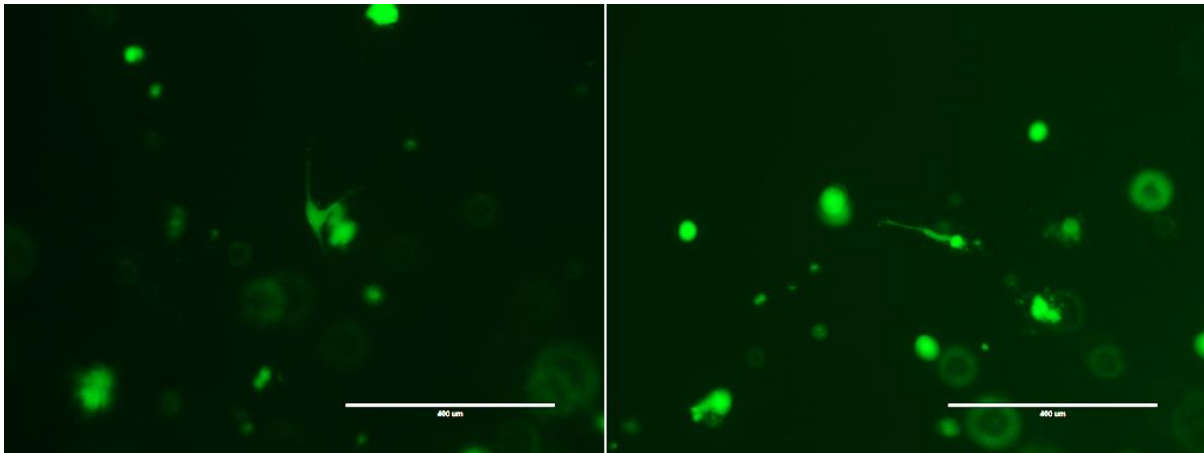


Figure 33. Imaging of live cells in the sample with 1% gel with 1:2 UP-LVG+RGD alginate and 4×cells on Day 1. The scale is 400 μm .

Over the control period, the gels with cell concentrations of 1× and 2× provided the most consistent results on the cell attachment. For these gel conditions, the first cells indicating adhering were found on Day 3. The number of elongated cells was higher in gels with the higher overall number of cells (Figure 34). Because cells were distributed on multiple different layers a ratio between the adhered and non-adhered was difficult to estimate with this imaging method.

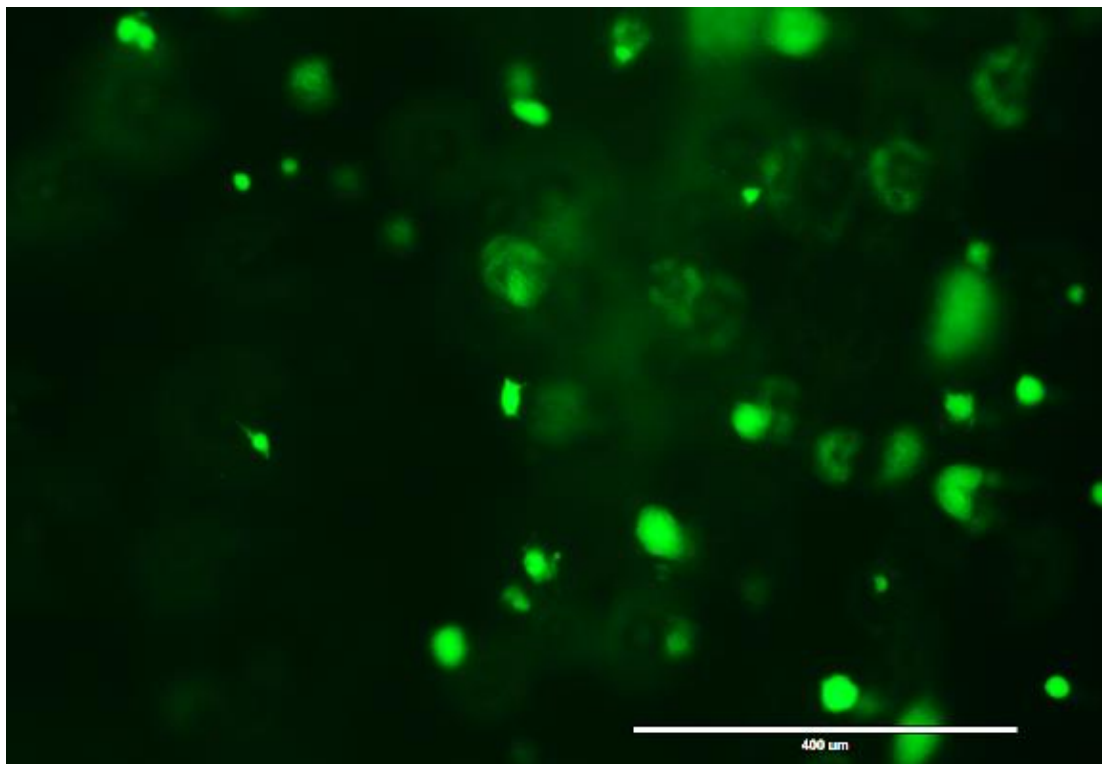


Figure 34. IMR90 in 1% gel with 1:2 UP-LVG+RGD alginate and 2×cell concentration on Day 3. The scale is 400 μm .

On Day 7 on the samples with 1% gel with 2×cell concentration, a noticeable number of cells were found to have likely migrated on the bottom of the well plate (Figure 35). The cells were found on one distinct plane of height at the very low part of the gel and some cells appeared to have spread similarly as when they had attached to the well plate in previous experiments. The migration out of the gel might have been caused by a gradient of nutrients and oxygen between free cell media and gel. The number of dead and live cells inside of the same gel sample is represented in Figure 36. In this figure, the number of live cells seems commendably high but so does the number of dead cells too. If compared to each other the number of live cells is greater, but the rather high number of dead cells could imply a lack of oxygen or nutrients inside the gel.

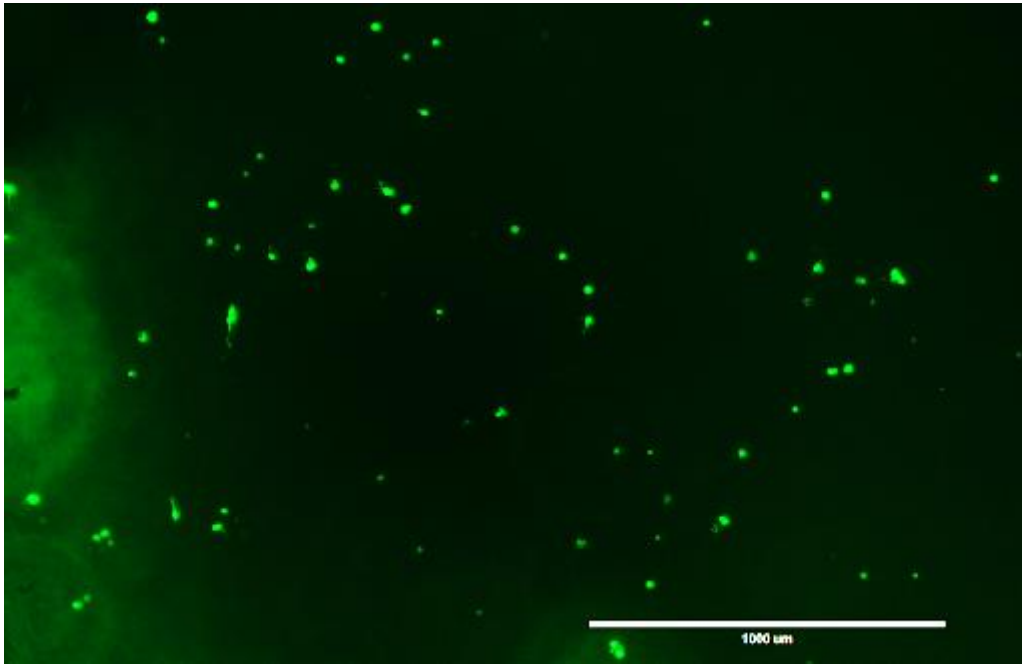


Figure 35. IMR90 likely adhered on the bottom of 96-well plate in the sample with 1% gel and 2×cell concentration on Day 7. The scale is 1000 μm .

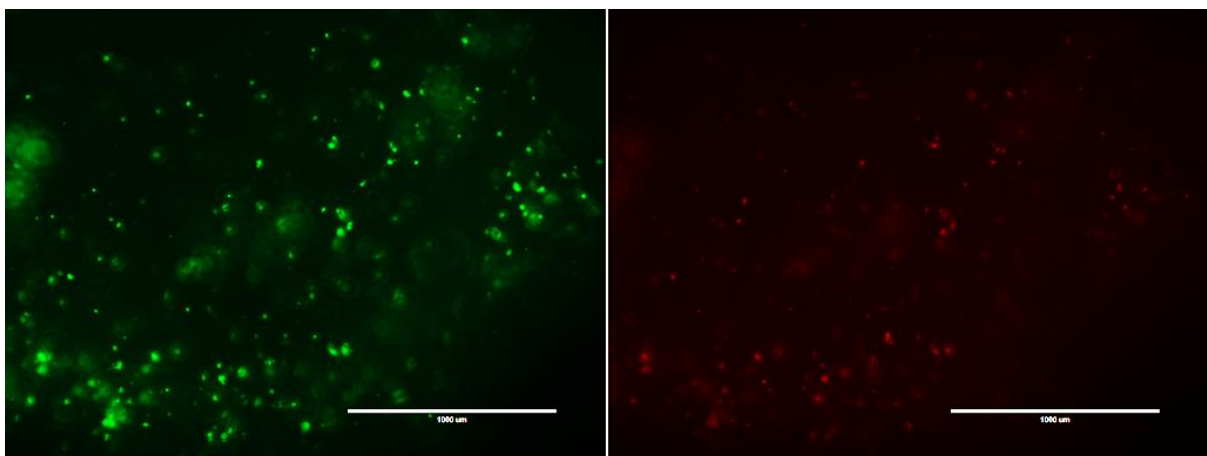


Figure 36. IMR90 cells inside 1% gel and 2×cell concentration on Day 7. Live cells (GFP) on the left and dead cells (RFP) on right. Images were taken at the same height and position of the same gel. The scale is 1000 μm .

The ratio between UP-LVG and the modified alginate was same for all conditions. Due to this the total amount of RGD-modified alginate was double in 2% gels. Despite this in the gels with 2% alginate, the cells were not found to have obtained similar elongated shape as in gels with 1% alginate. Due to the high amount of RGD-modified alginate in the gel, it might be more likely that the lack of elongated cells could have been caused by cells inability to penetrate the stiffer gel structure. Furthermore, during the follow-up period, a small number of cells were found to obtain morphology that could implicate spreading of cell and thus attachment (Figure 37).

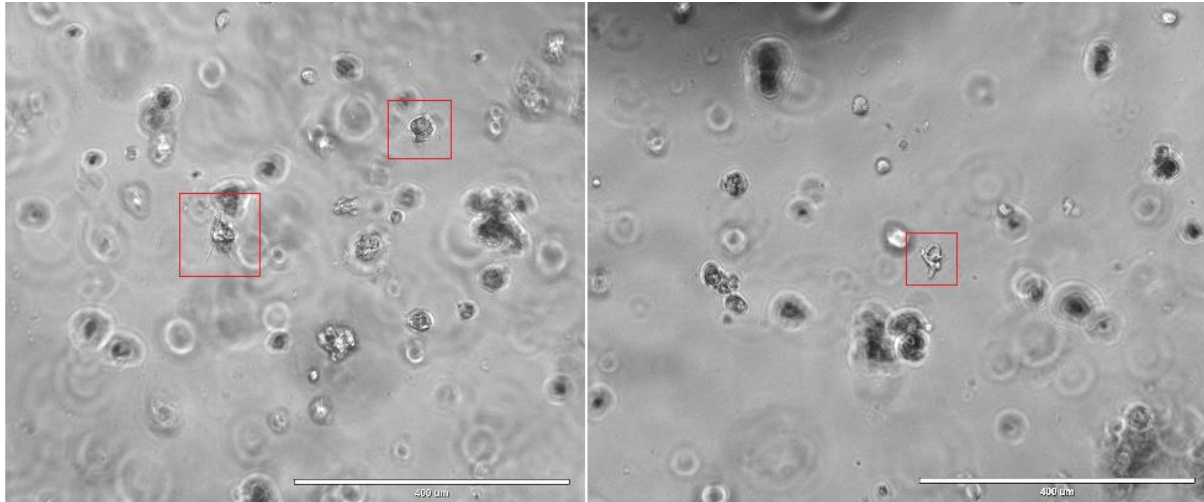


Figure 37. IMR90 cells inside 2% gels with 2xcell concentration on Day 5 (left) and on Day 7 (right). The scale is 400 μm .

Despite that, a decent number of cells remained viable in both 2% conditions till the end of the follow-up period a great number of dead cells were detected in the 2% gels with 2xcell concentration especially on Day 3 and Day 5. The change of media on Day 6 could have slowed down the rate of dying because on Day 7 there were not as many dead cells detected as on the two previous points of imaging. The high number of dead cells could have been caused by the increased need for oxygen and nutrients due to the higher number of cells and the lower rate of the exchange of gas and nutrient due to stiffer gel structure.

3.7.1 Imaging of gels with CLSM

In this experiment, some gels were also imaged using confocal laser scanning microscopy (CLSM) on Day 5 and Day 10. With CLSM it was possible to obtain 3D schemes by screening and combining multiple heights within the gels. However, imaging with CLSM did not cover the whole volume of the gel but only a selected and representative part of it.

In Figure 38, Figure 39 and Figure 40 are represented the 3D views obtained with CLSM on Day 10 of the 1% alginate gels with different cell concentrations. From these figures, the difference in the cell numbers between the samples is visualized. From each of these, multiple cells with an indication of attachment to the material can be detected. A high number of dead cells was found to be in the sample with the 4xcell concentration. Although considering that the sample initially had the highest number of cells, the ratio between live and dead cells seemed worse than for sample with 2xcell concentration. In the sample with 4xcells (Figure 40) a long object visible in the left had been stained by EthD-1 in the L/D assay. This is not be considered as dead cells.

When estimating the number of attached cells in the gels the sample with 2×cells seemed to have most of them in proportion to the total number of cells. But as stated, the images represent only a part of the gel and interpretation of the cell elongation changes depending on the angle from which the 3D scheme was viewed.

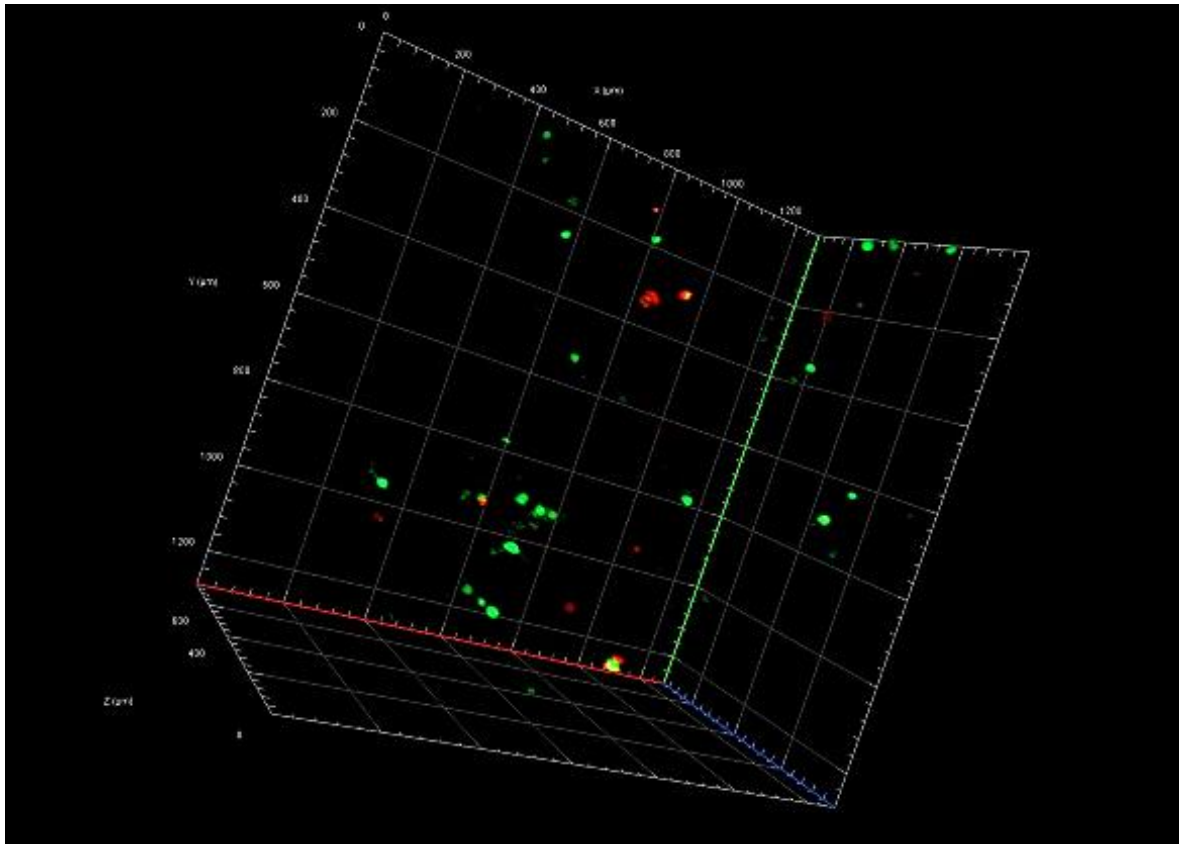


Figure 38. z-Stack of 1% gel with UP-LVG+RGD alginate (1:2) with 1×cells obtained with CLSM on Day 10. The dimensions of the grid are approx. 800×1200×1200 µm.

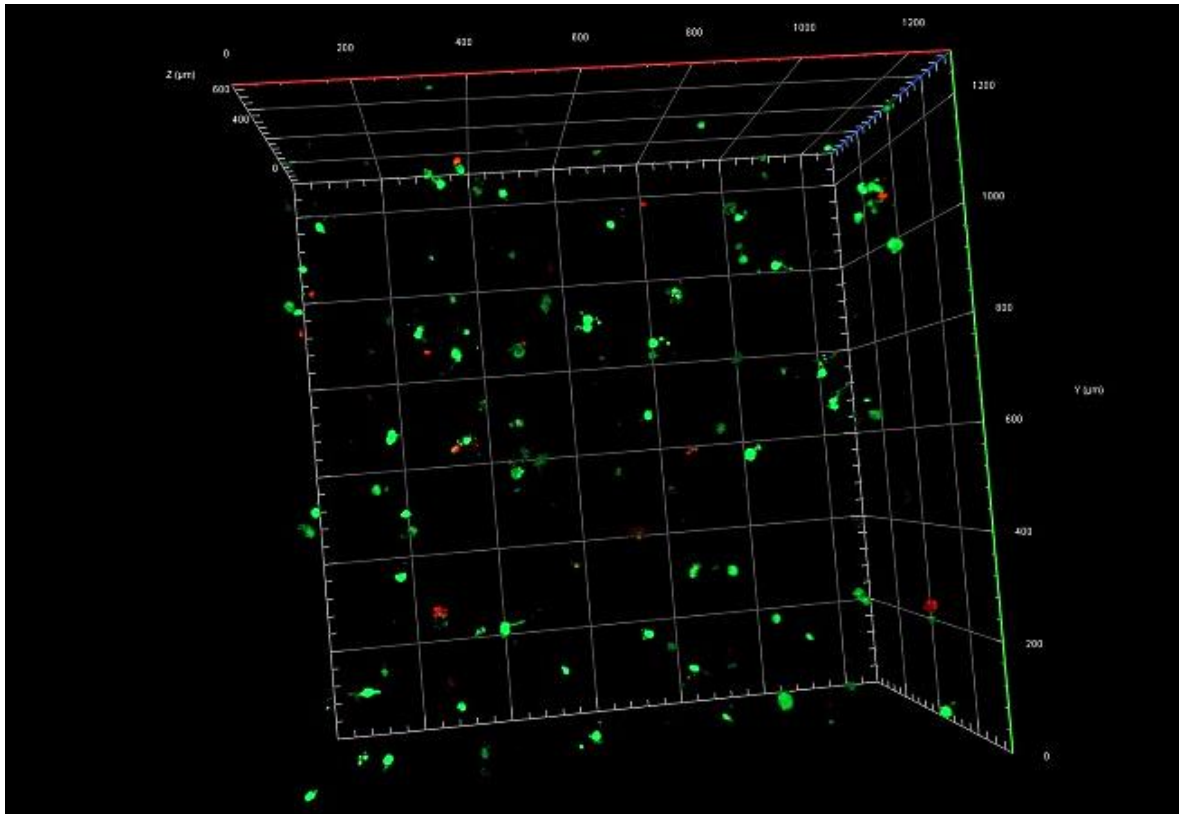


Figure 39. z-Stack of 1% gel with UP-LVG+RGD alginate (1:2) with 2x cells obtained with CLSM on Day 10. The dimensions of the grid are approx. 800x1200x1200 μm.

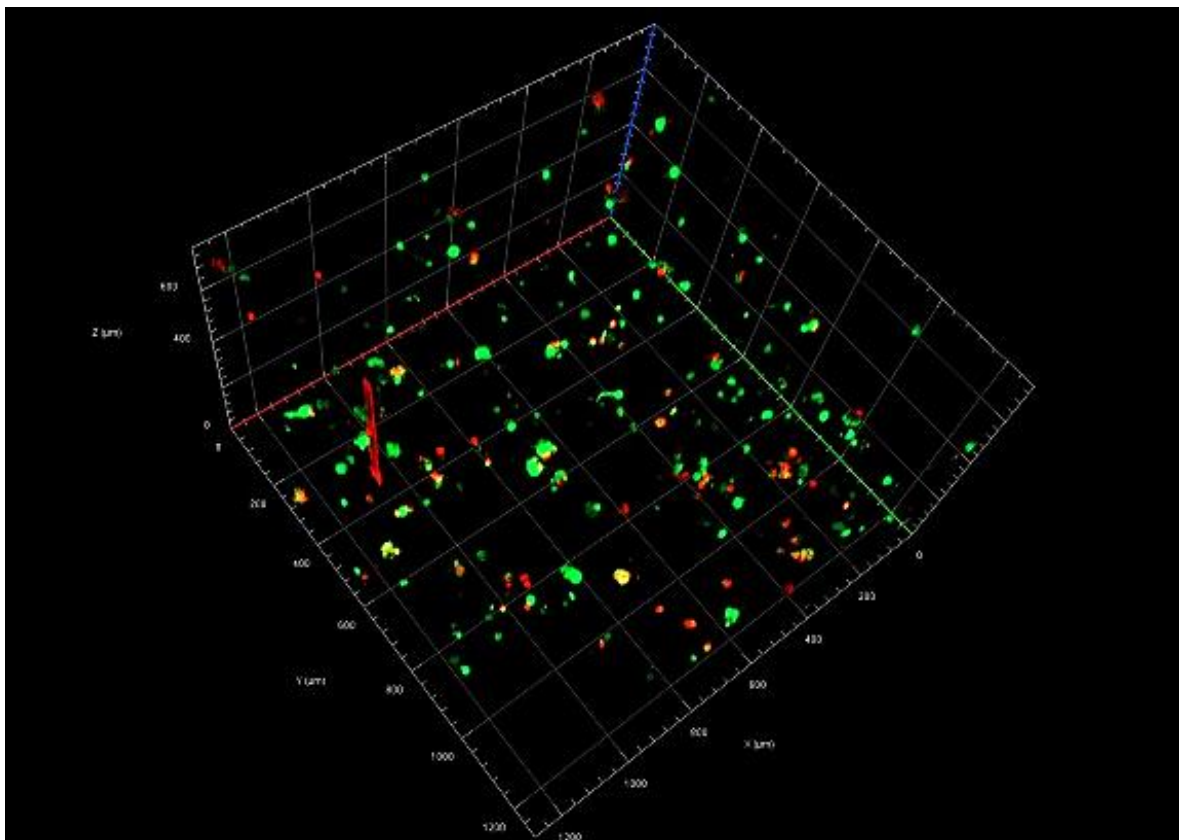


Figure 40. z-Stack of 1% gel with UP-LVG+RGD alginate (1:2) with 4x cells obtained with CLSM on Day 10. The dimensions of the grid are approx. 800x1200x1200 μm.

For better evaluation of the most efficient encapsulation condition, more parallels should be examined at multiple different time points over a similar time period.

CLSM was also used for imaging 2% gels with two different cell concentrations (Figure 41 and Figure 42). Cells in these images are principally round-shaped and seem to indicate very little attachment to the material. In the sample with 2×cell concentration, the amount of dead cells is higher than in the sample with 1% gel and 2×cell.

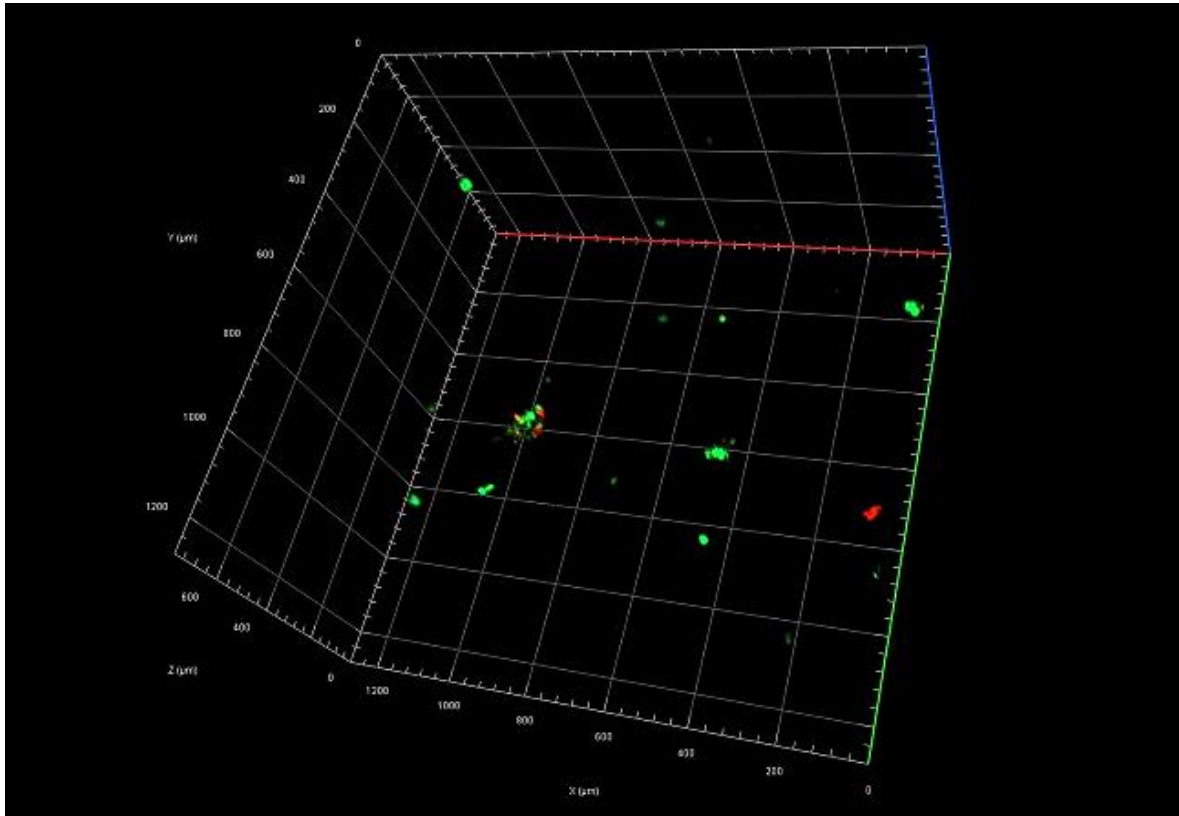


Figure 41. z-Stack of 2% gel with UP-LVG+RGD alginate (1:2) with 1×cells obtained with CLSM on Day 10. The dimensions of the grid are approx. 800×1200×1200 μm.

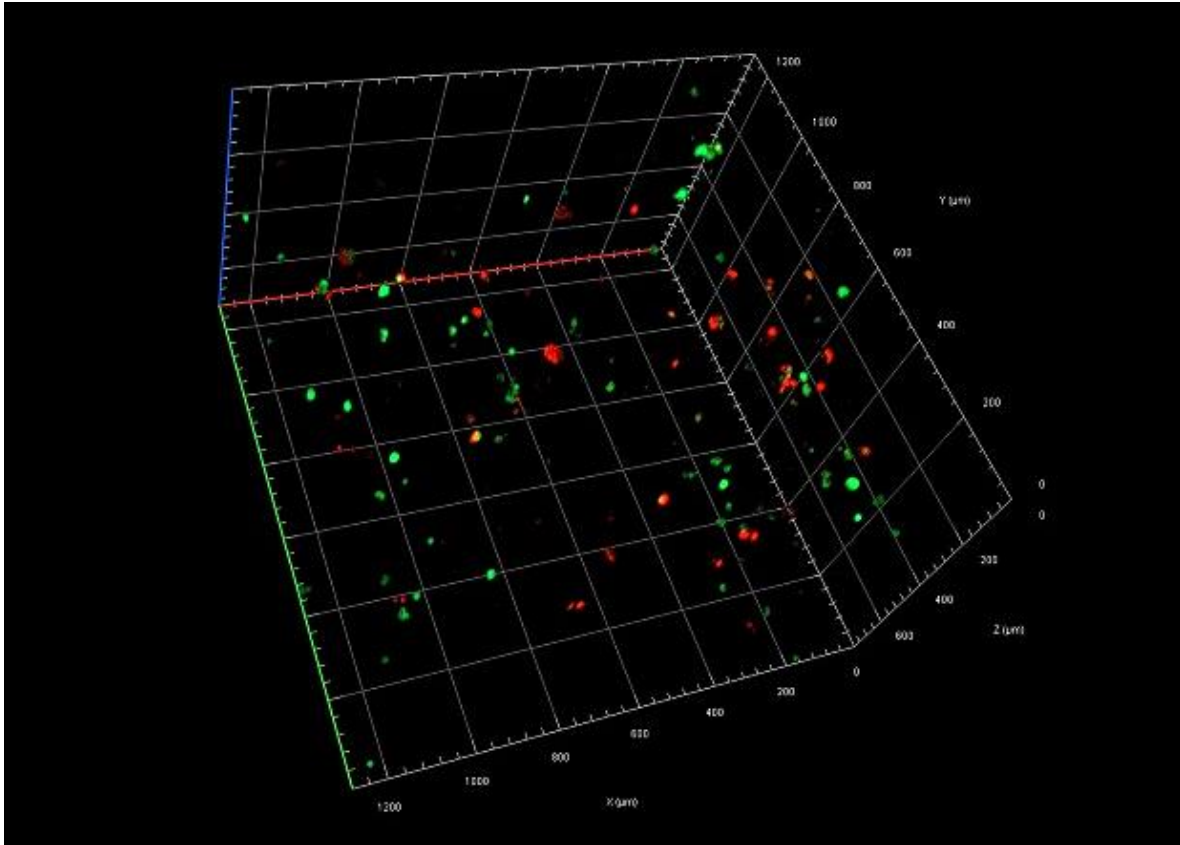


Figure 42. z-Stack of 2% gel with UP-LVG+RGD alginate (1:2) with 2×cells obtained with CLSM on Day 10. The dimensions of the grid are approx. 800×1200×1200 μm.

Samples with a 1×cell concentration in 1% and 2% gels were imaged with CLSM at two different time points. In Figure 43 are two 3D-schemes obtained from these two time points of the 1% gel sample. Cells with an elongated shape were visible in both of these images. However, the total number of cells seemed to have diminished during the control period.

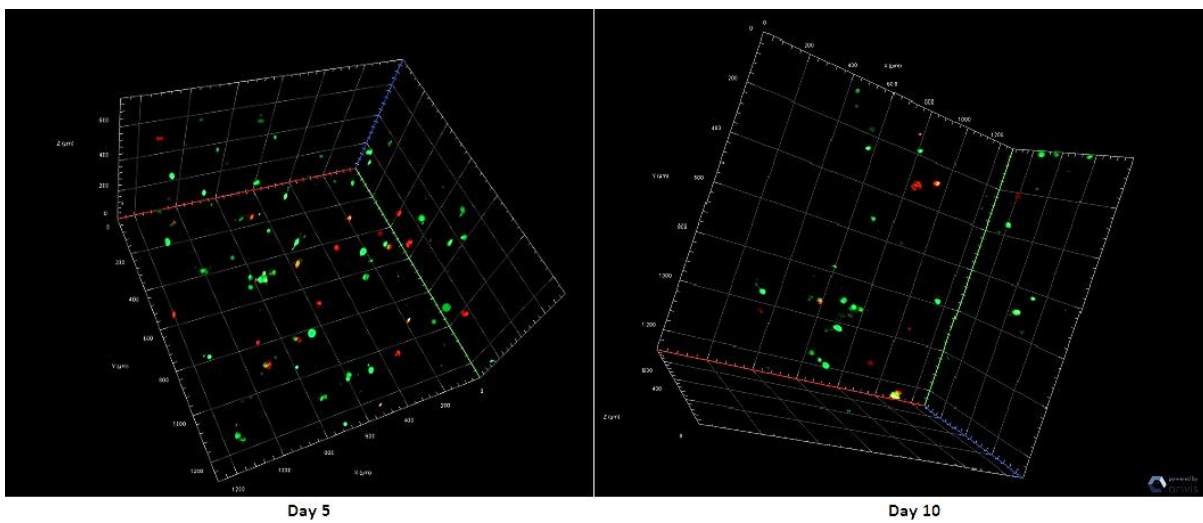


Figure 43. IMR90 in 1% gel with 1xcell concentration imaged with CLSM on Day 5 (left) and Day 10 (right). The dimensions of the grids are approx. 800×1200×1200 μm.

In Figure 44 are represented similar 3D views from samples with 2% gel from the same time points as the images from 1% gels. Cells appearing attached are visible in neither of these images. Despite this, the number of live cells seemed higher for this sample on Day 5 than it did for 1% gel sample and very few dead cells were found. However, on Day 10 the total number of cells was smallest for 2% gel sample.

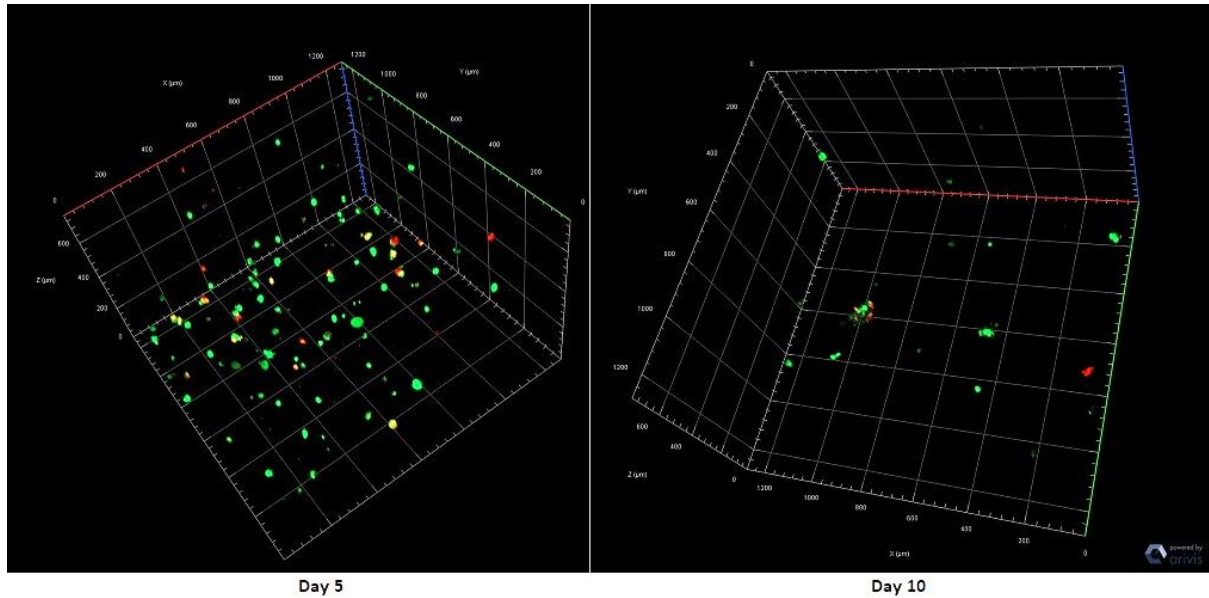


Figure 44. IMR90 in 2% gel with 1xcell concentration imaged with CLSM on Day 5 (left) and Day 10 (right). The dimensions of the grids are approx. $800 \times 1200 \times 1200 \mu\text{m}$.

3.8 Matrigel as a material for matrix

Matrigel is a commercially available material for cultivation and encapsulation of cells. This was tested with HepG2 and IMR90 cell lines in order to compare the support on survival and viability of cells to the survival in alginate-based hydrogels.

3.8.1 Cell cultivation on top of Matrigel

Cultivation of cells on top of Matrigel matrix was tested during the Experiment 4. L/D assay was performed as for alginate hydrogels in the same experiment. In Figure 45 are the results from the imaging. For these pictures, only GFP is imaged because there were no dead cells visible and the RFP would have only increased the background signal in here. Viability of cells was followed over a five-day period. The cell culture media was not changed during this time. The final concentration of Matrigel in the gels was 10,0 mg/ml.

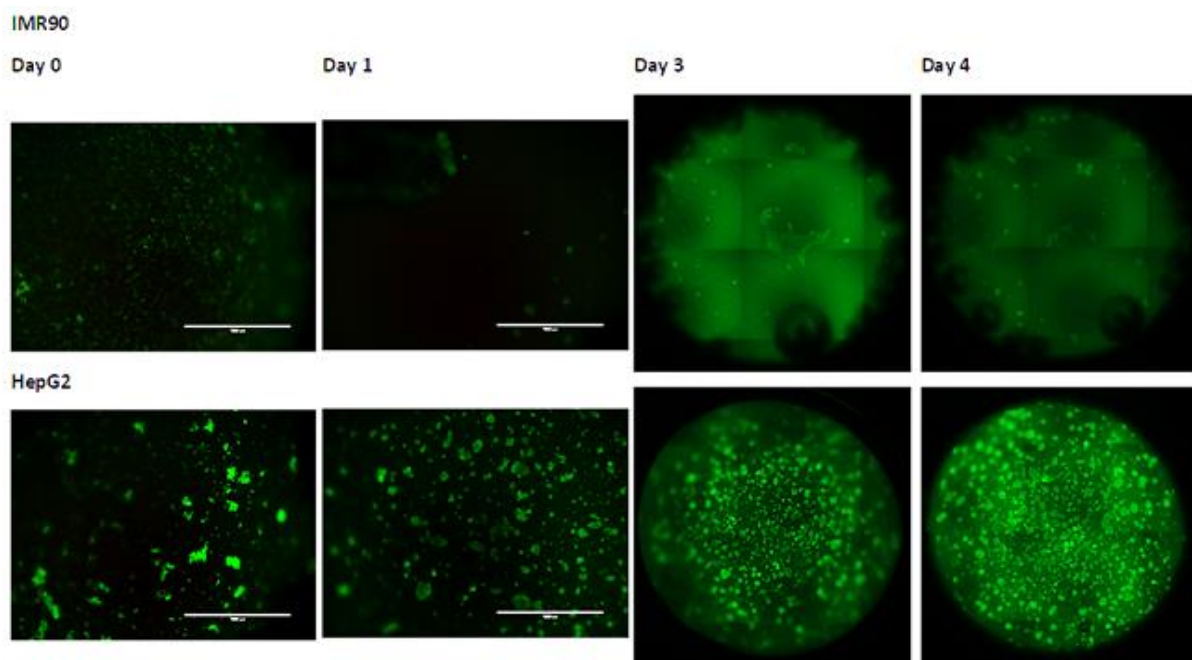


Figure 45. IMR90 and HepG2 cells cultivated on top of Matrigel®. The scale is 1000 μm for images on the left. In the images covering the well surface, the diameter of one gel is approx. 6,4 mm.

On the day of cell seeding, there were a great number of cells alive for both cell lines. After one day the HepG2 seemed very much viable but the number of IMR90 cells seemed to have plummeted. On Day 3 and Day 4 the whole surfaces of the gels were imaged to assess the distribution of cells. From these, it can be determined that HepG2 cells were evenly distributed and viable during the last day of the experiment on Day 4. For IMR90 the Matrigel gels seemed to be less favorable.

In the images of IMR90 from Day 3 and Day 4 cluster-like structures are visible approx. in the middle of the well. In an attempt to image this structure, it was found to be out of reach of the focus of the microscope. In Figure 46 the surface of the gel with cells growing on top of it is imaged with the peculiar cluster. This could be caused by a portion of cells detaching from the gel surface and then floating in the medium.

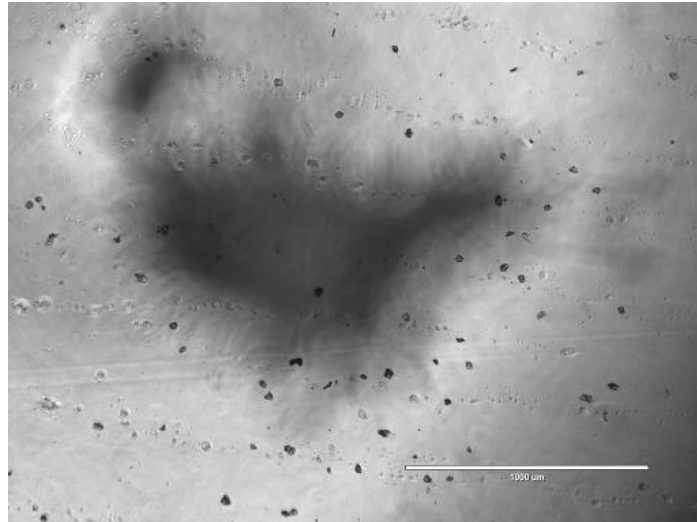


Figure 46. Phase imaging of IMR90 cells cultivated on top of Matrigel during Day 3. The scale is 1000 μm . (Original color and brightness)

The L/D assay solution was added on the samples in Experiment 4 at the same time and then incubated for 45 min in RT. After this, the plates with alginate-based hydrogels were imaged first and the plate with Matrigel last. The imaging of the first plates lasting approx. 2 h increased the incubation time of the Matrigel plate closer to 3 h in total. In an experiment where cells are cultivated on top of the gel, the exposure has been even greater compared to when cells are encapsulated inside of gel.

3.8.2 Encapsulation of cells into high concentration Matrigel

IMR90 and HepG2 cells were encapsulated also in Matrigel during Experiment 5. As in Experiment 5, the viability of the cells was followed over a 10-day period and the cell culture media was changed on Day 2 and Day 5. Again, only GFP was imaged for Matrigel encapsulated cells for the full well surface covering pictures. The concentration of Matrigel in gels for IMR90 cells was 4,9 mg/ml and 5,2 mg/ml for HepG2. The cells were prepared to chill (+4 °C) culture media and were kept on ice during the encapsulation procedure.

In Figure 47 are results obtained from microscope imaging covering the full well surface of samples with IMR90 cells. In this picture, the cells visible are located inside of the gels. On the day of encapsulation and on the following day the signal from the live cells is relatively high but seemed to decrease after the first days. In Figure 49 images from Day 5 and 7 are represented separately in a larger size. From this, it can be seen that a high number of cells were alive in the later part of the follow-up period. However, the cells appeared very small in size and less clustered as on Day 0 and Day 1.

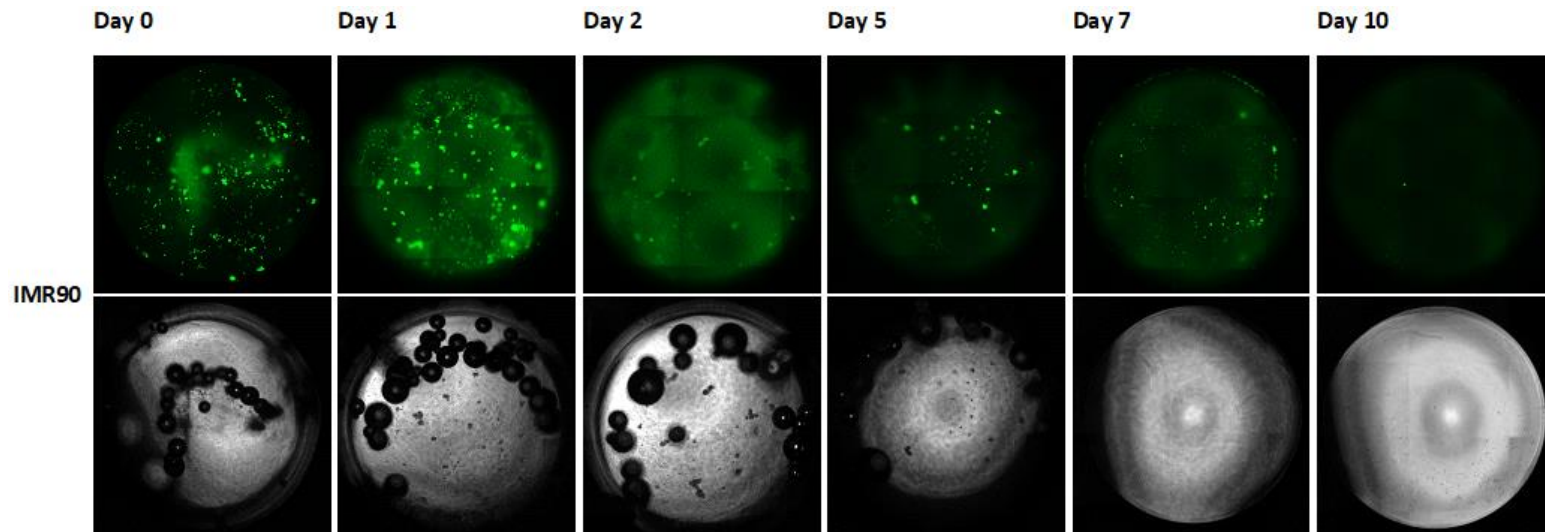


Figure 47. GFP and phase imaging of IMR90 cells encapsulated in Matrigel. Original contrast, brightness increased by 20% in phase images.

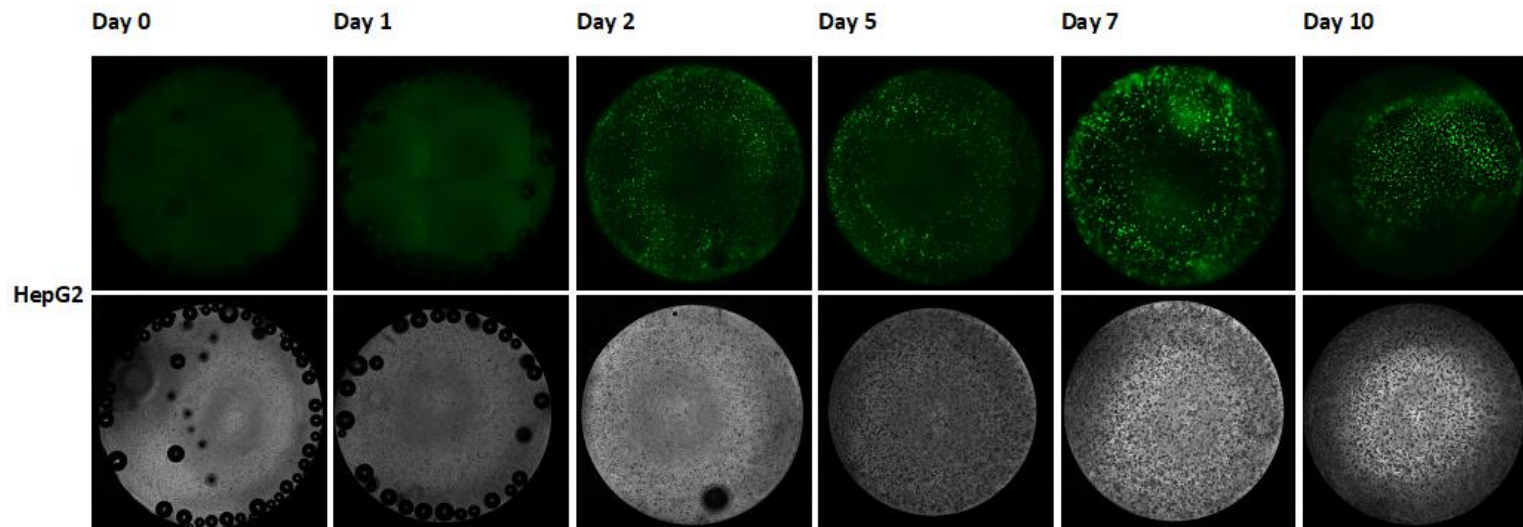


Figure 48. GFP and phase imaging of HepG2 cells encapsulated in Matrigel. Original contrast and brightness in phase images.

Day 5

Day 7

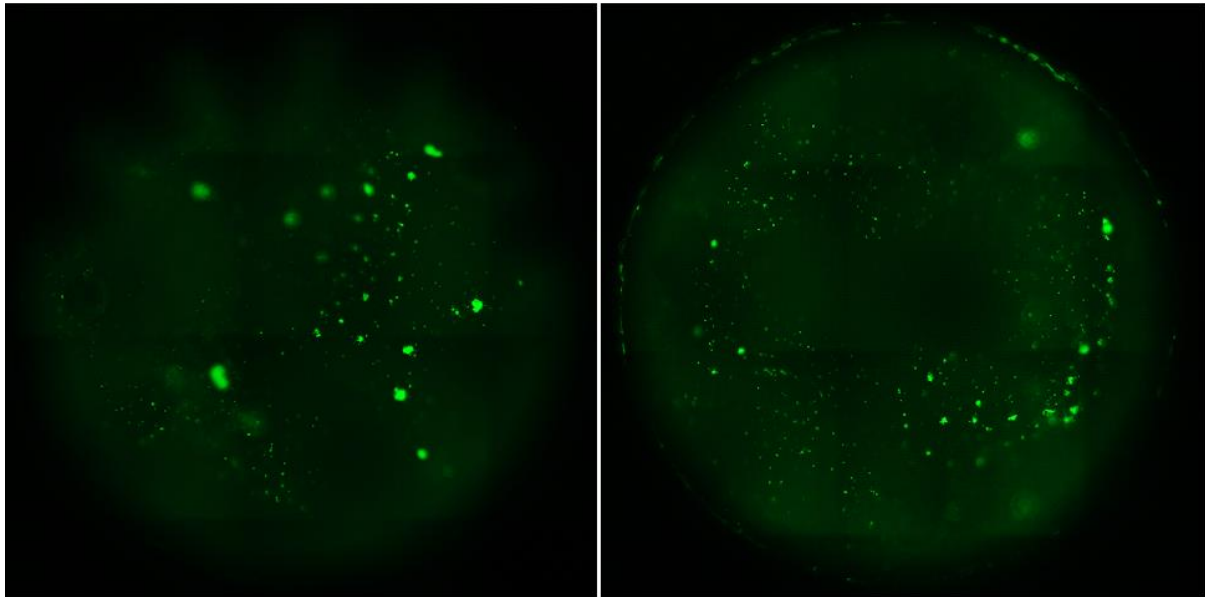


Figure 49. Imaging of live IMR90 cells inside 5mg/ml Matrigel on after 5 and 7 days from the encapsulation. The diameter of one gel is approx. 6,4 mm.

The very low number of detected live cells inside the gels on Day 10 in Figure 47 might be partly due to the migration of the IMR90 cells. In Figure 50 are images taken from the bottom of the well of the same samples from the last two time points of the control period. In these, the cells have obtained a shape indicating an attachment to the well surface on Day 7 and forward.

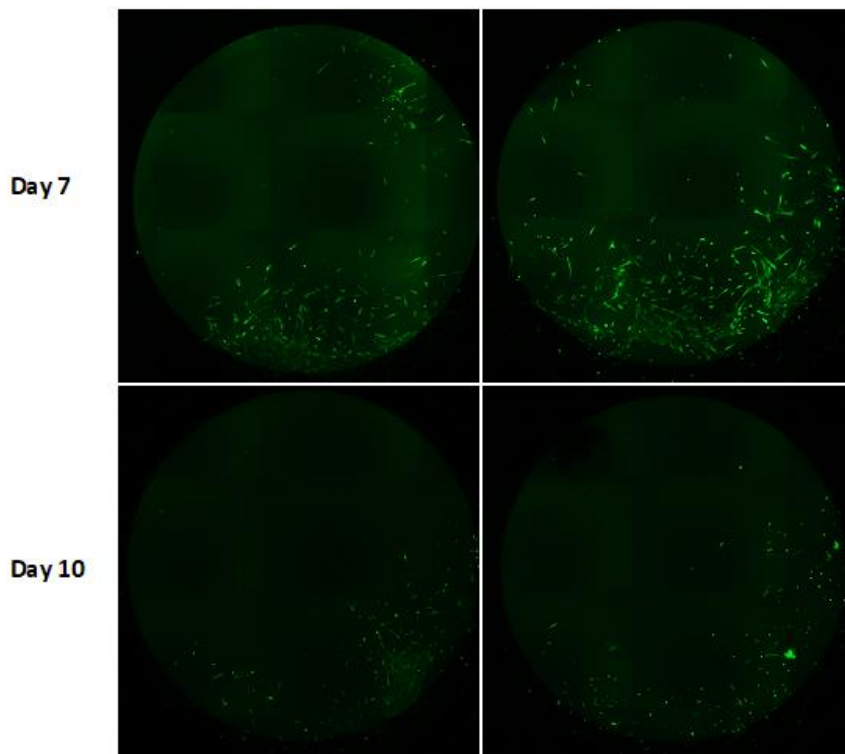


Figure 50. L/D imaging of IMR90 cells in the well plate surface and under the Matrigel on Day 7 and Day 10. The diameter of one gel is approx. 6,4 mm.

Even though a notable number of cells likely adhered on the well plate surface, some indication of cell attachment on the Matrigel was discovered already on Day 5 and also in another sample on Day 7 (Figure 51).

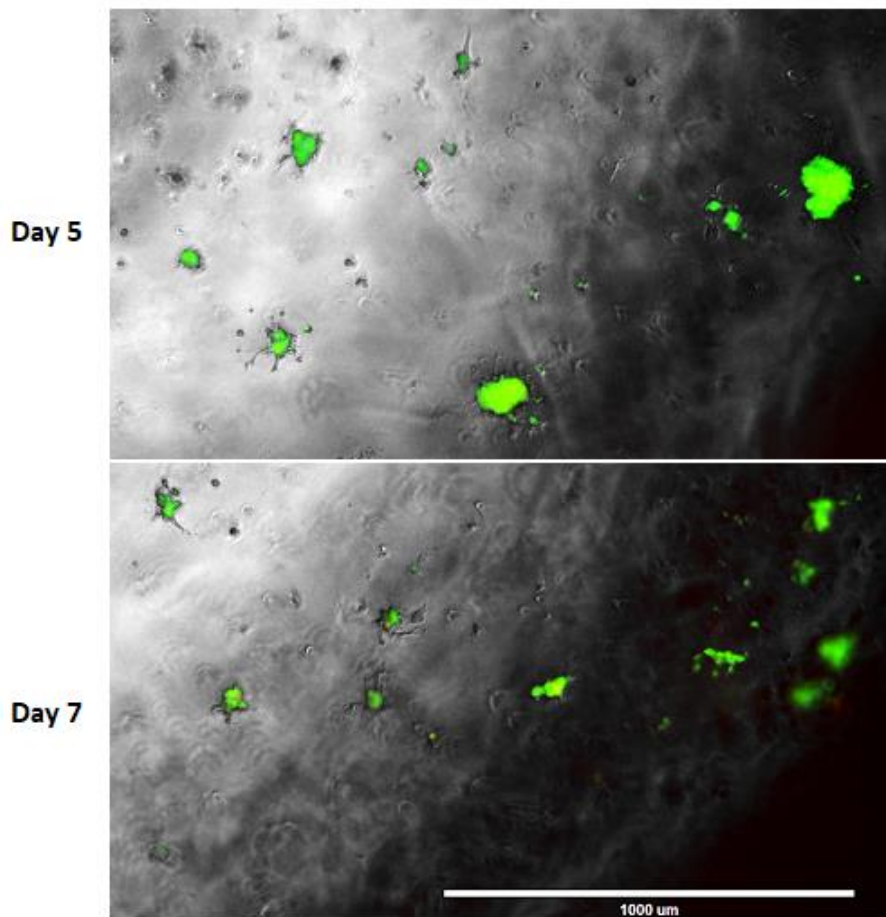


Figure 51. GFP/phase imaging of possibly adhered IMR90 cells inside of Matrigel on Day 5 (above) and on Day 7 (below). Brightness and contrast increased by 20%. The scale is 1000 μm .

Images taken at the beginning of the follow-up period had more vague staining of live cells than in images from the later part of the experiment for HepG2 (Figure 48). The increase in the live signal may have been due to proliferation and spreading of HepG2 that was detected on Day 10 (Figure 52). Generally, Matrigel seemed to support the survival and viability of HepG2 cells better than of IMR90 cells but the HepG2 cell line has proven to be more viable in other materials too when compared to IMR90.

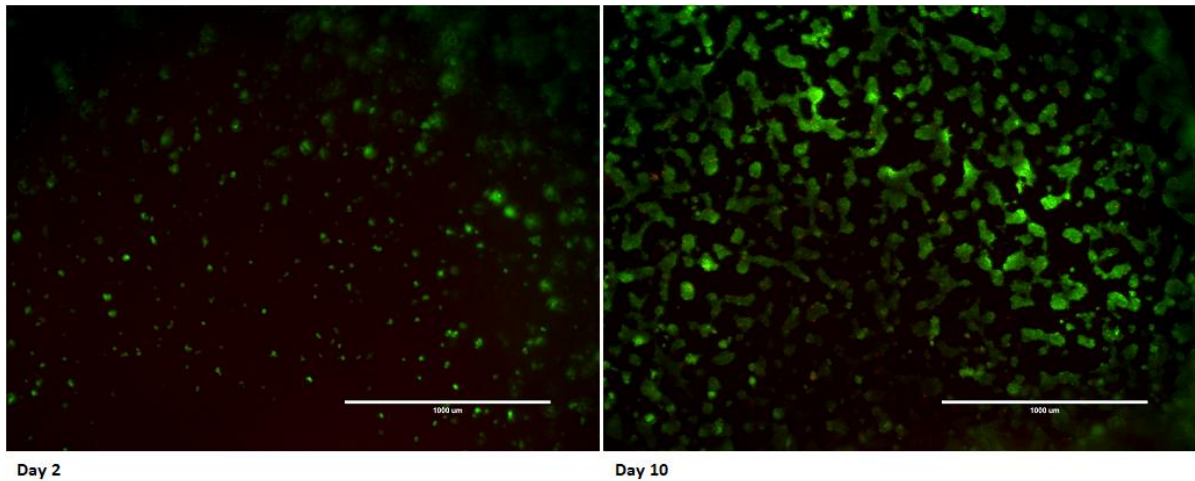


Figure 52. HepG2 in Matrigel during Day 2 and Day 10. The scale is 1000 μ m.

3.8.3 Encapsulation of IMR90 into high concentration Matrigel

Encapsulation of IMR90 cells into Matrigel matrix with higher (10,0 mg/ml) Matrigel concentration was studied. Again approx. 50 000 cells were encapsulated inside of gel with a total volume of 65 μ l. The viability of cells was followed over a 10-day period and the cell culture media in which the gels were in, was changed once during this period on Day 5.

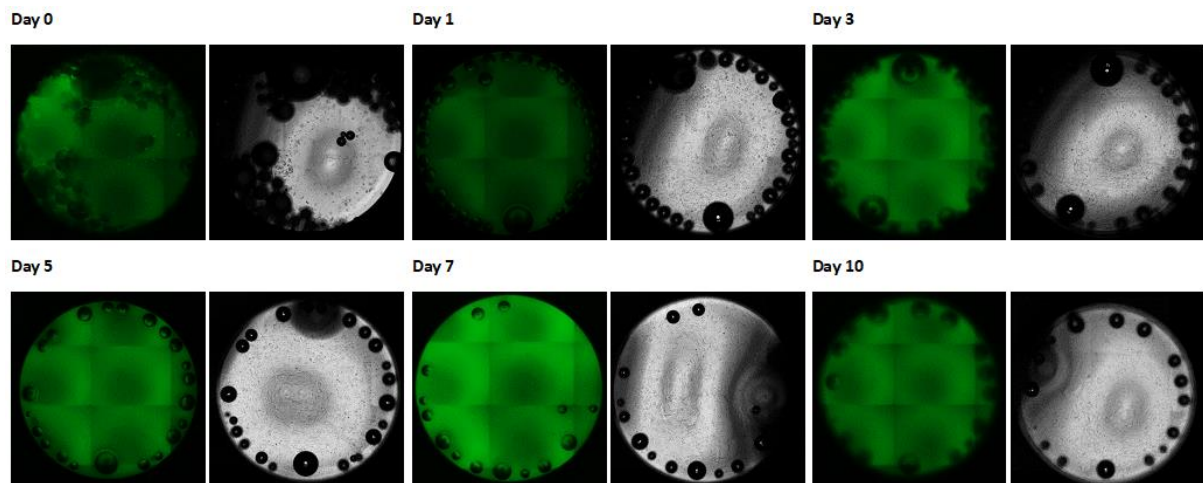


Figure 53. IMR90 cells encapsulated into high concentration Matrigel matrix. Both phase and GFP views represented for each time point. The diameter of one gel is approx. 6,4 mm.

During the control period, the L/D assay used proved to be even more improper for staining of Matrigel cultures than in previous experiments with Matrigel. The fluorescent signal from the cells was very vague in every time point examined due to a high background signal. On the day of the encapsulation, the cells (Day 0) were most visible (Figure 54) compared to the later points of when the gels were imaged.

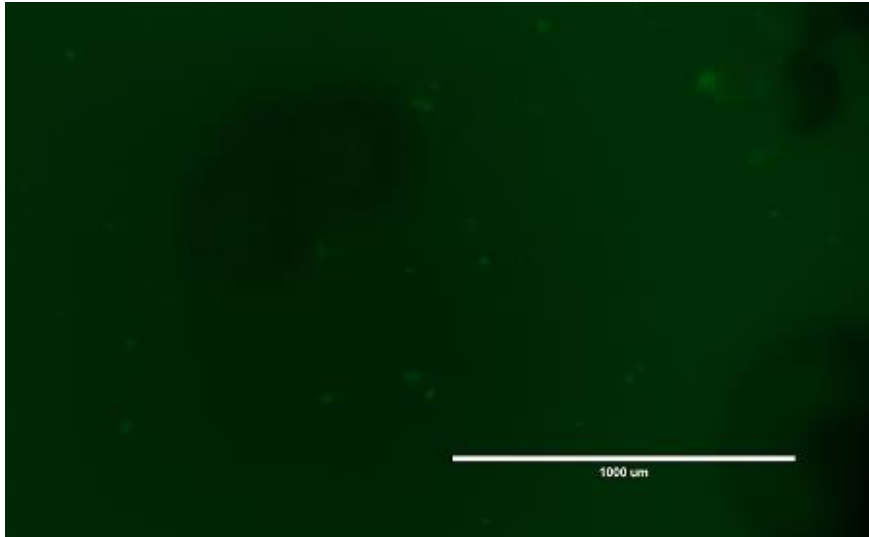
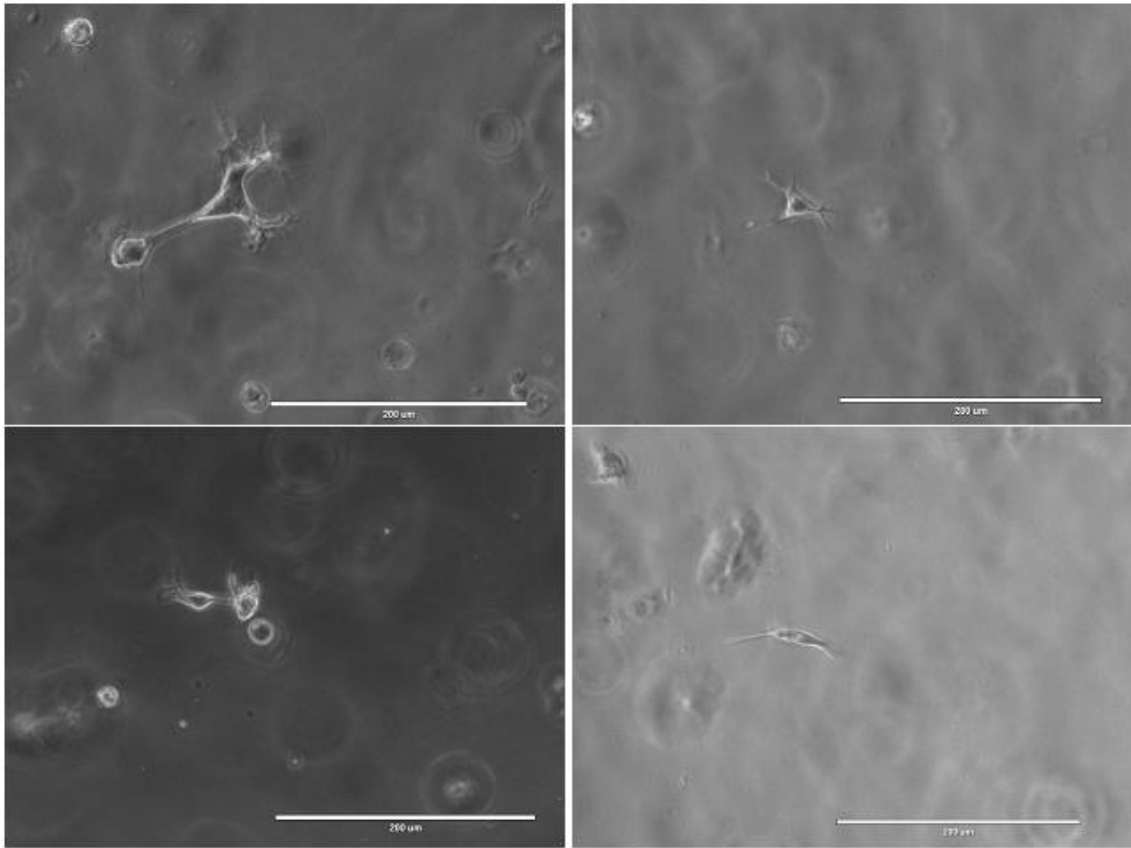


Figure 54. Imaging of live IMR90 cells in 10 mg/ml Matrigel gel on Day 0. The scale is 1000 μm . Original brightness and contrast.

The gels were stained with calcein and EthD-1 as in all L/D assays carried out here. As before the EthD-1 staining was found to be vague and very little dead cells were reliably detected. This time also the detection of live cells was found to be difficult too. It is possible that the L/D stains were binding to the Matrigel and thus caused the high background signal. Matrigel is derived from sarcoma of Engelbreth-Holm-Swarm mouse and might contain traces of the intracellular esterases that convert the calcein AM into fluorescent calcein. (39) (36)

When the incubation time of the staining was increased the cells became even less visible and faded in the background signal of GFP. Because of this, the evaluation of the cell morphology was done from images taken with non-fluorescent light (e.g. as in Figure 55). Unfortunately, the viability of the cells could not be determined from these.

As in the experiment where cells were encapsulated into Matrigel with the concentration of 5 mg/ml, in most samples, the IMR90 cells were also found on a very low level of the gel structure and likely attached to the surface of the well plate. However, unlike in the low-concentration gels, the number of cells inside the 10 mg/ml gels was significantly higher than outside of them. On Day 5 and forward part of the cells that were found inside the gel structure exhibited a morphology suggesting an attachment to the material (Figure 55).



Matrigel (10 mg/ml) - Day 5

Figure 55. IMR90 cells encapsulated inside a high concentration Matrigel matrix on Day 5. Original brightness and contrast. x20 objective used for each separate image. The scale is 200 μm .

4 Discussion

The primary target of the experiments was to find an optimal alginate-based hydrogel material that would be able to support the viability of IMR90 cells. In the experiments for this thesis and in previous experiments for this project, the overall survival of IMR90 had been more or less poor when used in encapsulation experiments and the viability had proven to be challenging to support. Because of this, the other cell line HepG2 was used in these experiments as a control.

4.1 Increasing the rate of survival

The focus of the first experiments was on improving the survival of encapsulated cells and extending the time that the cells remained viable inside of the 3D environment. Washing of gels after encapsulating the cells in it was carried out in order to remove excess calcium and other possible compounds that might have affected decreasingly to cell viability. Calcium is an important signaling molecule in mammals with multiple purposes and functions e.g. in synaptic signaling and muscle contraction. Intracellular and extracellular concentrations of calcium are strictly regulated. In vertebrates, the concentration of free calcium in the cytosol is less than 0,1 μM and it is kept low by active pumping into intracellular calcium storages and out of the cell. In extracellular space, the concentration of calcium is 1 mM. Pumping of calcium out of the cell against a higher concentration is energy consuming and requires ATP to function. (40)

In each experiment, Ca^{2+} was used as a gelling agent of alginate and was added in as CaCO_3 solution. The final concentration of Ca^{2+} for 1 % gels were 18 mM and 15 mM for 0,5 % gels. Although the most calcium ions bind to G-blocks in alginate the initial concentration of calcium in the gels is likely higher than cells generally experience in vivo. Washing of the gels was introduced in order to reduce the amount of free calcium in the system and thus inducing a more compatible environment for the cells. In the first experiment, a $1 \times 150 \mu\text{l}$ washing step with cell culture media was of the gel was performed and compared to gels that had not been exposed to washing. In the second experiment, washing was increased to $2 \times 150 \mu\text{l}$. Although no clear indication of the effectivity of the washing procedure was detected, it was hypothesized to improve the viability of the cells.

In the third experiment, cells were exposed to very low-temperature conditions (+4 °C) to study if the low-metabolic state of hypothermic cells would protect them from the mechanical and chemical stress the cells were likely exposed during the encapsulation procedure. For mammalian cells, a temperature of +4 °C is very low and cells exposed to temperature as low as this, experience severe hypothermia. Under these conditions, the natural cell cycle is arrested, and cells do not proliferate or grow. (41) Some studies have shown that a short time exposure to cold (1 h) following a reheating step to 37 °C has induced synchronization of the mitotic cycle in the cells. Cells from different cell lines have shown to enter mitosis 11-17 h after recovering from the cold shock. (42) Under serious cold stress, cells have been shown to have changes in their structure and morphology. In very cold temperatures (but above subzero) cells can appear less spread and more rounded, be generally smaller in size and have nuclei with contracted diameter. Severe cold shock can cause the cells to die and in a study by M.J. Carden et al. the survival rate of cells rewarming from +4 °C was 70-80% from the initial number of cells. (41)

Although the experiment gave a little support for the effectiveness of the cold-treatment for improving cell survival, more promising results from this was gained by Daria Zaytseva-Zotova in experiments related to this project. Because of this, it was decided that the cells would be exposed to hypothermia in further encapsulation experiments too.

4.2 Enhancing viability by promoting cell attachment

Because fibroblasts tend to obtain a very distinct shape when they adhere, the attachment of IMR90 cells to the 3D gel material was interpreted to some extent from their morphology. In most of the experiments, the cells were initially encapsulated inside of hydrogels. In many cases after cultivating the cells within these gels over different periods of time, there was no indication of attachment to the materials with cells that were undisputedly inside of the gel where they had been encapsulated. However, in some of these experiments, attachment indicating formations were discovered. In most of these cases, the cells were found to have formed a distinct layer of cells despite that they had presumably been evenly distributed within the whole gel volume by two vigorous steps of mixing (2000 RPM for 30 s after addition of cell-CaCO₃-suspension and again after GDL-solution) during the encapsulation process. When the layer formation was studied more closely it was found to be caused by cells adhering to the bottom of the well plate. In an attempt to avoid attachment to the well plate an insulating 'bottom' gel was used below the actual cell-matrix layer, but it proved not to prevent this especially in cases where the top material failed to form a stable gel.

In the experiment where cells were cultivated on top of alginate gels containing different cell adhesion promoting peptides, the RGD-modified alginate was found to promote cell attachment on IMR90. The RGD-modified alginate was then further tested and used for cell encapsulation experiments. First gels with UP-LVG+RGD alginate were tested in Experiment 5 with a ratio of 1:1. During this very little indication of attachment to the gel material was detected. Also, in one parallel of these samples during Day 1 and Day 2 cells were found to have formed a monolayer and seemed to have adhered to the well plate surface.

After obtaining contradictive results from gels with UP-LVG+RGD alginate, it was decided that the experiment should be repeated. Two different UP-LVG and RGD alginate ratios were then tested, 1:1 ratio for repetition and 1:3 ratio with 25% of UP-LVG and 75% of RGD-modified alginate, to study whether increasing the amount of RGD-peptide would have an effect on cell attachment. This time the results were found to be more coherent and an indication of cell attachment in both materials was detected. When comparing the results of these two conditions the 1:3 ratio seemed to have been more favorable over to 1:1 ratio gel, suggesting that increase in the amount of RGD-modified alginate would increase cell adhesion. A ratio of 1:2 of UP-LVG and RGD-alginate in gels were also tested. This ratio was found to promote cell adhering more better than gels with a 1:1 ratio and possibly less effectively than the 1:3 ratio.

As expected, the overall survival was higher for HepG2 cells as for IMR90 cells, in most gel conditions and treatments. The purpose of the HepG2 cell line was to provide output of the possible effects of the material to the cells inside the gels and a reference point to results obtained from experiments with IMR90 cells. No undisputable adhering to the gel matrix was detected with HepG2 cells but considering that this cell line is naturally rather circular and inclined for clustering, this was not as easy to determine as with IMR90.

4.3 Mechanical properties of ECM and the effect on cells

In natural solid tissues, ECM is the material surrounding the cells. Consisting of a plethora of proteins and sugars it provides a scaffold for organs and other tissues. ECM has also a role in cellular communication and regulation, e.g. in cell proliferation and differentiation. Different tissues vary greatly from each other functionally, structurally and mechanically and these differences can be rather apparent. For example, bone tissue is much harder compared to liver tissue and executes very different functions inside the body. All the biochemical and -physical properties of the ECM are profoundly prescribing for any certain tissues and these alter the fate of the resident cells from transcriptional level to interactions with other cells. (43)

Stiffness of ECM is one aspect of the biophysical property of every tissue. This is a feature that also differs in a great extent within the tissues found in the human body, from a hard-solid stiffness of bone tissue to liquid-like structure of blood. Most tissue-resided cells are accommodated to certain stiffness of the ECM and changes in it can have a profound effect on the cells. In some studies, it has been found that an increase of ECM stiffness will have an effect on the cell behavior and in some cases, it could endorse the formation of focal adhesion sites. The stiffness of the ECM has also found to alter the expression of multiple genes. (43) Because the effects the ECM has on cell behavior are eminent the properties of it should be considered when designing 3D matrixes.

The stiffness of tissues is very much related to the amount of mechanical stress the tissue is exposed to. In addition, cells resided in specific tissues are specialized to function in that certain type of environment with particular features. These features should also be applicable for engineered matrixes when considering the most optimal material for specific cell types. A figure obtained from an article by Butcher et al. (44) presents general stiffness profiles of a few common tissues (Figure 56) in the human body.

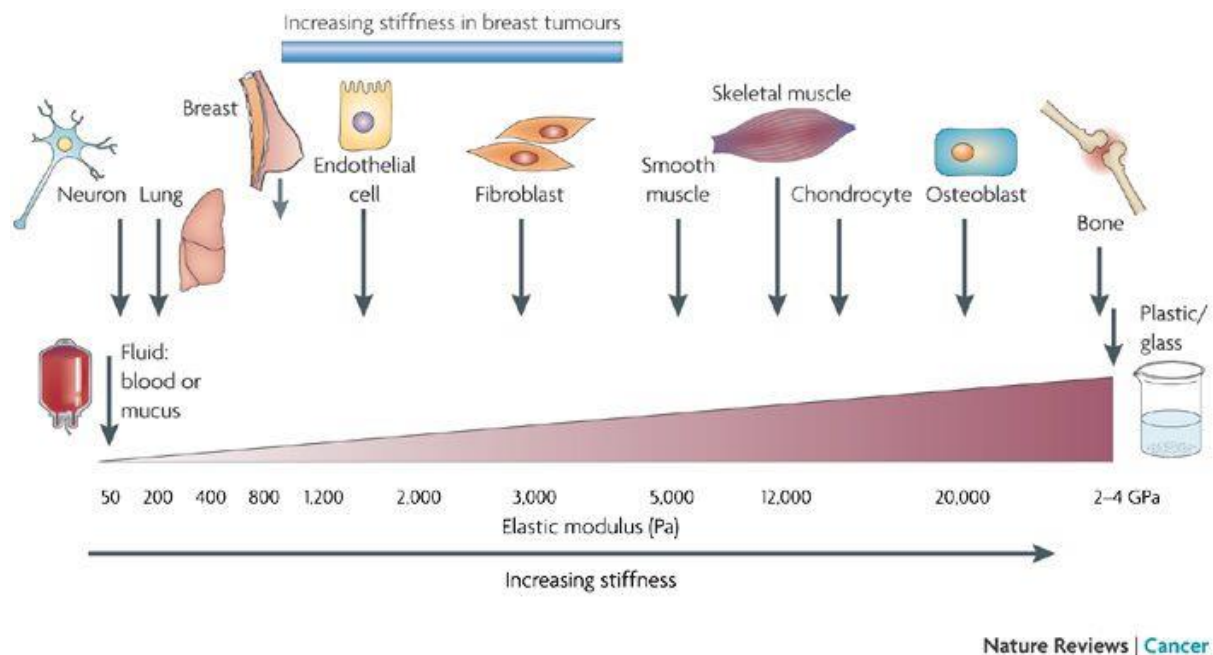


Figure 56. Stiffness profiles of human organs and resident tissues of presented cells. Image obtained from an article by Butcher et al. (44)

IMR90 is a lung-derived myofibroblast cell line. In Figure 56 the stiffness of lung tissue is stated to be around 200 Pa, whereas the stiffness what fibroblasts are likely to experience is approx. 3000 Pa. If the smooth muscle cell -like behavior of the IMR90 as in a study by Ehler et al. (28) should be considered, we find that the stiffness of these tissues is around 5000 Pa, which is even greater than ECM for normal fibroblasts. Interestingly, in some of the experiments, it was found that the IMR90 had adhered to the untreated surface of the 96 well plate that should not promote cell attachment and which expresses a great stiffness, possibly even greater than bone tissue. In all these cases the cells had conveyed on the bottom despite the presence of a bottom gel that was initially used to prevent the cells from reaching the well plate bottom.

Gels with grafted alginates are weaker than gels with only unmodified alginate. This was the reason why gels with generally higher alginate content were used for cell encapsulation experiments with grafted alginates. Article by Shea et al. (45) presented shear elastic modules for different alginate-based hydrogels. Elastic modulus describes the materials ability to resist deformation when exposed to shear stress and is used to assess the stiffness and elasticity of the material. In this article, the measured elastic modulus for hydrogel with 1,5% of unmodified alginate was 1300 ± 129 Pa and 629 ± 62 Pa for hydrogel with 1,5% of oxidized alginate. According to these measurements, the unmodified alginate has roughly a double the rate of stiffness to gels with the same amount of oxidized alginate.

As mentioned, alginate does not naturally promote cell adhesion. A feature that was also emphasized in the experiments carried out for this thesis. In the experiments, no cell attachment indicating morphology changes were detected in gels with only unmodified alginate. Only gels where the RGD-peptide had been incorporated, were found to provide adhesion of IMR90 cells. The first indication of this was found in Experiment 4 where cells were cultivated on top of alginate gels (Figure 17). In Experiment 5, it was debatable whether the cells had attached to the material or to the well plate in the samples where cell adhesion indicating morphology were found. To conclude this, the study was repeated with two different ratios of UP-LVG and RGD-modified alginate in Experiment 6.

In Experiment 6 it was also concluded that cells could indeed attach to the bottom of the well plate despite the non-adhesion promoting surface of them. Because of this tendency, it was considered if the IMR90 would actually prefer a harder matrix over softer materials. However, when the control period proceeded, an indication of cell adhesion in gels with UP-LVG+RGD alginate with the 1:3 ratio was detected. This was interesting because the gels with a 1:3 ratio were softer in structure than the UP-LVG+RGD alginate gels with the 1:1 ratio. This observation gave more emphasis for the cell attachment promoting feature of RGD-peptide, over the structural attributes of the gel.

In the experiment that followed this, two different gel strengths (1% and 2%) and three different cell concentrations (1x, 2x and 4x) were tested to further evaluate significant parameters. All the gels in this experiment had the same UP-LVG and RGD alginate ratios (1:2) but the total amount of RGD-alginate was higher in gels with the higher overall amount of alginate. In the results obtained from this experiment, it appeared that cells were not effectively able to spread into the stiffer 2% gel and morphology depicting adhered cells were mainly detected in gels with 1% alginate. This meant that IMR90 cells again preferred the softer gel matrix over the stiffer one.

An interesting feature in IMR90 behavior was detected when cells were cultivated on a well plate without a matrix material. Initially done to determine the morphology of cells when adhered on the bottom of the well plate and in order to compare this to the situations where it was suspected that cells had attached to the well plate despite the presence of hydrogel. Figure 57 represents the results of L/D assaying of the IMR90 cells cultivated without a gel matrix. If compared to results obtained from experiments 5 and 6, where a great number of the cells were found in the bottom of the well plate in OX+RGD alginate samples the difference in viability is notable. As seen in Figure 57, the number of live cells had decreased significantly after Day 1 and virtually no cells were alive on Day 10. This difference in survival rate is interesting because it suggests that the cells that grew below a layer of gel, remained more viable and were even able to proliferate during the 10-day follow-up period (as seen in Figure 19 and Figure 29 for samples with OX+RGD alginates). This suggests that even when in some cases the IMR90 favored the well plate over the gel, it still preferred to have the presence of the gel layer even though that the gel structure likely acted as a barrier decreasing the exchange of gases and nutrients between the cells and the media.

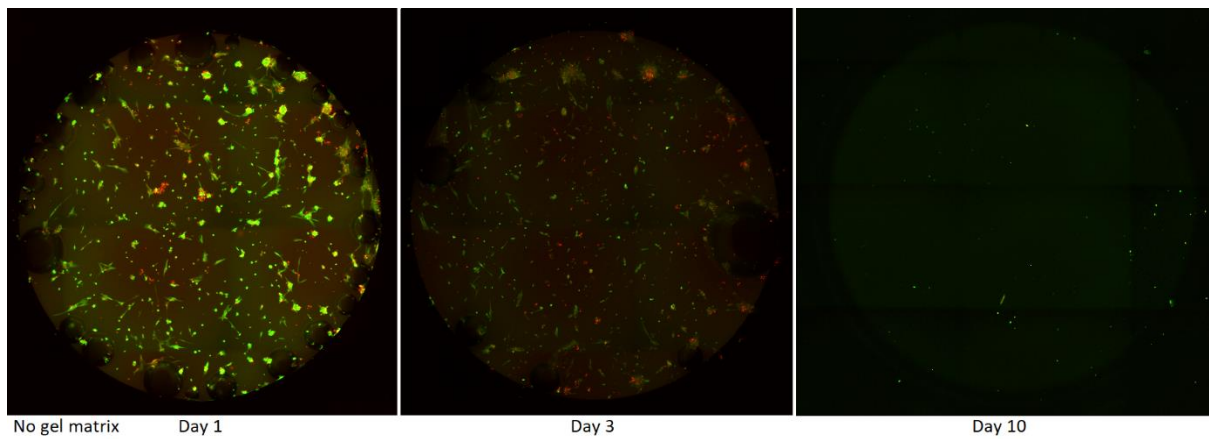


Figure 57. L/D imaging of IMR90 cell cultivated in 96-well plate without a matrix material on Day 1, 3 and 10. The diameter of one gel is approx. 6,4 mm.

4.4 RGD-modified alginate and cell adhesion

Cell viability and survival were studied at multiple different time points during the follow-up period to assess the number of cells and their survival. The changes in the cell numbers were considered as responses to the matrix material and culturing conditions. In the best scenario, the matrix would have provided an environment supporting proliferation of the cells resulting possibly in a higher number of cells that initially had been encapsulated.

A review article by Andersen et al. (2015) (46) the use of alginate-based hydrogels as a 3D matrix for cell culturing in different approaches is reviewed. In studies referred in the article, it had been found that the use of RGD-peptide modified alginate had affected the adhesion and proliferation of some cell lines. The article introduces a scaffold material for 3D cell culturing called NovaMatrix-3D that is an alginate-based scaffold material that also utilizes the RGD-peptide for promoting cell attachment.

Lines of different fibroblasts and few other cell lines were cultivated in NovaMatrix-3D system in a study referred in the article by Andresen et al. (46) (Original article cited not found). The results of the study had shown a proliferation of murine fibroblasts after weeks of culturing in alginate-based matrix without RGD-peptide. A line of lung-derived fibroblast cultivated in same material again without the coupled RGD-peptide had shown appreciable viability on day 15 of cultivation. Under these same material conditions viability was detected for murine leukemia suspension cells and human colorectal adenocarcinoma cells. Same material but with RGD-modified alginate was used for cultivation of human-derived ovarian adenocarcinoma cells and colorectal carcinoma cells. These were found to have remained viable at least 4 weeks. (46) According to this study, the need for RGD-peptide for adhesion is dependent on the cell line. This might explain the differences in survival between the two cell lines, IMR90 and HepG2 that were utilized for experiments for this study.

In one study alginate hydrogels coupled with RGD containing peptide sequence were used as a base layer for the cultivation of myoblast cells. In this study, 80 000 cells/cm² were seeded on top of gels with different G/M-ratios and RGD-peptide densities. It was found out that by increasing the amount of RGD-peptide in the gel the cell adhering to the surface was increased as well, but only to a certain point after which an increase in the amount of RGD-peptide did not have a substantial effect on adhering. Also, the study suggested that alginate coupled with RGD that had a high percentage of G-monomer promoted attachment of myoblasts better than ones with high amounts of M-monomer. (47)

Increasing the amount of RGD-peptide was also found beneficial for promoting cell attachment in the experiments carried out for this thesis. In the experiments, three different concentrations of RGD-modified alginate were used. The ratios of UP-LVG and RGD-alginate used were 1:1, 1:2 and 1:3. In Experiment 6, gels with ratios of 1:1 and 1:3 were compared and samples with a higher amount of RGD-alginate were found to promote cell adhering better. When the attachment of cells to the material was studied in Experiment 7, in gels with 1:2 ratio of UP-LVG and RGD alginates the adhering was found to be better than in gels with the ratio of 1:1, but the comparison to gels with the 1:3 ratio was not as straight forward. The total number of cells were found to differ between these two gel conditions and only the samples with a ratio of 1:2 had been imaged with CLSM, that was the better way of estimating the ratios between adhered and non-adhered cells.

Figure 58 and Figure 59 are L/D images obtained on Day 7 of the control period of two different gel conditions from separate experiments but with the same initial number of cells. Figure 58 is obtained from imaging of gel with a 1:3 ratio of UP-LVG+RGD alginates and Figure 59 of gel with a ratio of 1:2. In both these images, elongated cells are detected, but the total number of live cells is seemingly higher for the sample with a higher content of RGD-alginate (Figure 58). However, this could suggest that increase in the amount of RGD-alginate would improve the survival of cells, but it should be considered that these results are obtained from separate experiments and e.g. the passage number and age of cell is higher in the experiment with gels of 1:2 ratio.

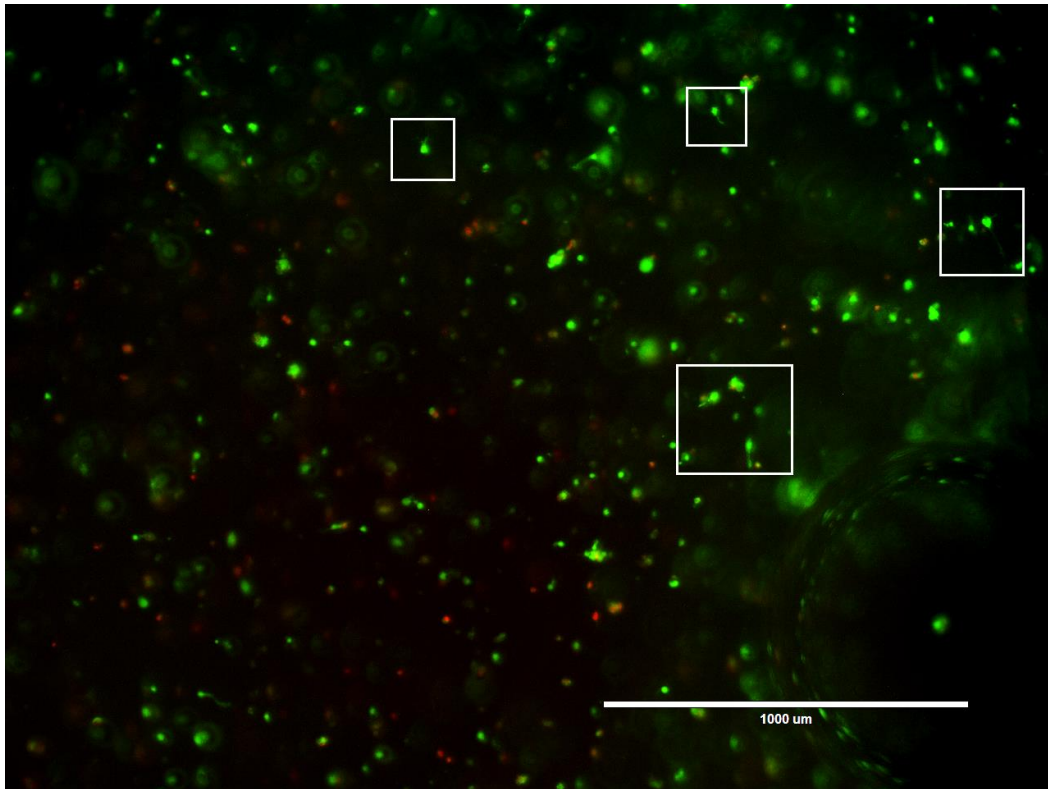


Figure 58. L/D imaging on IMR90 cells in 1% gel with 1:3 of UP-LVG+RGD alginates and 1xcell concentration on Day 7 in Experiment 6. Brightness and contrast increased by 20%. Some of the elongated cells are highlighted. The scale is 1000 μm .

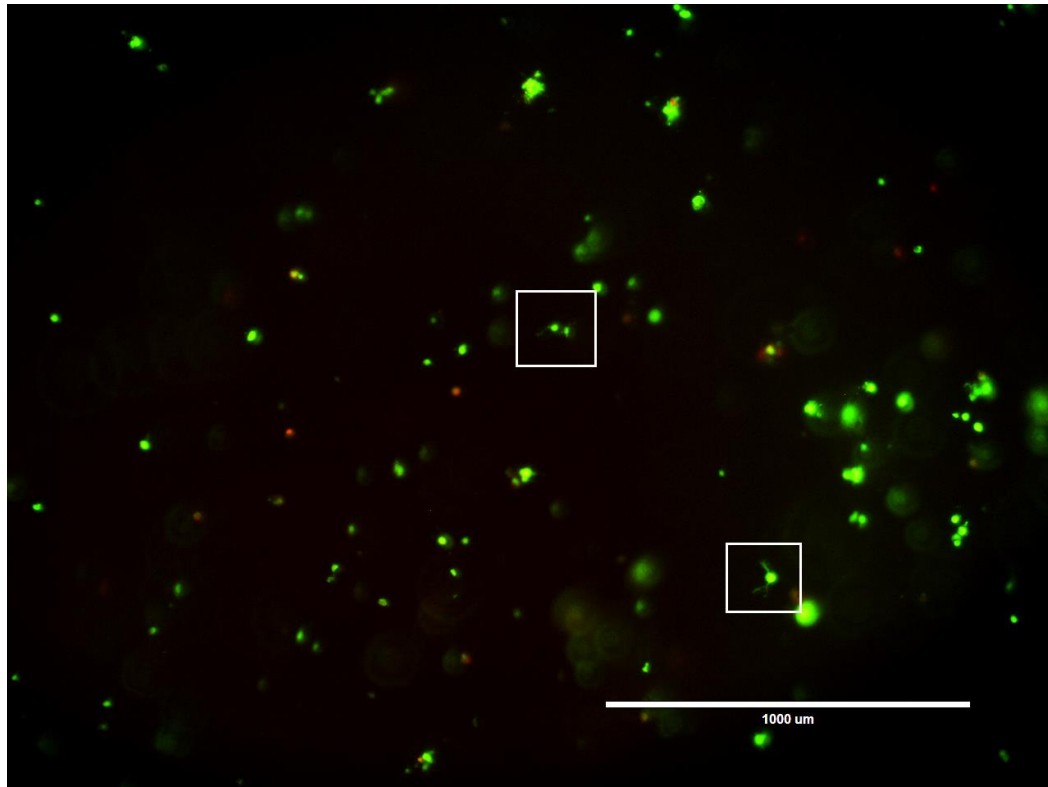


Figure 59. L/D imaging of IMR90 cells in 1% gel with 1:2 of UP-LVG+RGD alginates and 1xcell concentration on Day 7 in Experiment 7. Brightness and contrast increased by 20%. Some of the elongated cells are highlighted. The scale is 1000 μm .

In an article by Chaudhuri et al. (48) the effect of stress relaxation after in alginate-based hydrogels on cell adhesion was studied. In this study, alginate had been grafted covalently with polyethylene glycol (PEG) that has a function of preventing cell adhesion and suppressing the absorption of non-specific proteins. These advantages combined with a biocompatibility feature, PEG is widely studied for multiple approaches of tissue engineering and different biomedical applications. (49) In the study by Chaudhuri et al. (48) RGD-coupled alginate was used in hydrogels what were used for encapsulation of fibroblast cells. The morphology of these fibroblasts was then followed to determine their adhering to the material. The RGD coupled alginate was used in the encapsulation experiments due to the cell adhesion promoting properties of the RGD-peptide.

In the experimental setup of Chaudhuri et al. (48) the gels prepared had an alginate content of 2% and 2-3 million cells/ml. The volume of gels was 57 mm^3 resulting in a total cell number of $1,1-1,7 \times 10^5/\text{gel}$. Samples with different numbers and lengths of PEG chains were prepared on this same gel setup and then the ability of cells to spread was examined. The morphology of the cells was studied a week from encapsulation. In this study by Chaudhuri et al., it was found that an increase in the relaxation rate of the gels could to promote cell spreading and adhesion to the material. The rate of attachment was also increased by increasing the number of PEG-chains in alginate.

The volume of gel samples was not greatly different from the gels studied for this thesis, but the number of cells in one gel was closer to the 2xcell concentration used in Experiment 7. In this study cell spreading was discovered in gels with 2% alginate and a high rate of stress relaxation. In 2% gels with low rate relaxation, cells were not found to spread significantly. The results for low-rate relaxation gels are similar to what was

obtained in the experiments in here, where the cells were not found to obtain elongated shape when capsulated in 2% gels.

4.5 Effect of the cell number

In a study of myoblast differentiation, the number of cells used in experiments by Rowley and Mooney (47) was almost half (80 000 cells/cm²) of what was used in the on-top cultivation experiment (Experiment 4) for this study, where 50 000 cells were cultivated on top of a gel with surface area approx. 0,32 cm² ($1,56 \times 10^5$ /cm²). But in an experiment studying cell adhesion and proliferation, the number of cells used by Rowley and Mooney (47) was only 2400 cells/cm².

In a study by T.M. Abney et al. (1) it was found out that despite the initial number of myofibroblast cells (which the IMR90 is also) inside of collagen-based 3D matrix, the cells were found to approach a threshold value of 1 million cells in 1 ml of the collagen matrix. When the initial number had been higher, the cells were found to die to point of the 1 million/ml or proliferate if the initial number had been smaller. In the experiments here, the most used cell concentration was approx. 0,77 million cells in 1 ml of the matrix material. In experiments where the number of cells was increased the concentration was approx. 1,5 million/ml for the 2×-samples and for the 4×-samples the number of cells were approx. 3 million cells/ml. If the cells were to behave as they did in the collagen matrix in the study and would have strived to obtain the concentration of 1 million cells/ml also in alginate gels, the aforesaid cell concentration would have placed in between the 1× and 2× concentrations. This could have meant that the decrease in cell number in 2×-samples was due to the cells internal drive to a smaller population but unfortunately an increase in cell number was not detected in 1×-samples in the manner as the study suggested.

4.6 Imaging of gels and the L/D assay

The procedure of imaging the gels in 96-well plates with the light microscope used in these experiments had no possibility for determining or pre-setting the height plane of imaging. Due to this the height could not be set to be the same for every assessment point. As a result, the plane of imaging had to be found manually each time by first adjusting the focus on the top of the gel and then slowly moving it through the gel towards the bottom of the well. The gels were surveyed throughout every time, but only selected planes were imaged. The imaged planes were the ones that had approximately highest number of cells detected on them or otherwise were the best representatives of the viability and distribution of cells in the sample. A problem with this type of imaging was that only one layer of the whole three-dimensional complex could be imaged at the time and the images only gave an estimation of the number of viable cells in the gel. Furthermore, the gels tended to form a meniscus that warped the gel and caused a distortion in the focus plane. This can be seen in the pictures where the area covering the whole well has been imaged and the center of image is nicely in focus, but on the edges of the gel the cells seem to be out of focus.

In the course of this study, the L/D assay was carried out multiple times for assessing the viability of the cells in all the experiments. However, the intensity of the signal from this assay was found to differ in a rather large extent between the time points in the control periods and between the two different cell lines. The changes from time point to another could be considered expected, if the intensity would gradually decrease or increase over the time. However, in many cases the signal was found to differ more or less randomly and independently from what had been observed in the previous time point. To some extent, this was suspected to be caused by differences in the samples but in some cases both parallels showcased similar behavior. It was also thought that it could be an indication of changes in metabolic activity of the cells, but when sudden and even contrary changes in the intensities of both signals of the L/D assay had been detected, the metabolic activity might not then have been the effect behind it. After surveying this phenomenon over several experiments, the possible effect of the media changes during the control period began to emerge. In some cases, the signal from L/D assay was found to increase on days after the change of the cell culture media in which the gels were submerged during incubation. The discarding of old media from the samples might have removed debris from dead cells and other compounds excreted by the cells, that were interfering with the stains of the L/D assay and increasing the background signal in the imaging.

Another evident variable that seemed to affect the signal intensity was the line of cells that had been encapsulated into gels. In many cases, the signal detected from IMR90 was found to be much weaker than the signal from HepG2 cells. To assess whether the difference was due to inherent features of the cell lines, cells from both lines without any gel matrix were subjected to L/D assay and imaged after 45 min of incubation in RT. The results obtained did not suggest a significant difference between the cell lines (presented in Figure 7). This meant that the often-witnessed vague signal from IMR90 was likely caused by other variables. The gel compositions and encapsulation procedures were similar for both lines and in many cases the same staining solution was used for both. The one difference between samples with the different cell lines was the cell culture media used for washing of gels and cell culturing. For IMR90 the media was DMEM with 10% FBS, 1% l-glutamine, 1% Pen-Strep, 1% NEAA and 0,1 mM SP and For HepG2 RPMI with

10% FBS, 1% l-glutamine and 1% Pen-Strep was used. It could be that a component in the media might have interfered with the staining and reduced the signal strength of IMR90.

Despite the few challenges in the imaging with the microscope used, the imaging procedure was similar for gels with both lines. The time of incubation was 45 min in minimum in all L/D assays performed. Though in some cases when a great number of samples and parallels were to be assayed and imaged on the same day, the incubation time was sometimes extended to 2 h. This might have had an effect to the intensity of the L/D signal, but in cases when samples with different cell lines were imaged at the same time, the samples with more detectable signal were imaged first in order to extend the time of incubation for the samples with less visible signal.

4.7 Results obtained with Matrigel

Matrigel™ (Corning Life Sciences and Becton Dickinson) is used for preparation of basement membrane matrixes. Matrigel™ is an extraction from Engelbreth Holm-Swarm (EHS) mouse sarcoma. This is a tumor containing high amounts of different extracellular matrix proteins such as laminin and collagen IV, growth factors and glycoproteins. Being a derivate from a natural source Matrigel is intrinsically biocompatible and has been successfully used in different 3D cell culture studies. On the downside materials like this are complex, in a risk of contamination and can have significant variability in between batches. (50) (39) (2)

In these experiments, the successfulness of the use of Matrigel as a material for cell-matrix seemed to be much depended on the concentration and stiffness of the Matrigel and on the type of the cell line. When used as a base for monolayer culture the Matrigel proved to be challenging for the IMR90. From Figure 45 the viability and the number of cells decreased notably during a 4-day control period for this cell line. On the contrary, for HepG2 the number of cells seemed to have increased over the same time period. There was also little indication of attachment to the material for IMR90 but for HepG2 the cells formed structures similar to normal culture flask cultivation (Figure 5).

Matrigel was also used as a 3D matrix with two different concentrations (5 mg/ml and 10 mg/ml). Both cell lines were used in encapsulation into low concentration gels and again the HepG2 was found to be generally more viable compared to IMR90 (Figure 47 and Figure 48). During this experiment, a considerable number of IMR90 cells also likely migrated out of the gel matrix and adhered on the bottom of the well suggesting a greater preference on the non-treated well plate surface over the Matrigel (Figure 50). Despite the decreased viability and cell migration, few IMR90 cells found inside of the gel matrix expressed a morphology of adhered cells (Figure 51).

Only IMR90 cells were used in encapsulation into high concentration Matrigel. During this experiment, the number of cells that remained inside the gel was higher than in the experiment with Matrigel with a concentration of 5 mg/ml but again, cells were found on the well plate surface as well. Cell attachment was again detected for the cells inside of this gel matrix (Figure 55). But despite that cell attachment on the Matrigel was detected in multiple samples, the number of cells that did not indicate an attachment to the gel matrix remained notably higher than the number of cells that did throughout the follow-up periods for both encapsulation experiments with Matrigel.

Matrigel was used twice with the higher concentration (10 mg/ml) in the experiments, for on-top cultivation and as a 3D matrix. As the staining of the L/D assay proved to be challenging for detecting encapsulated live/dead cells, it was concluded from the bright field images, that encapsulation provided better viability for IMR90. This provides evidence that IMR90 likely did not suffer from nutrient or oxygen deficiency inside of the matrix and that the exchange of these had been sufficient inside the gels.

Collagen being a profuse component in Matrigel (39) is also abundant in ECM of tissues where fibroblasts reside. Conversely, the ECM of myofibroblasts is less rich in collagen and consists firstly of fibrin and fibronectin. (31) This could be an aspect in the applicability of Matrigel for IMR90 line and could shed some explanation for the results obtained with Matrigel in the experiments. According to an article by Caliarì and Burdick Matrigel is widely used as material for 3D cell culturing, but it has a few disadvantages that can reduce the repeatability and comparability of the experiments carried out with it. Source of some this

uncertainty is the variability between batches due to the complex composition of the tumor-derived material. (51)

4.7.1 Comparison of alginate gels and Matrigel

When comparing the viability of cells encapsulated in Matrigel to the viability detected in alginate gels the results vary to some extent. Generally, the cells remained viable in both encapsulations with Matrigel over several days and in both experiments probable cell adhesion was detected. However, the viability of IMR90 cells in Matrigels seemed generally less promising than what was detected in gels with the RGD-alginate. When compared to results obtained from experiments where the amount of RGD-alginate in gels was higher than 50% the number of live cells on the last day of the control period was significantly higher in these than in any sample with Matrigel on Day 10.

Although the viability of cells inside the high concentration Matrigel was difficult to determine at some time points, the morphology of cells inside these gels was studied. The cells that had supposedly adhered to the Matrigel appeared similar to cells that were assumed to have attached to gels containing the RGD-peptide. Also, in both on-top cultivations (on Matrigel and on alginate gel with RGD-peptide) the morphology of cells seemed rather similar for Matrigel and alginate-based gel. Despite finding adhered cells in Matrigels, the highest numbers of cells with the spread-out appearance were detected in gels with UP-LVG+RGD alginate and the ratio being over 50% of RGD-modified alginate.

In a study by Collins et al. (52) IMR90 cells were used in a study where Matrigel was used as a 3D matrix. As a part of this study 5000 IMR90 cells were encapsulated in gels with a concentration of 4 mg/ml of Matrigel and total volume of 64 μ l. The proliferation of cells was assessed after 2 and 5 days and although no proliferation was detected on Day 2, the cell number had almost doubled to Day 5. The proliferation of cells was assayed with quantitative WST-1 proliferation assay. These results from the study by Collins et al. could be considered opposites to the results obtained within this thesis, where no probable cell proliferation was detected on any Matrigel-based gels and on the contrary the cell numbers seemed to significantly decrease over time. This is particularly interesting because the gel parameters were rather similar in these two studies. In our study the concentration of Matrigel in the 'low concentration Matrigel'-experiment was 1 mg/ml higher and the volume of gel was 1 μ l greater than in the experiment by Collins et al. The most significant difference between the experiment setups was the initial cell number that was ten times greater in experiments in here than in the study by Collins et al. (52)

4.8 Future perspectives

In the encapsulation experiments, the amount of RGD-modified peptide in alginate seemed to be the most important separate variable for improving attachment of IMR90 cells to the matrix material. Increasing the amount of RGD-modified alginate might be a matter of interest to be tested in the future. However, increasing the ratio of RGD-alginate further and over 75% of the total amount of alginate might become problematic especially in gels where the total amount of alginate is 1% or less. This is because gels made with RGD-modified alginate are generally weaker in structure and might not form a stable gel. By increasing the total amount of alginate in solution might make it possible to increase the ratio of RGD-alginate in gels and still obtain gels with a stable structure.

The results obtained from Experiment 6 and 7 suggested that there was some difference in cell survival between the gels with the ratios of 1:3 and 1:2 of UP-LVG and RGD-alginates. Although the proportional amount of adhered cells to the total number of cells might not have been greatly different between these two gel conditions, the number of live cells seemed greater in gels with the 1:3 ratio of UP-LVG and RGD alginates. Because the gel conditions were only tested with a small number of parallels in two separate experiments, the comparison of the two different ratios should be further tested to better determine the actual effect of the higher RGD-alginate ratio.

It was hypothesized that the overall viability of the cells might be improved by increasing the initial number of cells so they would be able to communicate and generate cell-cell contacts easier. The recommended confluency to be achieved with IMR90 cell line in prior to splitting procedure for subcultivation to maintain the appropriate vitality of the subsequent line was 70-80% (27). At this high rate of confluency cells are largely and visibly connected with each other (Figure 4). In Figure 7 the coverage or 'confluence' of approx. 50 000 cells when on a surface of one well of 96-well plate can be estimated. Though, in this image the cells have not been cultivated on the plate, so they do not exhibit their normal elongated and more spread shape and thus appear generally smaller in size. However, in the experiments conducted with the same number of cells, the cells had been distributed within a multilayered structure, where the number of close neighbors was decreased despite the total number of cells within the gel.

By increasing the number of cells, the demand of oxygen and nutrients would also be increased, and the volume of culture media used during culturing might prove to be insufficient and result in a decrease in cell survival. A positive aspect considering this was that in the experiments where the cells had attached to the well plate, they remained more viable under a gel layer than they did without it. This suggested that the gel did not critically limit the exchange of nutrients and gases. Moreover, only after gels with 2% alginate content were used for cell encapsulation in Experiment 7 an indication of restricted exchange was suspected. In the samples where the initial number of cells was doubled to what had been used in the experiments before, the number of dead cells was found to be higher in the 2% gels than in 1% gels with the same initial number of cells.

The reason for having the cell number constant for most of the experiments was to have results that would be comparable between the different experiments and gel conditions. Only after gaining positive results from cell adhering as a result of the use of RGD-modified alginate, the increase of cell density was thought to be relevant. In the samples where the initial cell number was increased a higher number of cells with elongated morphology were detected in images obtained with both light microscope and CLSM. Although maybe

evident that a higher number of cells would result in a higher number of adhered cells, the ratio of attached cells to the total number of cells seemed encouraging. In samples where the number of cells was doubled from the initial 50 000 cells/well, proved able to sustain the cell viability to somewhat same extent as in gels with a smaller number of cells. In these samples, a high number of live cells were detected even on the last day of the control period. However, the number of dead cells was greater in these gels than in gels with the initial 50 000 cells.

In the experiments, two cell lines with different origin and morphology were used. Since maintaining the viability of the IMR90 line had proven to be challenging, it could be of interest to introduce another cell line to the experimental setup. In the article by Andersen et al. (46) a myoblast line C2C12 were encapsulated in alginate-based hydrogels including the RGD-peptide and was reported to have proliferated and maintained its viability over several weeks. Considering the similarity with the cell matrix used in the study by Andersen et al. it would be interesting to test if as encouraging results could be achieved with the matrix used in the experiments in here.

The effect of washing of the gels after encapsulation was only shortly studied in the first experiments and the washing procedure tested first in Experiment 2 was used in all encapsulation experiments that followed it. Although the effect of the washing on cell survival was not fully demonstrated in the first experiments, it had been found to positively effect on it in other experiments conducted for this project. Due to this the effect of increasing the number of washes could be an interesting aspect for future experiments.

The L/D assay and imaging used in these experiments for determining cell viability was a qualitative method for assessing the survival of the cells and the development in the overall number of cells inside the gel. As stated, imaging of three-dimensional gels with a light microscope also proved to have its restrictions and determining of the most representative height and place in each sample relied on the experience and opinion of the person operating. A quantitative method for determining cell numbers more reliably could provide information that would be more comparable between the samples and less prone to a discussion about the distribution and place of the cells in the gels. For example, this could be achieved through flow cytometry after first dissolving the gels. However, this would not replace the need for imaging of gels that still provides valuable information about the migration and morphological changes of the cells.

The length of the time period over what the encapsulated cells were followed lasted maximum for 10 days in these experiments. This was partially due to the underlying motive for the screening of the most potential conditions for supporting the viability and adhering of cells. Since gels with a high ratio of RGD-alginate were found to promote these features, a follow-up period extending over 14-20 days might be interesting to be studied to obtain more knowledge about the survival and possible migration or further changes in the morphology of the cells.

5 Conclusion

Cultivating IMR90 cells inside of hydrogels with a combination of UP-LVG alginate and RGD-modified alginate with a total amount of 1% alginate in gel were found to be most essential factors in promoting cell attachment to the material. In the experiments, an effective amount of RGD-alginate for promoting cell adhering was found to be a minimum ratio of 1:2 of RGD-modified and UP-LVG -alginates. The 1:2 ratio was considered more effective than the 1:1 for attachment but the results suggested that the 1:3 might be able to promote a better overall survival of the cells than the 1:2 ratio. In addition, the total amount of alginate in the gel was found to affect to cells ability to obtain the elongated shape distinct for IMR90. The spreading of cells was not detected in same extent in 2% gels than in 1% gels despite the amount of RGD-alginate used.

Although the effect of increased cell number was only studied at one separate experiment the results gained from it suggested that by increasing the initial number of cells from 50 000 cells/well (7.7×10^5 cells/ml) to 100 000 cells/well (1.6×10^6 cells/ml) or higher, might result in a higher number of viable and adhered cells after a week of cell cultivation. Exposing cells to hypothermic conditions prior to encapsulation was considered to improve cell survival over the process compared to cells that were prepared and encapsulated in RT. Cell survival was also considered to have improved by the washing steps performed on the gels after 2h gelling with encapsulated cells.

The benefit of using a two-layered gel structure with top and bottom gel did not demonstrate a vital improvement for a cell culture matrix. As the initial purpose of the bottom gel was to prevent the cells from migrating on the bottom of the well plate, on some occasions cells were discovered to have done that despite this 'gel barrier'. Furthermore, the use of bottom gels increased the height of the gel structure to an extent that imaging them with the available CLSM equipment was not feasible unless the gels were removed from the 96-well plates and transferred on a Petri dish. However, the use of bottom gel made handling of gels more easy and managed to stabilize the structure of the whole gel making it more easy to transfer gels without risking the integrity of the sample.

When comparing the survival of IMR90 fibroblasts in alginate gels to their survival in Matrigel, the results were generally found to be more encouraging for alginate-based gels. Interestingly even when comparing Matrigel to alginate gels without any cell attachment promoting peptides the alginate gels seemed to support viability for a higher number of cells for over a longer period of time than Matrigel did. However, it should be noted that challenges were encountered when the L/D assay that was used to assess the viability and cell number in all samples, was used for Matrigels. In many Matrigel samples, the background signal for both stains was found to be relatively high. This might have affected the assessment of cell numbers and especially of dead cells.

6 References

1. **Genin G.M., Abney T.M., Wakatsuki T., Elson E.L.** Cell-Cell Interactions and the Mechanics of Cells and Tissues Observed in Bioartificial Tissue Constructs. [book auth.] Harley B. (eds) Wagoner Johnson A. *Mechanobiology of Cell-Cell and Cell-Matrix Interactions*. Boston : Springer, Boston, MA, ISBN: 978-1-4419-8082-3, 2011.
2. *Polysaccharide matrices used in 3D in vitro cell culture systems.* **D.Diekjürgena, D.W.Grainger.** Salt Lake City, USA : University of Utah, ScienceDirect, 2017, Vol. 141. <https://doi.org/10.1016/j.biomaterials.2017.06.020> .
3. **S.A. Lelièvre, T.Kwok, S.Chittiboyina.** Architecture in 3D cell culture: An essential feature for in vitro toxicology, Pages 287-295,. *Toxicology in Vitro, Volume 45.* s.l. : Elsevier ScienceDirect, ISSN 0887-2333, <https://doi.org/10.1016/j.tiv.2017.03.012>, 2017.
4. *3D Cell Culture Systems: Advantages and Applications.* **Maddaly Ravi, V. Paramesh, S.R. Kaviya, E. Anuradha, F.D. Paul Solomon.** 1, s.l. : Journal of Cellular Physiology, 2014, Vol. 230. <https://doi.org/10.1002/jcp.24683>.
5. **Dorina Diekjürgen, David W. Grainger,** Polysaccharide matrices used in 3D in vitro cell culture systems, Pages 96-115. *Biomaterials, Volume 141.* Utah : ScienceDirect, ISSN 0142-9612, 2017.
6. *Tissue Engineering: Current Strategies and Future Directions.* **J. L. Olson, A. Atala, J. J. Yoo.** 1, s.l. : Chonnam Med J., 2011, Vol. 47. doi: 10.4068/cmj.2011.47.1.1.
7. *Cell Commun. Signal. - 3D tumour models: novel in vitro approaches to cancer studies.* **Nyga, A., Cheema, U. & Loizidou, M. J.** 239, s.l. : Springer Netherlands, 2011, Vol. 5. Online ISSN: 1873-961X DOI: <https://doi.org/10.1007/s12079-011-0132-4>.
8. **M.Borgogna, E.Marsich, I.Donati, S.Paoletti, A.Travan.** Hydrogels. [book auth.] F.Alhaique, T.Coviello P.Matricardi. *Polysaccharide Hydrogels, Characterization and Biomedical Applications.* New York : Pan Stanford, ISBN 9789814613613, 2015.
9. **Thakur S., Thakur V.K., Arotiba O.A.** History, Classification, Properties and Application of Hydrogels: An Overview. [book auth.] Thakur M. Thakur V. *Hydrogels.* Singapore : Springer, Singapore, Online ISBN: 978-981-10-6077-9, 2018.
10. **Garner J., Park K.** Chemically Modified Natural Polysaccharides to Form Gels. [book auth.] Mérillon JM. (eds) Ramawat K. *Polysaccharides.* s.l. : Springer, Cham, ISBN: 978-3-319-16297-3, 2015.
11. **Aminabhavi T.M., Deshmukh A.S.** Polysaccharide-Based Hydrogels as Biomaterials. [book auth.] Kalia S. (eds). *Polymeric Hydrogels as Smart Biomaterials.* s.l. : Springer, Cham, Online ISBN 978-3-319-25322-0, 2016.
12. **Gudmund Skjåk-Bræk, I. Donati, S. Paoletti.** Alginate Hydrogels: Properties and Applications. *Polysaccharide Hydrogels - Characterization and Biomedical Applications.* New York : Pan Stanford, <https://doi.org/10.1201/b19751>, 2015.
13. **Ivan Donati, Sergio Paoletti, Bernd H. A. Rehm.** *Material Properties of Alginates.* Berlin : Springer, Berlin, Heidelberg, 2009. 978-3-540-92678-8.

14. **Christensen, B. E.** *BIOPOLYMERS - Compendium TBT4135*. Trondheim : NTNU, 2018.
15. *Alginate: Properties and biomedical applications*. **K.Y. Lee, D.J. Mooney**. 1, Cambridge, Seoul : Harvard University, Hanyang University, Elsevier, 2011, Vol. 37. <https://doi.org/10.1016/j.progpolymsci.2011.06.003>.
16. *Cellular Cross-linking of Peptide Modified Hydrogels*. **T. Boontheekul, J.L. Drury, D.J. Mooney**,. 2, Michigan : University of Michigan, American Society of Mechanical Engineers , 2004, Vol. 127. doi:10.1115/1.1865194.
17. *Efficient functionalization of alginate biomaterials*. **Marianne Ø. Dalheim, Julie Vanacker, Maryam A. Najmi, Finn L. Aachmann, Berit L. Strand, Bjørn E. Christensen**. Trondheim Norway, Brussels Belgium : Elsevier, 2015, Vol. 80. <https://doi.org/10.1016/j.biomaterials.2015.11.043>.
18. *A Synthetic Peptide Containing the IKVAV Sequence from the A Chain of Laminin Mediates Cell Attachment, Migration, and Neurite Outgrowth**. **K.Tashiro, G.C. Sephel, B.Weeks, M.Sasakig, G.R. Martinn, H.K. Kleinman, Y.Yamada**. 25, Maryland : Laboratory of Developmental Biology and Anomalies, National Institute of Dental Research, National Institutes of health, 1989, Vol. 264. PMID: 2777785.
19. *Peptide-modified alginate surfaces as a growth permissive substrate for neurite outgrowth*, p.191-368. **N.O. Dhoot, C.A. Tobias, I.Fischer, M.A. Wheatley**. 2, s.l. : Journal of Biomedical Materials Research Part A, 2004, Vol. 71A. <https://doi.org/10.1002/jbm.a.30103> .
20. *Alginate: properties and biomedical applications*. **Kuen Yong Lee, David J. Mooney**. Cambridge, Seoul : National Institute of Health, 2012. doi:10.1016/j.progpolymsci.2011.06.003.
21. *RGD modified polymers: biomaterials for stimulated cell adhesion and beyond*. **Ulrich Hersel, Claudia Dahmen, Horst Kessler**. 24, Munchen Garching, Germany : Elsevier, 2003, Vol. 24. [https://doi.org/10.1016/S0142-9612\(03\)00343-0](https://doi.org/10.1016/S0142-9612(03)00343-0).
22. *RGD AND OTHER RECOGNITION SEQUENCES FOR INTEGRINS*. **Ruoslahti, Erkki**. La Jolla, California : La Jolla Cancer Research Center, The Burnham Institute,, 1996, Vol. 12. <https://doi.org/10.1146/annurev.cellbio.12.1.697>.
23. *Hydrogel Formation via Cell Crosslinking*. **K.Y. Lee, H.J. Kong, R.G. Larson, D.J. Mooney**. 21, Michigan : WILEY VCH, University of Michigan Cardiovascular Center, 2003, Vol. 15. <https://doi.org/10.1002/adma.200305406>.
24. **Pavelka, Margit and Roth, Jürgen**. Fibroblast, Fibrocyte, Macrophage. *Functional Ultrastructure: An Atlas of Tissue Biology and Pathology*, pp.248-249. Vienna : SpringerLink Books, ISBN: 9783211835647, E-ISBN: 9783211263921, 2005.
25. **Marco Gattorno, Alberto Martini**. Chapter 3 - Inflammation and Its Mediators. [book auth.] Ronald M. Laxer, Carol B. Lindsley, Lucy R. Wedderburn Ross E. Petty. *Textbook of Pediatric Rheumatology (7th Edition) Pages 14-32*, ISBN 978-0-323-24145-8. s.l. : Elsevier Inc., 2016.
26. *Fibroblasts form a body-wide cellular network*. **Helene M. Langevin, Carson J. Cornbrooks, Douglas J. Taatjes**. 1, s.l. : Histochemistry and Cell Biology, 2004, Vol. 122. ISSN: 0948-6143, E-ISSN: 1432-119X, DOI: 10.1007/s00418-004-0667-z.

27. **ATCC**. IMR-90 (ATCC® CCL-186™). *ATCC in partnership with LGC standards*. [Online] ATCC. [Cited: 15 January 2019.] http://www.lgcstandards-atcc.org/products/all/CCL-186.aspx?geo_country=no#characteristics.
28. *Human foetal lung (IMR-90) cells: Myfibroblasts with smooth muscle-like contractile properties*. **Elisabeth Ehler, Eduard Babiychuk, Annette Draeger**. 4, s.l. : Austrian Science Fdn, Austrian Ministry of Science, 1996, Vol. 34.
29. *Vinculin and metavinculin: Oligomerization and interactions with F-actin*. **P.M.Thompson, C.E.Tolbert, S.L.Campbell**. 8, Chapel Hill, NC USA : University of North Carolina at Chapel Hill, ScienceDirect, 2013, Vol. 587. <https://doi.org/10.1016/j.febslet.2013.02.042>.
30. **G.Ramaswamy, M.WarrenBidez, C.E.Misch**. Chapter 6 - Bone Response to Mechanical Loads. *Dental Implant Prosthetics (Second Edition)*. s.l. : ScienceDirect, <https://doi.org/10.1016/B978-0-323-07845-0.00006-3>, 2015.
31. *Mechanoregulation of the Myofibroblast in Wound Contraction, Scarring, and Fibrosis: Opportunities for New Therapeutic Intervention*. **Livingston Van De Water, Scott Varney, James J. Tomasek**. 4, Albany New York, Oklahoma City Oklahoma : Center for Cell Biology and Cancer Research, Albany Medical College, Department of Cell Biology, University of Oklahoma, 2013, Vol. 2. DOI: 10.1089/wound.2012.0393.
32. **Soto-Gutierrez A., Navarro-Alvarez N., Kobayashi N**. Hepatocytes. [book auth.] Monga S. (eds). *Molecular Pathology of Liver Diseases. Molecular Pathology Library*. Boston MA : Springer, 2010.
33. *Hepatic Tissue Engineering*. **Shan J., Stevens K.R., Trehan K., Underhill G.H., Chen A.A., Bhatia S.N**. Boston : Springer, Boston, MA, Part of the Molecular Pathology Library, 2011, Vol. 5. Online ISBN: 978-1-4419-7107-4, DOI: https://doi.org/10.1007/978-1-4419-7107-4_22.
34. **D.López-Terrada, S.W. Cheung, M.J. Finegold, B.B.Knowles**. Hep G2 is a hepatoblastoma-derived cell line. *Human Pathology, ISSN 0046-8177*. 2009, Vol. 40, 10.
35. *Modulation of the liver specific phenotype in the human hepatoblastoma line Hep G2*. **J.H. Kelly, G.J. Darlington**. 2, s.l. : Springer-Verlag, , 1988, Vol. 25. Online ISSN 1475-2689, <https://doi.org/10.1007/BF02626182>.
36. **Scientific, ThermoFisher**. Invitrogen™ LIVE/DEAD™ Viability/Cytotoxicity Kit, for mammalian cells. *ThermoFisher Scientific*. [Online] [Cited: 21 January 2019.] <https://assets.thermofisher.com/TFS-Assets/LSG/manuals/mp03224.pdf>.
37. —. EVOS™ FL Auto Imaging System. *ThermoFisher Scientific*. [Online] ThermoFisher Scientific. [Cited: 4 April 2019.] <https://www.thermofisher.com/order/catalog/product/AMAFD1000>.
38. —. HEPES. *ThermoFisher Scientific*. [Online] ThermoFisher Scientific. [Cited: 4 April 2019.] https://www.thermofisher.com/no/en/home/life-science/cell-culture/mammalian-cell-culture/reagents/hepes.html?gclid=Cj0KCQjw1pbIBRDSARIsACfUG11kO1ELbSXuUR0ITw9XuBVcU_8xT9aYtV5YKx6i0nhEuLS2iGYFhiMaAroQEALw_wcB&s_kwid=AL!3652!3!184018110216!p!!g!!hepes%20bu.

39. **Sciences, Corning Life.** Corning® Matrigel® Basement Membrane Matrix, Phenol Red-free, *LDEV-free, 10 mL, Product Number 356237. *Corning Life Sciences* . [Online] Corning Life Sciences . [Cited: 10 February 2019.] <https://ecatalog.corning.com/life-sciences/b2c/US/en/Surfaces/Extracellular-Matrices-ECMs/Corning%C2%AE-Matrigel%C2%AE-Matrix/p/356237?clear=true>.
40. *TMEM203 Is a Novel Regulator of Intracellular Calcium Homeostasis and Is Required for Spermatogenesis.* **P.B. Shambharkar, M.Bittinger,B.Latario, Z.Xiong, S.Bandyopadhyay, V.Davis, L.Victor, Y.Yi, V.Reginald, M.Labow.** s.l. : PLoS ONE, 2015. PLOS ONE. 10. e0127480. 10.1371/journal.pone.0127480.
41. *Biochemical insights into the mechanisms central to the response of mammalian cells to cold stress and subsequent rewarming.* **A. Roobol, M.J. Carden, R.J. Newsam, C.M. Smales.** 276, Canterbury, UK : University of Kent, FEBS, , 2008. doi:10.1111/j.1742-4658.2008.06781.x.
42. *Cold-Shock and the Mammalian Cell Cycle.* **C.L. Rieder, R.W. Cole.** Albany New York, Woods Hole Massachusetts : Landes Bioscience, 2002. ISSN: 1538-4101, DOI: 10.4161/cc.1.3.119.
43. *Remodeling and homeostasis of the extracellular matrix: implications for fibrotic diseases and cancer.* **T.Cox, J. Erler.** 2, Copenhagen Denmark, Darlinghurst Australia : ResearchGate; Disease Models and Mechanisms, 2011, Vol. 4. DOI: 10.1242/dmm.004077.
44. *A tense situation: forcing tumour progression.* **D.T. Butcher, T. Alliston, V. M. Weaver.** California, San Francisco, Philadelphia : NatureReviews Cancer, 2009, Vol. 9. doi:10.1038/nrc2544.
45. *Physical properties of alginate hydrogels and their effects on in vitro follicle development.* **Erin R.West, Min Xu, Teresa K.Woodruff, Lonnie D.Shea.** 30, Chicago USA, Evanston USA : Elsevier, 2007, Vol. 28. <https://doi.org/10.1016/j.biomaterials.2007.07.001>.
46. *3D Cell Culture in Alginate Hydrogels.* **Therese Andersen, Pia Auk-Emblem, Michael Dornish.** 2, Sandvika : FMC BioPolymer AS, 2015, Vol. 4. doi:10.3390/microarrays4020133.
47. *Alginate type and RGD density control myoblast phenotype.* **Jon A. Rowley, David J. Mooney.** 2, Ann Arbor, Michigan : University of Michigan, Colleges of Engineering and Dentistry, 2002, Vol. 60. <https://doi.org/10.1002/jbm.1287>.
48. *Varying PEG density to control stress relaxation in alginate-PEG hydrogels for 3D cell culture studies.* **Sungmin Nam, Ryan Stowers, Junzhe Lou, Yan Xia, Ovijit Chaudhuri.** Stanford CA USA : Elsevier, 2019, Vol. 200. <https://doi.org/10.1016/j.biomaterials.2019.02.004>.
49. *Cell Adhesion and Spreading on an Intrinsically Anti-Adhesive PEG Biomaterial.* **Marga C. Lensen, Vera A. Schulte, Mar Diez.** Berlin : InTech Europe, InTech China, 2011. DOI: 10.5772/24273.
50. *Hydrogels as extracellular matrix mimics for 3D cell culture.* **M.W. Tibbitt, K.S. Anseth.** 4, Boulder, Colorado : University of Colorado, Wiley InterScience, , 2009, Vol. 103. DOI 10.1002/bit.22361.

51. *A Practical Guide to Hydrogels for Cell Culture*. **S. R. Caliari, J. A. Burdick**. 5, Pennsylvania, Philadelphia USA : HHS Public Access, 2016, Vol. 13. doi:10.1038/nmeth.3839.
52. *Microstructures in 3D Biological Gels Affect Cell Proliferation*. **James J. Norman, John M. Collins, Sadhana Sharma, Brenda Russell, Tejal A. Desai**. 3, Boston, Illinois, San Francisco : Mary Ann Liebert, Inc., 2008, Vol. 14. DOI: 10.1089/tea.2007.0077.
53. **K.H. Bouhadir, K.Y. Lee, E.Alsberg, K.L. Damm, K.W. Anderson, D.J. Mooney**. Degradation of Partially Oxidized Alginate and Its Potential Application for Tissue Engineering. *Biotechnology Progress*, p.791-978. 2008, Vol. 17, 5.
54. *Changes in Free Radicals System of Imr-90 and C-32 Cells During Photodynamic Therapy*. **M. Latocha, B. Pilawa, D. Kuřmierz, A. Zielińska, D. Nawrocka**. 4A, Sosnowiec, Poland : Medical University of Silesia, Polish J. of Environ. Stud., 2006, Vol. 15.
55. **S. Sethuraman, U. M. Krishnan, A. Subramanian**. *Biomaterials and Nanotechnology for Tissue Engineering*. s.l. : Taylor & Francis Group, CRC Press, 2016. ISBN 1498743749, 9781498743747.
56. **Therese Andersen, Helene Heier-Baardson, Jan Egil Melvik, Michael Dornish**. *NovaMatrix-3D™ - Alginate Foam Matrix for 3D Cell Culture and Tissue Regeneration*. Sandvika, Norway : NovaMatrix, FMC BioPolymer AS.

Appendix A. Citrate-HEPES buffer

Citrate-HEPES-buffer

	Art.nr	Cons (mM)	Mol	g/l
Na ₃ Cit (140 mM)	71405-1KG	140	0.028	41.2
Fructose (560 mM)	CF8008019AG	560	0.112	100.9
NaCl (700 mM)	1.06404.1000	700	0.140	40.9
HEPES (250 mM)	H7006-100G	250	0.050	59.6
IF-water				1000

mol weight Na ₃ Cit	294.1	g/mol
mol weight Fructose	180.2	g/mol
mol weight NaCl	58.4	g/mol
mol weight HEPES	238.3	g/mol

Adjust the pH to 7,4

Appendix B. Cell culture mediums and sub cultivation

General composition of each cell culture media used for each cell line utilized in the experiments:

IMR90

90%	DMEM (D5546) by SigmaAldrich
10%	FBS (F7524) by SigmaAldrich
1%	L-Glutamine, 200 mM (RNBG8374) by SigmaAldrich
1%	Pen-Strep (15140-122) by Gibco
1%	Minimum Non-essential Amino Acids (11140-035) by Gibco
1%	Sodium pyruvate solution (11360-070) by Gibco

HepG2

90%	RPMI Medium (1640) by Gibco
10%	FBS (F7524) by SigmaAldrich
1%	L-Glutamine, 200 mM (RNBG8374) by SigmaAldrich
1%	Pen Strep (15140-122) by Gibco

Other chemicals used in sub cultivation:

Trypsin, TrypLE™ Express (12605-010) by Gibco

The PBS-solution used in sub culturing procedures and preparation of cell suspension for encapsulation had been prepared at Sintef by the people working in the cell laboratory.

Appendix C. List of Experiments

Experiments conducted within this thesis with the corresponding experiment number and aim of each experiment. The sample conditions, cell lines used, and length of each follow-up periods also listed.

Experiment 1

Aim:	Effect of washing of gels
Gel conditions:	0,5% UP-LVG
Cell lines used:	HepG2 and IMR90
Length of follow-up:	5 days

Experiment 2

Aim:	Effect of 25 mM HEPES and washing of gels
Gel conditions:	0,5% UP-LVG
Cell lines used:	HepG2 and IMR90
Length of follow-up:	IMR90 for 8 days, HepG2 for 7 days

Experiment 3

Aim:	Effect of 'cold-treatment'
Gel conditions:	0,5% UP-LVG
Cell lines used:	HepG2 and IMR90
Length of follow-up:	10 days

Experiment 4

Aim:	Effect of peptide grafted alginates on cell adhesion
Gel conditions:	1,0 % UP-LVG 1,0 % UP-LVG + IKVAV-modified alginate (1:1) 1,0 % UP-LVG + YIGSR-modified alginate (1:1) 1,0 % UP-LVG + RGD-modified alginate (1:1) 1,0 % UP-LVG + OX (1:1)
Cell lines used:	HepG2 and IMR90
Length of follow-up:	5 days

Experiment 5

Aim:	Effect of RGD-modified alginate
Gel conditions:	0,5 % UP-LVG 1,0 % UP-LVG + RGD-modified alginate (1:1) 1,0 % OX + RGD-modified alginate (1:1)
Cell lines used:	HepG2 and IMR90
Length of follow-up:	10 days

Experiment 6

Aim:	Effect of amount of RGD-modified alginate for IMR90 adhesion
Gel conditions:	0,5 % UP-LVG 1,0 % UP-LVG+RGD-modified alginate (1:1) 1,0 % UP-LVG+RGD-modified alginate (1:3) 1,0 % OX+RGD-modified alginate (1:1) 1,0 % OX+UP-LVG (1:1)
Cell lines used:	IMR90
Length of follow-up:	10 days

Experiment 7

Aim:	Effect of gel stiffness and cell number
Gel conditions:	1% UP-LVG+OX 1:2 with 1×cells 1% UP-LVG+RGD modified alginate 1:2, 1×cells 1% UP-LVG+RGD modified alginate 1:2, 2×cells 1% UP-LVG+RGD modified alginate 1:2, 4×cells 2% UP-LVG+RGD modified alginate 1:2, 1×cells 2% UP-LVG+RGD modified alginate 1:2, 2×cells
Cell lines used:	IMR90
Length of follow-up:	10 days

